MEASUREMENTS IN COMPRESSOR CASCADE WAKE

By
M. A. SAYEED KHAN

DEPARTMENT OF AERONAUTICAL ENGINEERING
INDIAN INSTITUTE OF TECHNOLOGY KANPUR

JANUARY, 1980

MEASUREMENTS IN COMPRESSOR CASCADE WAKE

A Thesis Submitted
in Partial Fulfilment of the Requirements
for the Degree of
MASTER OF TECHNOLOGY

By
M. A. SAYEED KHAN

to the
DEPARTMENT OF AERONAUTICAL ENGINEERING
INDIAN INSTITUTE OF TECHNOLOGY KANPUR
JANUARY, 1980

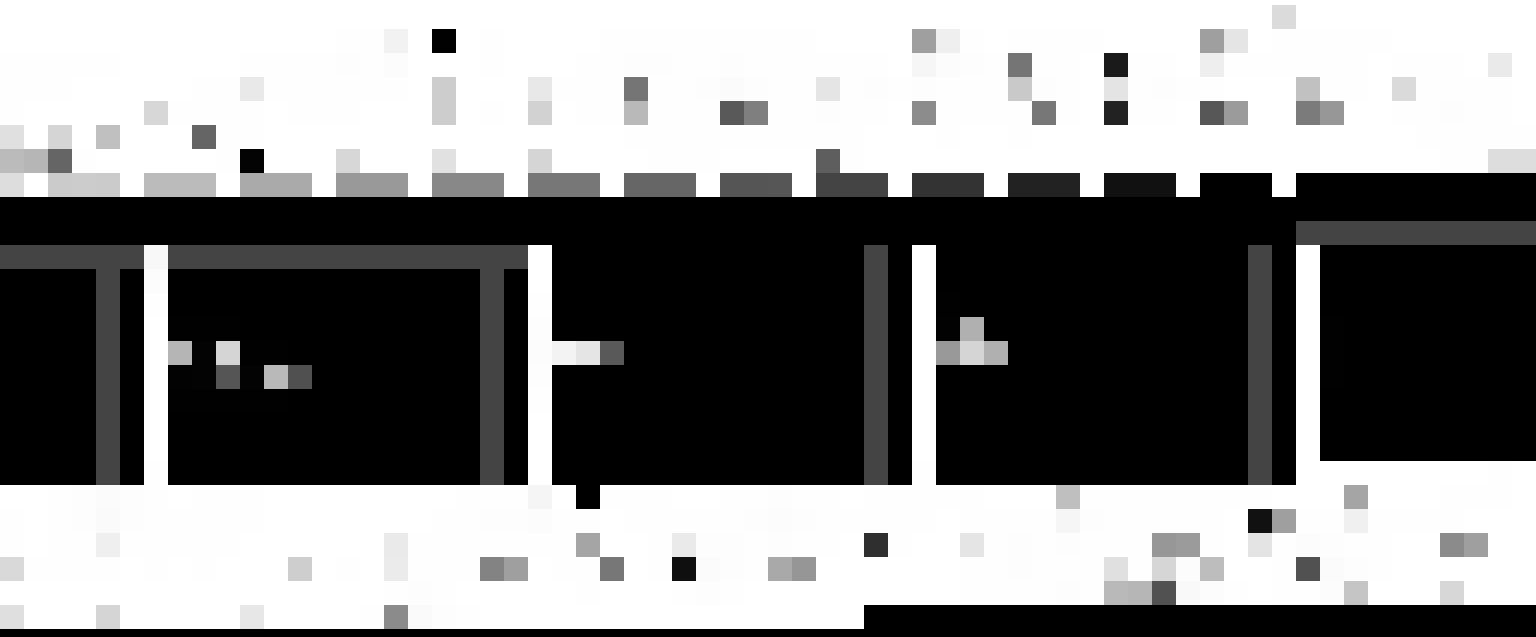

14.9.79
2i

C E R T I F I C A T E

This is to certify that the thesis entitled, "Measurements in Compressor Cascade Wake", is a record of the work carried out under my supervision and that it has not been submitted elsewhere for a degree.

R. K. Sullerey
Assistant Professor
Department of Aeronautical Engineering
Indian Institute of Technology, KANPUR

A C K N O W L E D G E M E N T S

At the very out set I wish to express my deep sense of gratitude to Dr. R.K.Sullerey for suggesting me the problem and providing me the most benevolent guidance and constant encouragement throughout the course of these investigations.

I thank Mr.R.Krishna Murthy of Aeronautical Engineering Department work-shop, under whose supervision the test set-up was prepared.

My thanks are also due to Mr.S.C.M. Yadav, and the staff of the departmental work-shop who prepared the test set-up and lent their services during the experimental investigations.

Thanks are also due to Mr.Saksena for tracing the graphs in a record time.

M.A.Sayeed Khan

الجامعة

TABLE OF CONTENTS

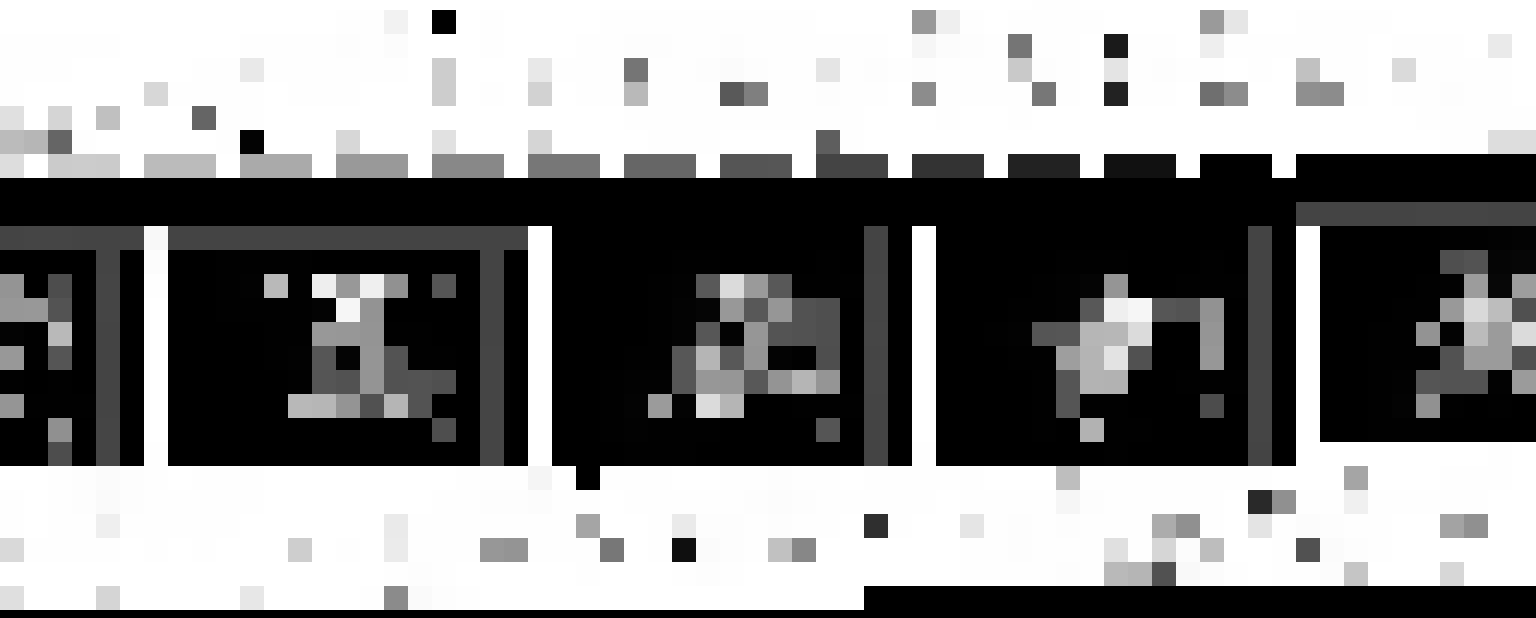

ABSTRACT

The study of the characteristics of the wakes of a cascade of airfoils has direct relevance to the aerodynamic design of axial flow compressors and turbines. Knowledge of flow properties of cascade wake is necessary to predict rotor stator interaction, the noise generated due to inlet wake, and blade row vibrations induced by upstream wakes. In the present investigations, mean flow measurements have been carried out on a compressor cascade wake at three different values of free stream turbulence upto a turbulence intensity of 2.78% . The Reynolds number based on blade chord was 1.31×10^5. *A three dimensional spherical probe was used for measurements. A special calibration rig was fabricated for this probe and it was accurately calibrated. Measurements include the mean velocity and freestream turbulence intensity for three incidence angles. The velocity profiles were asymmetric about the center-line. Using appropriate velocity and length scales, similarity in velocity profiles was observed for all the three stream turbulence levels. The effect of stream turbulence on wake decay was not significant upto a stream turbulence of 2.78%.*

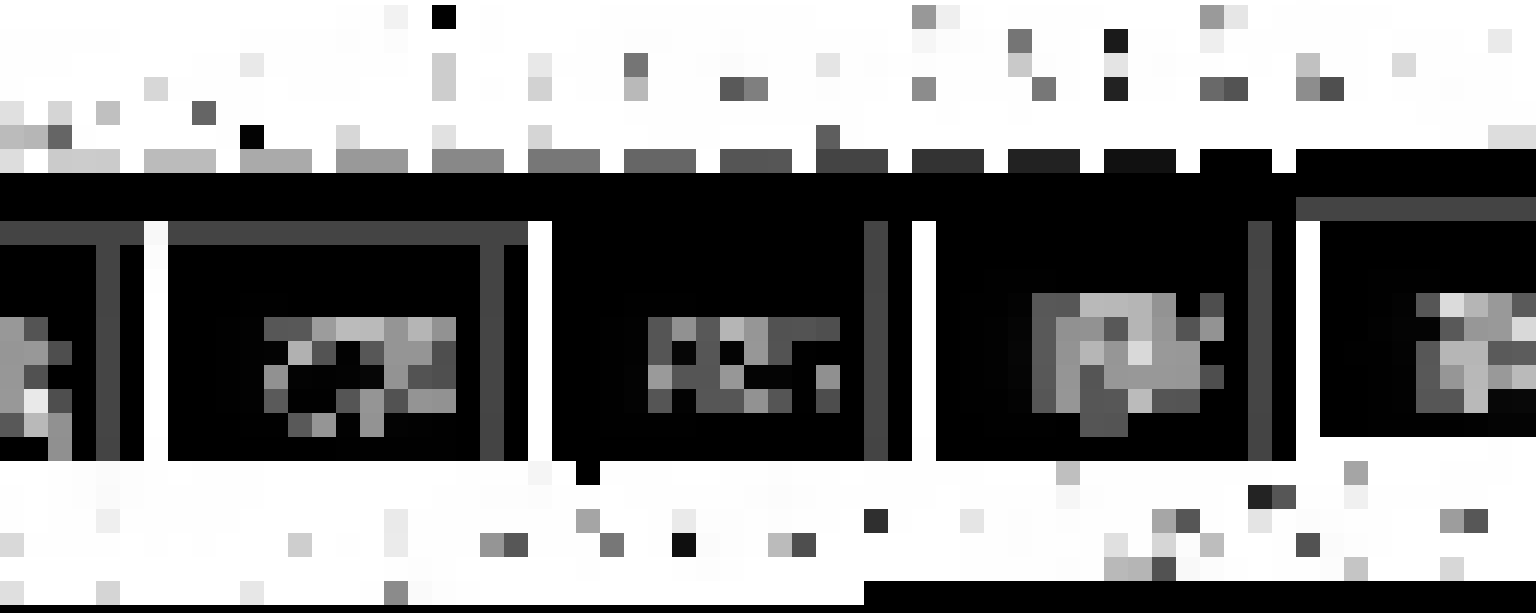

NOMENCLATURE

c Chord length

U Wake velocity

U_e Wake edge velocity

U_c Wake centre-line velocity

x distance from the trailing edge along the wak centre-line.

y Distance across the wake from and perpendicular to wake centre-line.

U_o Scaling velocity $(U_e - U_c)$

L_{os} Scaling length (on suction side), It is the distance on suction side of wake centre-line, from the point of minimum velocity to a point where velocity is $\frac{1}{2}(U_e - U_c)$

L_{op} Scaling length (on pressure side), It is the distance on pressure side of wake centre-line, from the point of minimum velocity to a point where velocity is $\frac{1}{2}(U_e - U_c)$

L_o Mean scaling length $\frac{L_{op} + L_{os}}{2}$

U_{et} Wake edge velocity at trailing edge.

x_o/c Virtual origin.

δ Pitch angle

Ψ Yaw angle

K_δ Inclination factor as a function of δ with constant Ψ.

K_Ψ Inclination factor as a function of Ψ with constant δ.

h Manometer readings (mm w.g)

Suffix 1, 2, 3, 4, 5, Corresponds to holes 1, 2, 3, 4, and 5 respectively (Figure 2)

V_{12} Velocity factor (function of δ & Ψ)

P_{st} Static pressure factor.

h_q dynamic head.

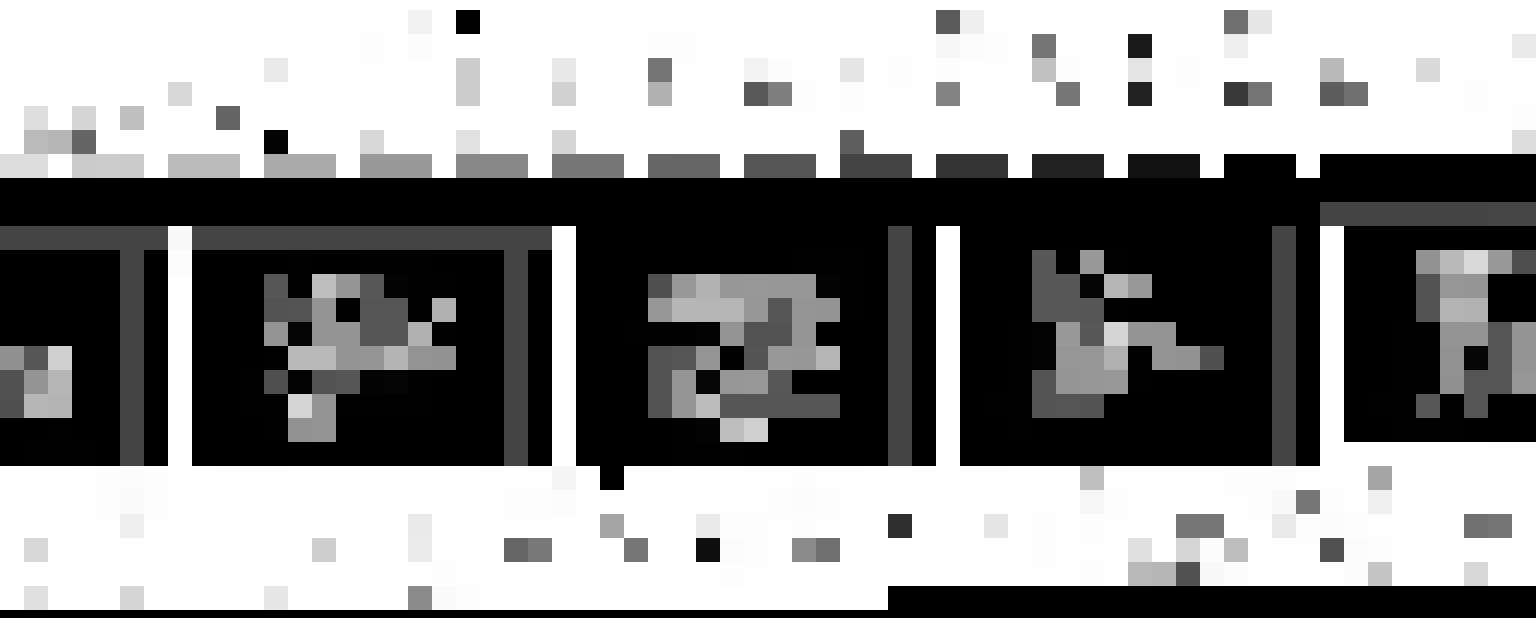

h_{stat} Static head of the pitot static tube.

H_o Total head of the pitot static tube.

W Free-stream velocity

ρ_w Density of water

ρ_a Density of air

g acceleration due to gravity.

μ Coefficient of viscosity.

V_{RMS} Root mean square value of voltage, in millivolts.

V Bridge D.C. Voltage in volts.

V_o Bridge voltage at zero flow velocity.

q_o Free-stream dynamic pressure.

H_1 Total pressure in the wake.

p_1 static pressure in the wake.

$H_c = \frac{H_o - H_1}{q_o}$

$S_1 = \frac{H_o - p_1}{q_o}$

y_w distance normal to wake centre-line velocity from position of H_c Max. to the point at which readings are taken.

d interval at which C_d is determined.

m parameter depending on geometry.

[redacted]

LIST OF FIGURES

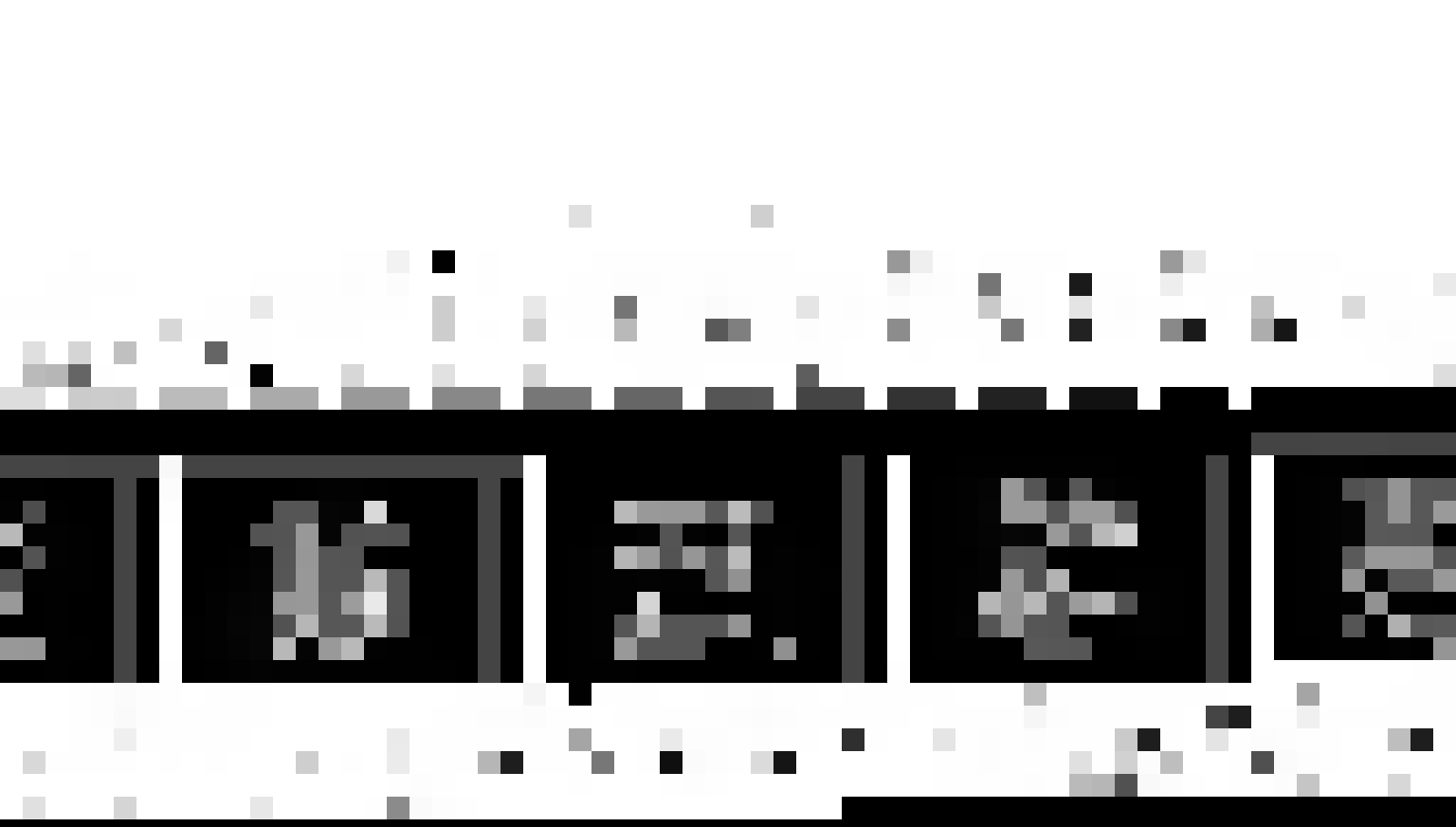

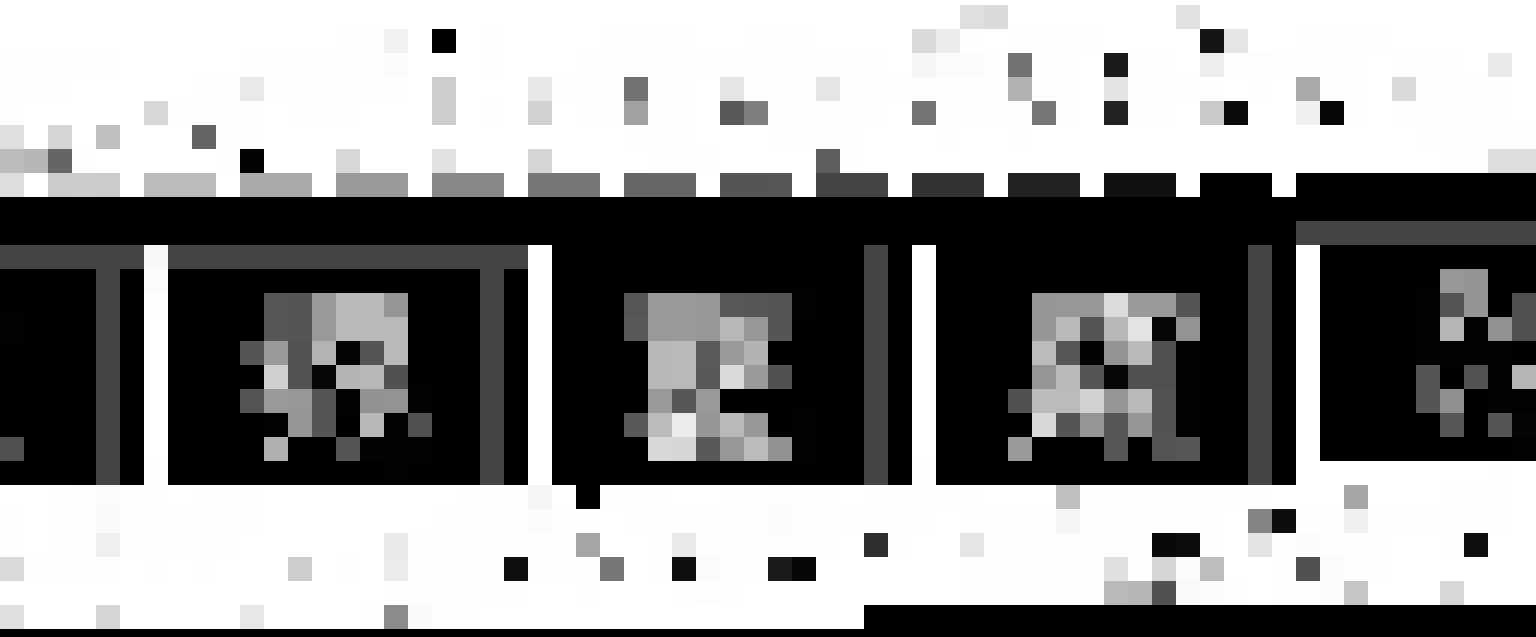

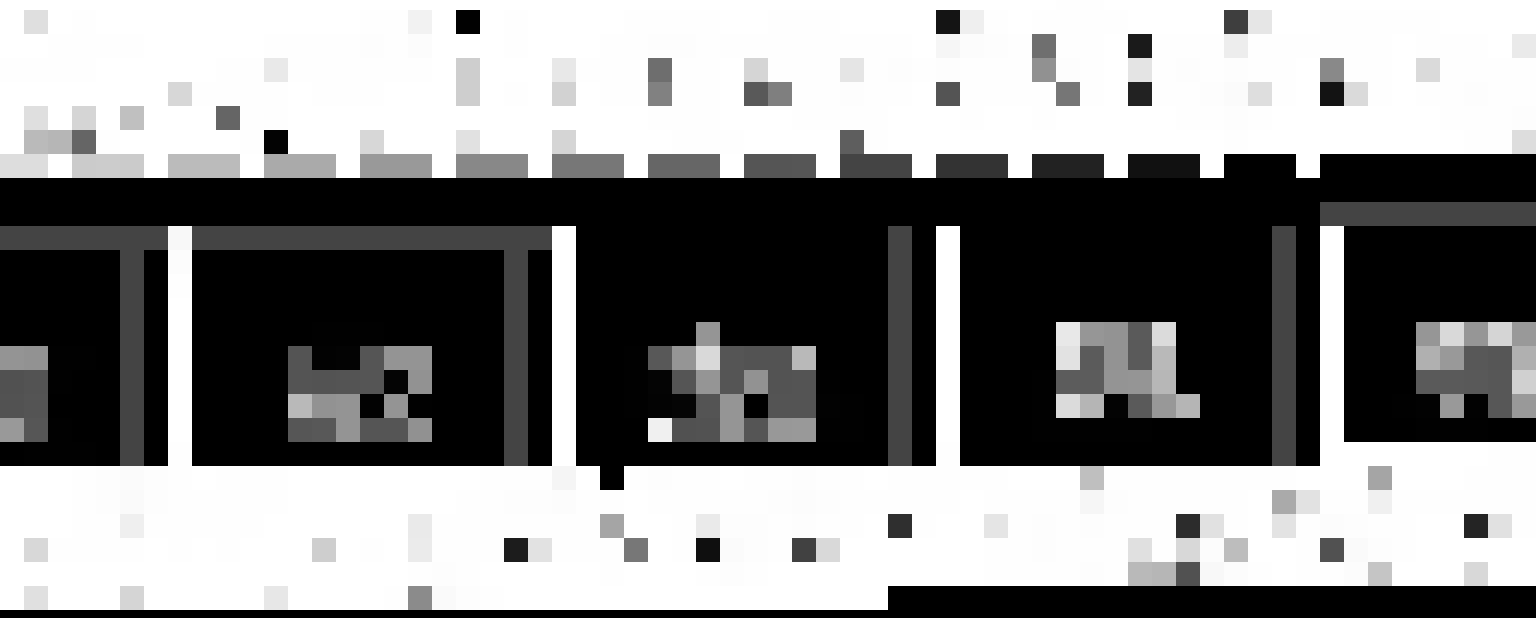

CHAPTER 1
INTRODUCTION

The flow through the blading of an axial flow turbomachine is an extremely complicated three-dimensional phenomenon. It has significant viscosity effects and gradients of flow phoperties in the three physical dimensions (axial, radial, and circumferential), as well as in time. In addition, boundary-layer growth, separation, and tip clearance affect the flow to a great extent. Since a complete solution to such a problem is not currently obtainable, it is treated by making simplifying assumptions.

The three dimensional aspect of the main flow is considered to be described essentially by inter-related two dimensional flow in two principal planes. First, the flow in the blade-to-blade or circumferential plane containing the tangential direction and describes the turning effects of the blade. Secondly, under the assumption of axial symmetry, the average quantities in the blade-to-blade plane are used to describe the distribution of the flow in the hub-to-casing or meridional plane.

The two dimensional blade-to-blade flow surface is taken as cylindrical. This cylindrical surface is developed into an infinite plane cascade. The cascade consists of a group of blades of constant profile mounted in a parallel fashion. For an actual blade of varying section the mean section would yield the average performance.

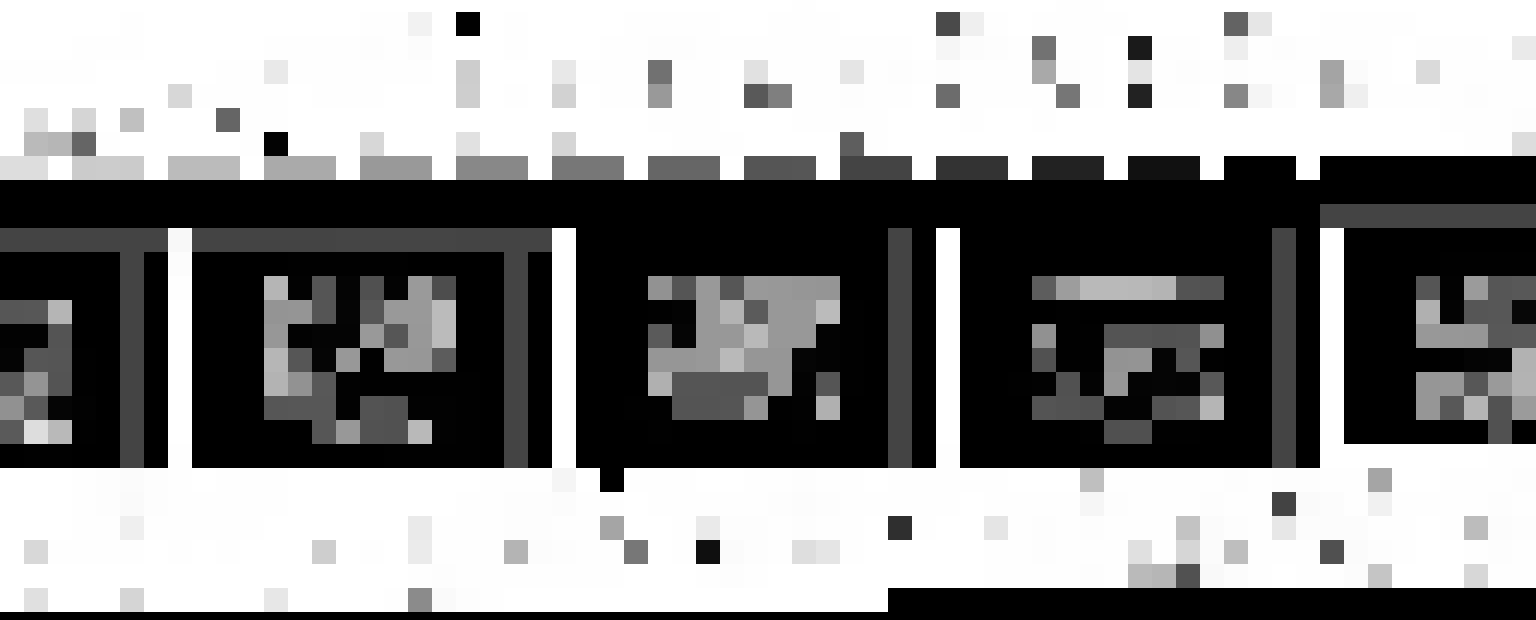

The knowledge of characteristics of wake behind a cascade of airfoils has a wide range of significant scientific and engineering applications. Its structure has an important role in understanding the vibrations produced by the periodic forces in an axial flow turbomachine. As the flow through a row is turned by the blades, the boundary layers formed on either surfaces of each blade form wakes behind the blade row. The cascade wake is turbulent and usually grows in thickness downstream. Associated with the wake are velocity and pressure variations. This unsteady, periodic flow-field surrounding the blades induces bending and torsional vibrations of the blade. As a consequence it may lead to structural failure of the blades.

1.1 Review of available literature:

Numerous studies have been carried out in the past on wake flows of isolated airfoils. These studies show that the similarity in the mean velocity profile exists close behind the airfoil and that the wake centre-line velocity recovers to about 80% of the freestream velocity within a quarter chord length from trailing edge.

Spence (1) gave a general expression for the wake decay, free of the geometry of the airfoil, in terms of wake centre-line velocity, wake edge velocity, distance from trailing edge and the chord length.

Chevray and Leslie (2) investigated experimentally the wake of a thin flat plate at a

Reynolds number of 1.5 X 10^4. The flow was found to be uniform over 75% of the span (wind-tunnel width) at the trailing edge and over 60% of the span at the last downstream station 240 cm from trailing edge. The wake was found to be symmetrical, and grew gradually downstream. The quasi-periodic motion often associated with the wakes of two dimensional bluff bodies was absent.

Bradshaw (3) predicted the mean velocity characteristics of the near wake of symmetrical airfoil using a 'mixing length' fit to data of Chevray & Kovasznay (2). It was concluded that the mixing length fit is not valid once the inner wake spreads.

In the outer layer, the flow was no longer self-preserving. Shear stress profiles showed a large error accumulated for distances greater than 50 cm from the trailing edge. The mixing length fit is not valid for asymmetric wakes.

The experimental data due to Lieblein & Roudebush (4) on Low speed wake characteristics of two dimensional cascade and isolated airfoil sections showed that the wake centre-line velocity attained 75 to 85% of the free-stream value within quarter chord length downstream of the blade. The variation of wake momentum thichness, air outlet angle, and mixing loss were also indicated to occur within a short distance behind the blade.

The wake of a cascade of airfoils differs from that of an isolated airfoil in several ways.

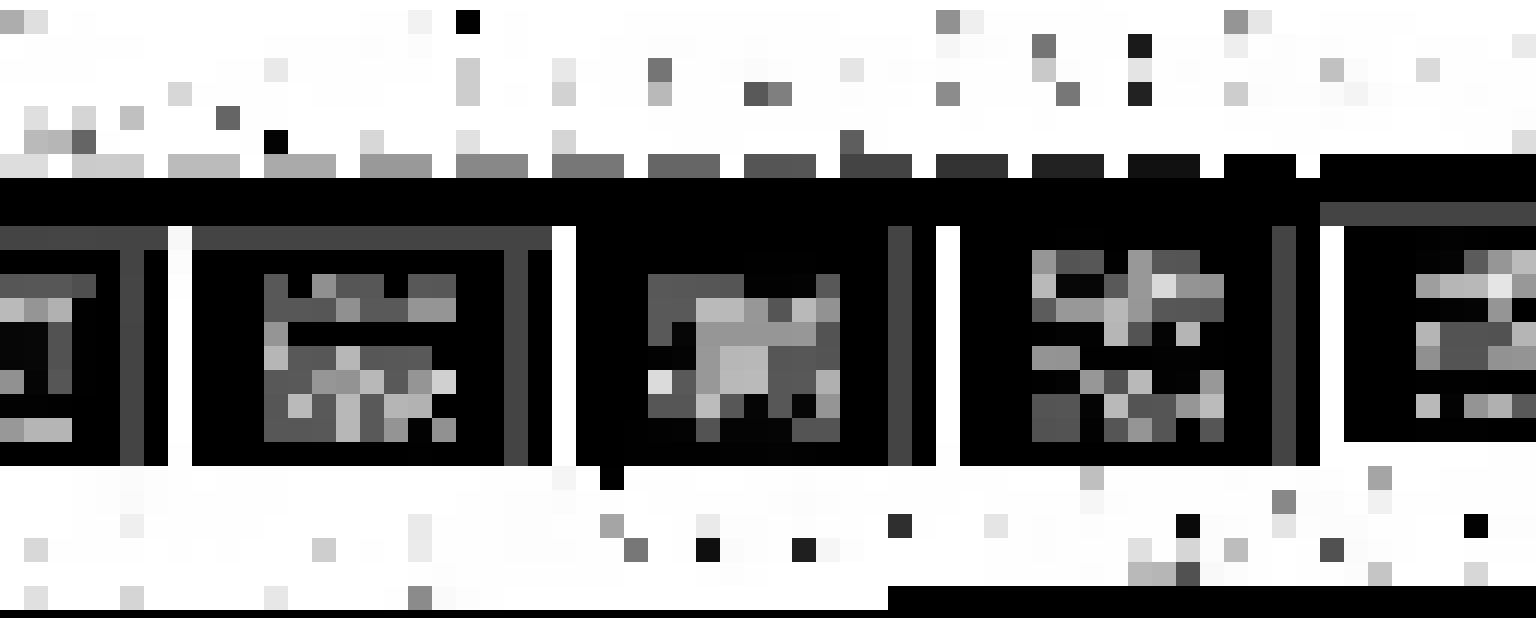

(a) The wake of a cascade decays slower than the wake of an isolated airfoil. (b) The cascade wake encounters an adverse pressure gradient because the wake edge velocity decreases with downstream distance. While the isolated airfoil encounters favourable pressure gradient due to the increase in wake edge velocity with downstream distance. (c) Since the wake edge velocity increases in an isolated airfoil, the momentum thickness decreases. While in cascade it increases due to decreasing wake edge velocity.

Raj and Lakshminarayana (5) carried out analytical and experimental investigations of the near and far wake characteristics of a cascade of cambered airfoil at a Reynolds number of 3×10^5.

The theoretical study of Ref.(5) was based on similarity consideration applied to the turbulent boundary-layer equations, assuming self-preservation and neglecting curvature terms. The continuity and momentum equations in incompressible flow, neglecting viscous diffusion and normal stress are

$$\frac{\partial U}{\partial x} = 0$$

$$U \frac{\partial U}{\partial x} + V \frac{\partial U}{\partial y} + \frac{\partial \overline{uv}}{\partial y} = U_e \frac{\partial U_e}{\partial x}$$

where x is the distance from the airfoil trailing edge along the wake centre-line, y is the distance across the wake from and perpendicular to the wake centre-line, U and V are mean velocities in x and y directions respectively, u and v are mean turbulent velocity components in x and y direction and U_e is the wake edge velocity. It was shown that

$U_e(x) \backsim x^{-m}$; $U_c(x)/U_e(x) \backsim x^{-(1-m)/2}$; and $b(x) \backsim x^{(m+1)/2}$; where b is the wake width and U_c is the wake centre-line velocity.

The experimental investigation in Ref.(5) was carried out with NASA-$(8A_2I_{86})^{10}$ blade section cascade of seven blades with the following salient specifications.

Air inlet angle $\beta_1 = 45^\circ$

Solidity $c/S = 1.505$ (where S is blade spacing and c is chord)

Incidence $i = -6^\circ, 0^\circ, 2^\circ$

Reynolds No. $Re = 3 \times 10^5$.

Free stream turbulence $Tu = 0.16\%$.

Measurements were taken upto $x/c = 0.72$ downstream from trailing edge. A five-hole prism shaped probe was used in combination with three pressure transducers, to measure the resultant direction of the flow and the stagnation and static pressure.

The results obtained in Ref.(5) are ---

(i) The wake is asymmetrical. The mean velocity profiles become symmetrical about the wake centre-line, when two different scaling lengths are used for each side of the wake. This confirms the self preservatory assumptions.

(ii) The wake edge velocity changes continuously giving rise to either slower decay of the wake defect (as with decreasing free-stream flow) or faster decay (with accelerating mean flow). The wake centre-line velocity increases with downstream distance from trailing edge and the value of $\frac{1}{2}(-m+1)$ and C_d vary with solidity and incidence.

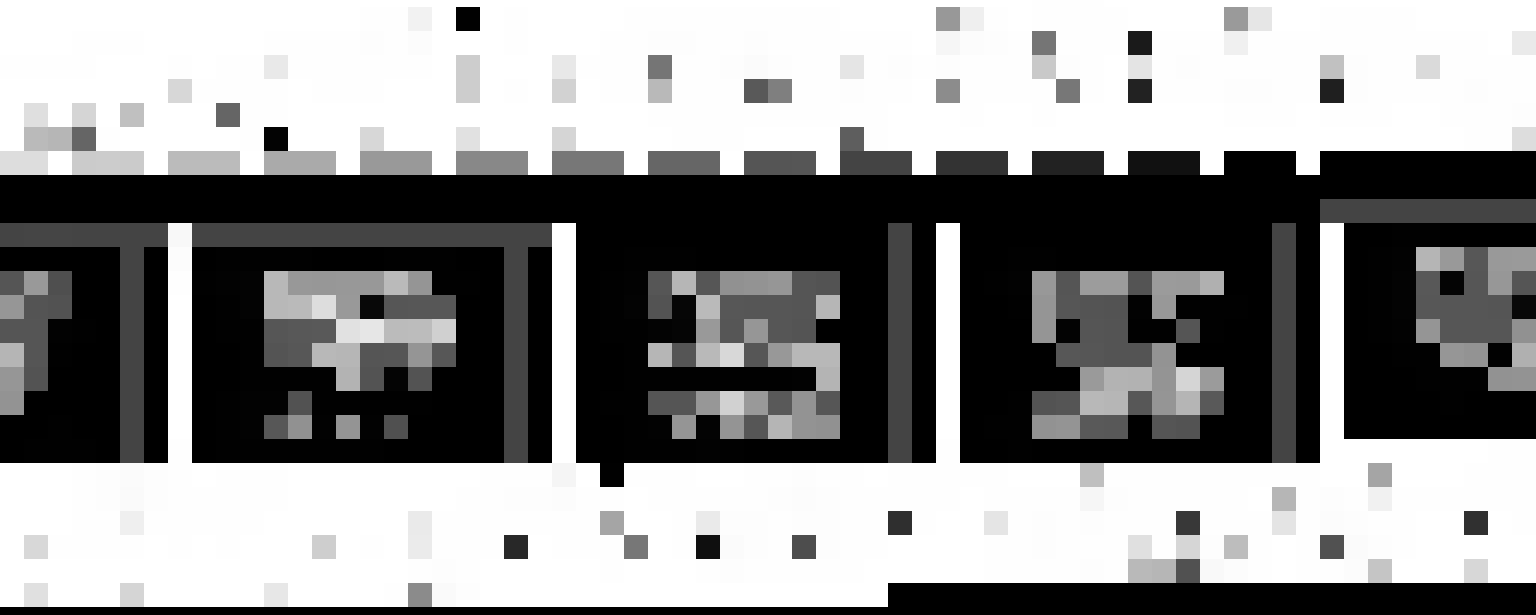

Table 1

	$\frac{1}{2}(-m+1)$	C_d
Isolated airfoil (6)	0.487	0.013
Cascade c/S=0.92 (4)	0.450	0.016
Cascade c/S=1.505 (5)	0.390	0.030

Where 'm' is a parameter that depends on various geometric factors.

(iii) Turbulence intensities are higher in cascade wake than in flat plate wake.

Gustafson and Davis (7) considered the boundary layer equations containing longitudinal curvature terms. The continuity and momentum equations used ignoring viscous stresses are

$$\frac{\partial u}{\partial x} + \frac{\partial}{\partial y}((1+ky)v) = 0$$

$$\frac{1}{1+ky}\, u \frac{\partial u}{\partial x} + v \frac{\partial u}{\partial y} + \frac{kuv}{1+ky} + \frac{1}{\rho(1+ky)} \frac{\partial p}{\partial x} = \epsilon \frac{\partial^2 u}{\partial y^2} + \frac{2k\epsilon}{1+ky} \frac{\partial u}{\partial y}$$

$$\frac{1}{\rho} \frac{\partial p}{\partial y} = \frac{ku^2}{1+ky}$$

where $p(x,y)$ is the pressure, u and v the mean turbulent velocity components, $k(x)$ the curvature, and the Reynolds stress has been replaced by an eddy viscosity law, $-u'.v' = \epsilon \frac{\partial u}{\partial y}$, where $\epsilon(x)$ is the eddy viscosity, assumed to be a function of x. Solutions were obtained separately for local similarity, and global similarity considerations. The similarity solutions tend to become poorer near the trailing edge, but the local similarity solution in general gave a better agreement with experimental data of Ref.(5). The agreement improved further downstream but was reasonably good at 10% of chord from trailing edge, at small incidence. The value of m was as follows.

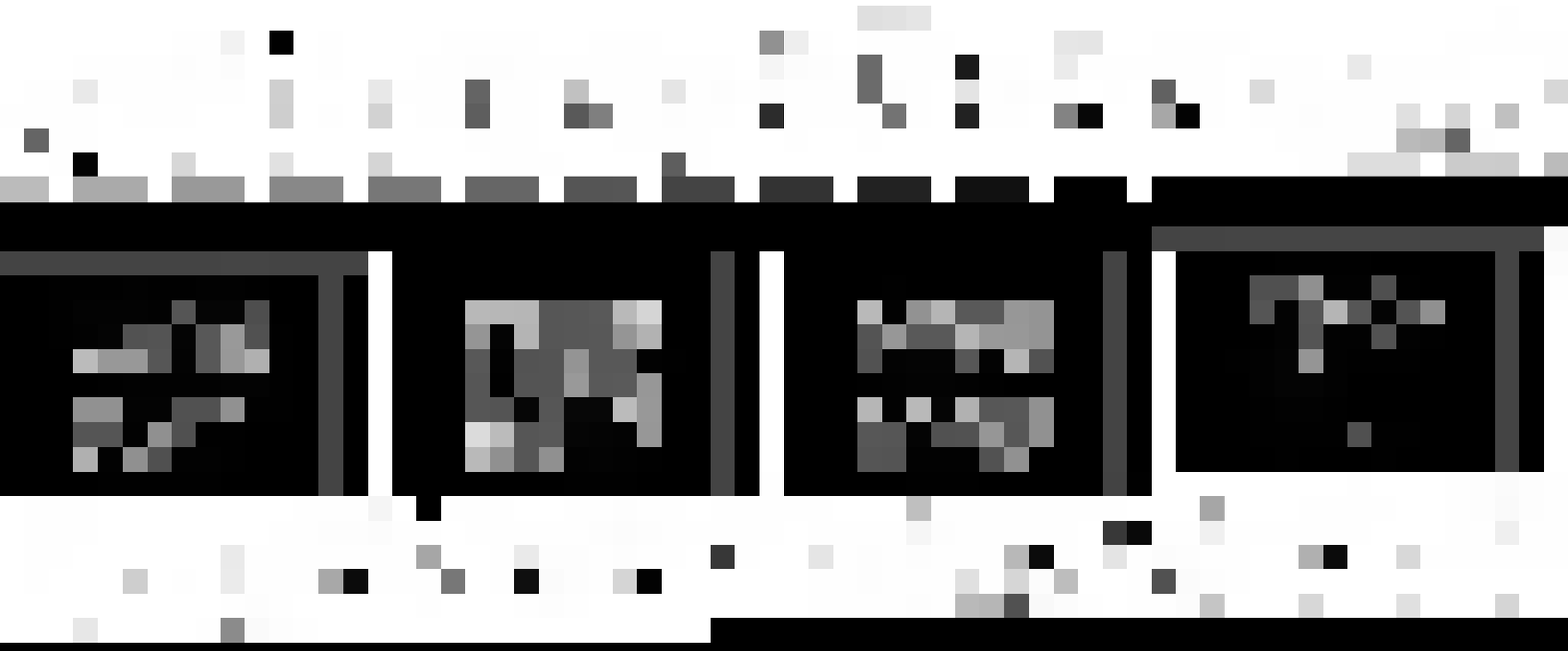

Table 2

Angle of incidence i	m
2^{o}	0.0198
0^{o}	0.0473
-6^{o}	0.1157

Schlichting and Das (8) measured the turbulence intensity encountered in a multistage axial flow compressor. The turbulence intensity increased from stage to stage downstream. A value as high as 5 to 6% in the sixth stage of axial flow compressor was obtained which remained constant at this asymptotic value further downstream. Schlichting and Das (8) suggested that turbulence variation may influence the allowable pressure gradient at which boundary layer begins to separate.

Evans (9) studied the freestream turbulence effects on the turbulent boundary layer and showed that an increase in turbulence level increased the fullness of the velocity profile, kinetic energy, shear stress, and skin friction; and showed decrease in displacement and momentum thickness.

Evans and Harlock (10) modified the existing boundary layer calculation procedure by including extra terms in both the turbulence model equation and the momentum integral equation to account for freestream turbulence. The investigation showed good agreement with flat plate boundary layer measurements in a turbulent freestream. Due to the decay of turbulence level in the streamwise direction in the experiments the effect of turbulence was overestimated in the calculations.

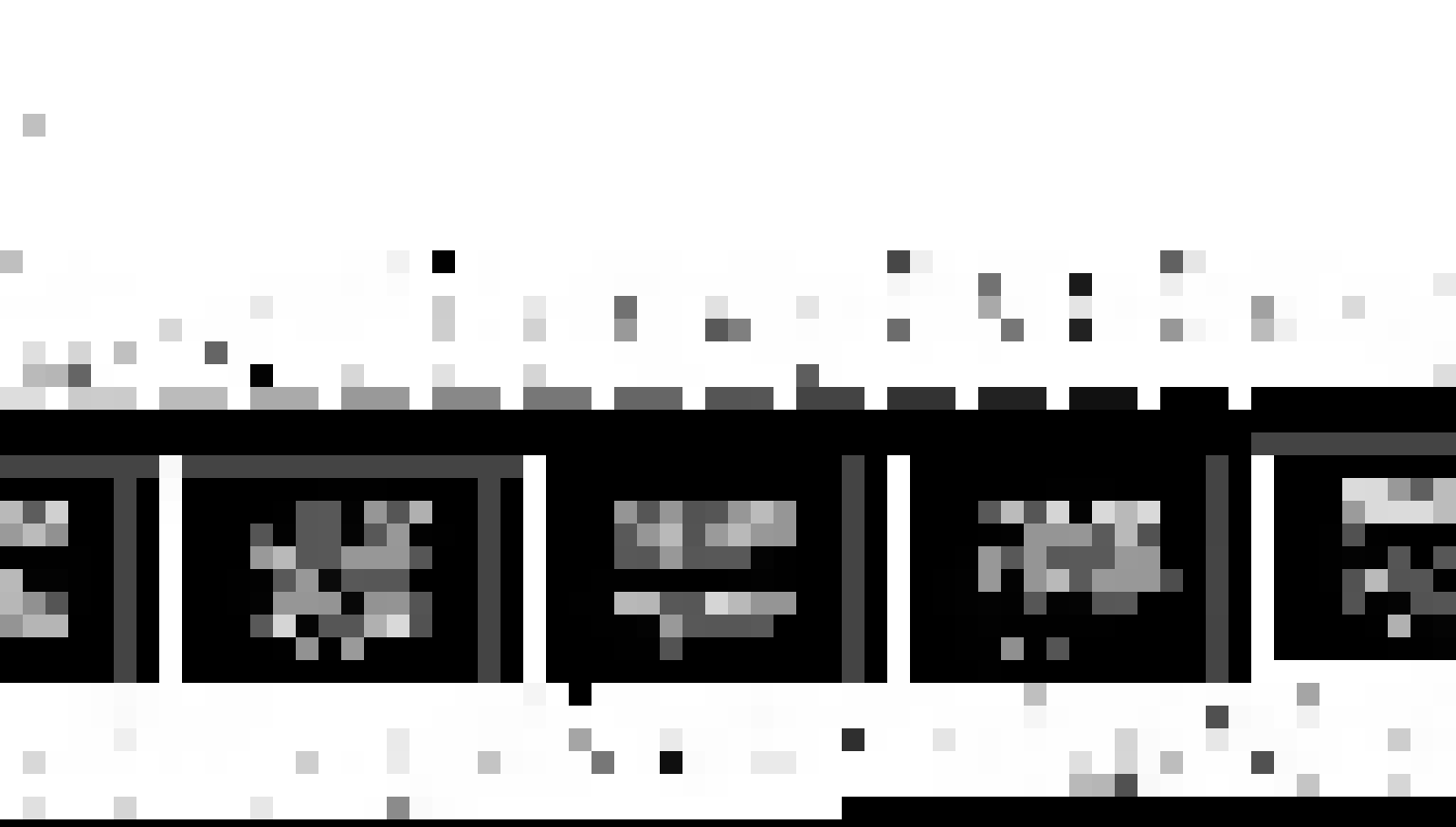

Citavy and Norbury (11) studied the performance of a compressor PVD (Prescribed velocity distribution) cascade and the behaviour of the separation bubble, at several Reynolds numbers and turbulence intensities of upstream flow. It was observed (Ref. 11) that the aerodynamic loading (i.e. the suction peak) increased with increase in Reynolds number for turbulence level greater than 0.35%. At maximum Reynolds number (Re) of 2 X 10^5 separation bubble occured even at turbulence intensity (Tu) of 4.4%. At Reynolds number of 1.52 X 10^5 separation bubble occured at turbulence intensity of 0.35%, at Re=0.93 X 10^5 it occured at Tu=2.1% and at Re=0.69 X 10^5 the separation bubble occured at Tu=4.4% accompanied by a sudden change in the pressure distribution. In particular, the suction peak decreased. It was also observed that the transition within the separated shear layer took place latter in lower turbulence intensity than in higher. Bursting occured at lower Reynolds number when the turbulence intensity was high.

Table 3

Tu	Re_b
0.35%	*1.52 X* 10^5
4.4%	*0.69 X* 10^5

Where Re_b *is the Reynolds number at bursting of the bubble and Tu is the turbulence intensity. However, the effect of turbulence intensity on laminar separation did not seem to be very strong.*

No attempts have been made in the past to investigate the effects of inlet turbulence on

the wake characteristics . Eagleson, Huval and Perkins (12) suggested that at higher levels of freestream turbulence, the wake decay characteristics may be different. The data of Eagleson etal (12) for a flat-plate wake in a water tunnel indicated that the near-wake decay law changed from $x^{-\frac{1}{2}}$ to x^{-1} when the turbulence level was around 4 to 7%. In the present investigations efforts are made to study the near and far wake characteristics of a cascade of compressor blades. The measurements are taken under different free-stream turbulence intensities in a low speed cascade tunnel for three incidences.

1.2 Scope of present investigations:

It was established in Ref.(8) that the turbulence intensity increased with the number of stage in the multistage compressor. From design point of view, it is therefore desirable to know the near and far wake characteristics of a cascade at higher freestream turbulence levels.

In the present investigations mean velocity was measured in the wake region close behind the cascade of compressor blades at various axial and transverse locations. The Reynolds number was maintained at 1.31×10^5. The turbulence intensities generated were 1.18%, 1.61% and 2.78% for -4°, 0° and 12° angle of incidence for the cascade. The five hole spherical pitot probe (Ref. Gupta & Sullery (13)), traversed by means of a three translational degree of freedom traversing mechanism, fitted with five digit mechanical counters was used for mean velocity measurements. The airfoil section chosen for the purpose is (Figure 1)

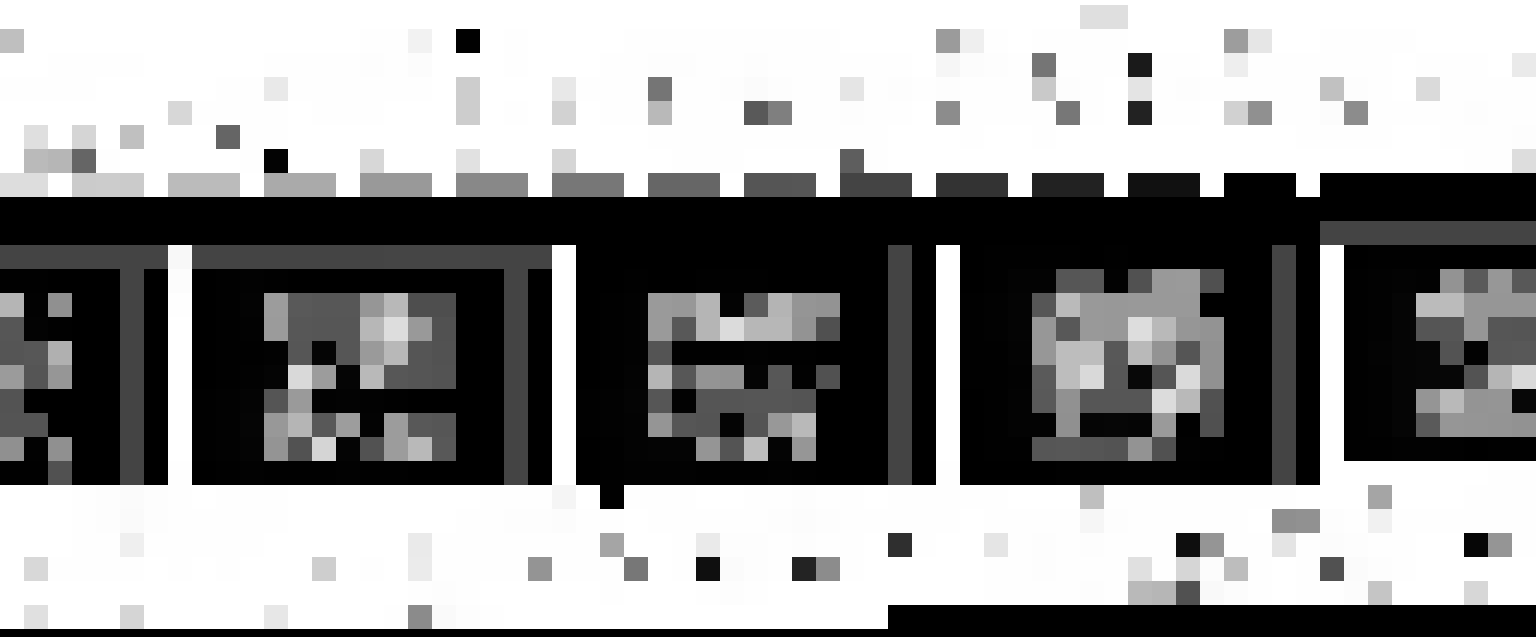

NACA 65-$(12A_{10})_{10}$ (Ref.14). All pressure readings were taken with a multimanameter inclined at 60° to the horizontal plane, with an accuracy of 0.5 mm.

Grids were used for the generation of turbulence upstream of the cascade, (Ref.11). The turbulence intensity was measured using DISA 55A01 hotwire anemometer.

The experimental programme included the effects of freestream turbulence intensity on the characteristics of the wake behind the compressor blade cascade.

المراجع

CHAPTER 2

TEST SET-UP

2.1 Wind Tunnel:

The existing cascade wind tunnel at the Propulsion Lab of the department was used for carrying out the present experimental investigations. The salient specifications of the tunnel are as follows.

Test section	38.10 cm X 30.48 cm
Max. Speed	44.44 m/s
Min. Speed	6.10 m/s (At temperature of 25°C & pressure of 72 cm of Hg),
Motor H.P.	30
R.P.M.	1460

Shutter arrangement near the eye of the blower provides for control of the air speed in the above mentioned range.

2.2 The Cascade and the Test Section:

The tests were carried out on a cascade with five blades. The cascade blades were fabricated from seasoned wood and were given a shellac finish. The blade profile Figure(1) has following specifications.

Chord length	$c = 10.16$ cm
Blade span	$S = 30.48$ cm
Solidity	$\frac{c}{S} = 1.33$

Mean velocities were measured at an inlet angle $\beta_1 = 45^\circ$. The test section had two aluminium plates one at the top and the other at the bottom which kept the cascade in place. Holes were provided in

the top plate near the leading edge of the blade for measuring the free-stream velocity and turbulence intensity.

2.2.1 Modification in the test section:

The two side walls of the test section were cut to different sizes so that the flow from the exit of cascade does not strike the walls, thus enabling more accurate measurements. The side walls were made of perspex sheets so that the upstream probes were visible while setting them along the flow.

2.3 Instrumentation:

The upstream velocity measurements were carried out with the help of pitot static tube. The turbulence intensity was measured with the hot wire probe of 0.003 mm diameter platinum wire and the DISA 55A01 constant temperature hotwire anemometer.

A five-hole spherical probe was used for down stream measurements (Figure 2). Hegge Zijnen (15) showed that when the angle between the central hole and the other holes lie between 40° and 45° the sensitivity of the probe is at its maximum. The probe was attached on a brass tube with its centre line in the axial direction. Five stainless steel tubes of 0.02 cm diameter were used as connectors between the probe and the manometer tubes. A multimanometer inclined at 60° to the horizontal using water as the manometric fluid was used for measuring the pressure heads. The five hole probe was attached to a three dimensional traversing mechanism (Figure 3).

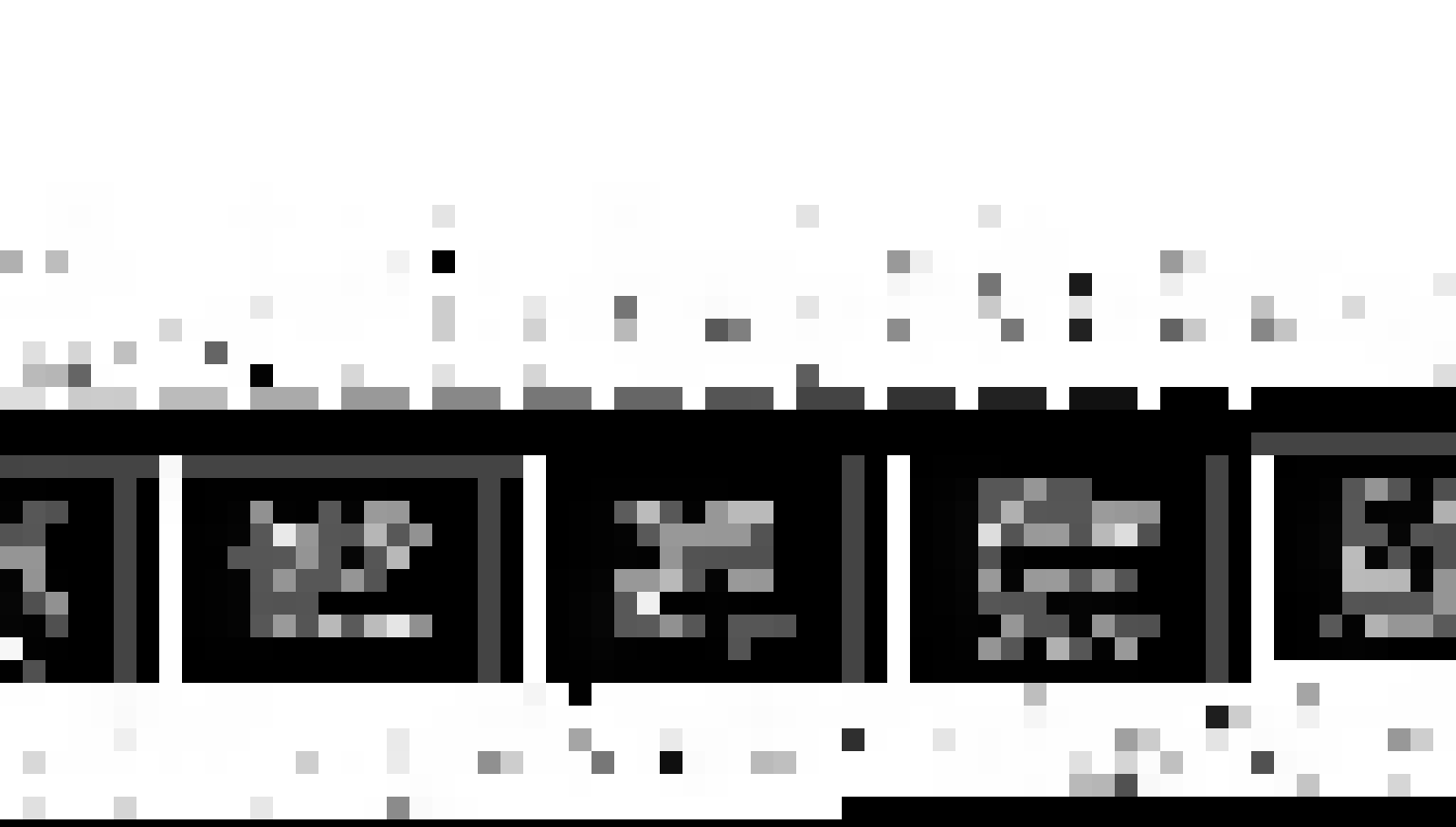

2.4 Calibration Rig:

The calibration rig Figure (4),(5) & (6) used for calibration of the probe consists of three perpendicular axes x,y and z, with a common intersecting point coinciding with the centre of the sphere of the probe. Thus enabling the centre of the sphere of the probe to remain fixed, at any position of the axes. The axes of the rig have been fitted with protractor scales to read the rolling, yawing and pitching angles.

2.5 Turbulence Grid:

The grid used to generate the turbulence intensity of 1.61% was made of 0.24 cm wire with a spacing of 2.22 X 2.22 cm, Figure (7). It was put immediately before the test section.

The other turbulence intensity of 2.78% was generated by a grid of steel bars 1.27 cm. diameter with a spacing of 5.08 X 5.08 cm Figure (8). This grid was kept at a distance of about 80 cm upstream of the test section. This spacing was maintained by a duct of 80 cm length of the same cross-section as that of the test section.

The turbulence intensity decays upstream of the cascade. The values quoted here correspond to position at the inlet to the blade passages of the cascade.

2.6 Calibration method for the five-hole spherical pitot probe:

For calibration (Ref. CFR Nowack (16)) the probe-head was set at a distance of about

18 cm from the convergent section of the tunnel in line with its axis. The holes 2 and 4 (Figure 2) were set in the vertical plane and consequently 3 and 5 in the horizontal. Pressure readings of the five measuring holes were taken on the inclined multimanometer. To determine zero reading of the protractor scale of the calibration rig a fine adjustment of the probe was necessary until manometer readings of the holes 2, 3, 4 and 5 gave the same value. During calibration, increment of 10^{o} were selected for the yaw angle(ψ) at constant pitch angle(δ). Manometer readings of each positions were noted. After each setting of the yaw angle in the range of -60^{o} to $+60^{o}$, the pitch angle(δ) was varied in steps of 5^{o} in the range between -60^{o} and $+60^{o}$.

Flow velocity at the convergent end of the wind tunnel was held constant and was periodically controlled after each setting by a pitot static tube which was removed from the flow field during calibration (Figure 27 and 28). The same probe arrangement was also used to note static pressure.

From the manometer readings, curves were drawn for the inclination factors K, velocity factor V and pressure factors P_{st} as a fuctions of $\pm\ \delta$ and $\pm\ \psi$ (Figure 12, 13, and 14). In order to check reproducability, several positions of the probe were repeated at different speeds of different days. It was found that the factors held practically the same values.

CHAPTER 3
TESTING TECHNIQUE

The existing cascade wind tunnel was suitably modified, as already mentioned, and used for present investigations. Model was fitted in the test section and rotated to set at zero incidence. The five-hole pitot probe was fitted on the traversing gear assembly (Figure 9). The probe was held at a position hebind the cascade model at the blade mid span and was screwed to the traversing gear at this position. The travers was so positioned ~~positioned~~ that the probe was along the centre-line of the blade (Figure 10). A pitot static tube and a hot wire probe was provided near the leading edge of the cascade blades (Figure 11).

3.1 Experimental Procedure:

The tunnel was made to run and the mass rate from the blower was adjusted so as to get a Reynolds No. of 1.31×10^5. The free-stream velocity was measured with the pitot static tube. And the free-stream turbulence with hot wire probe. Both pitot static tube and the hot wire probe were then removed from the test-section. The five-hole probe was traversed normal to the wake centre-line. Readings were taken at an interval of 0.1 cm till uniform velocity was reached on both sides. The probe was then traversed along the centre-line away from the trailing edge of the blade and the measurements across the wake were repeated. The stations along the centre line away from the trailing edge are given in Table 4.

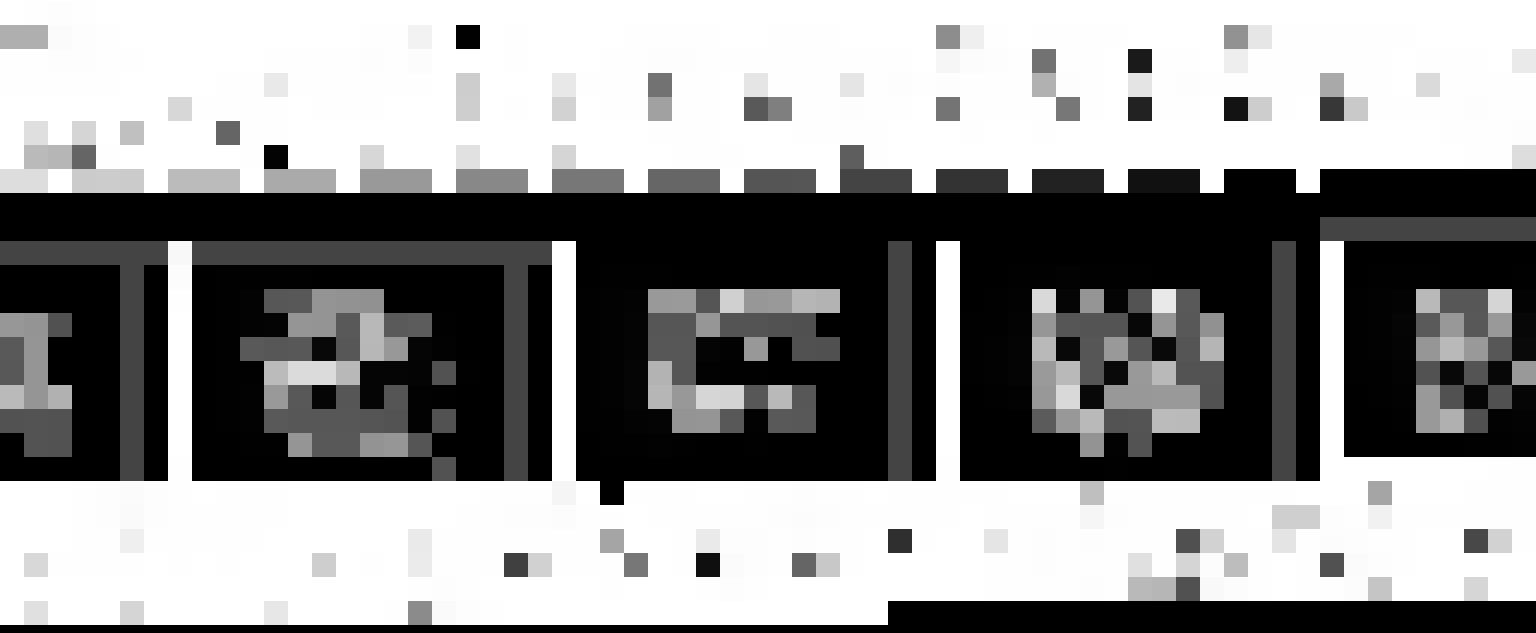

Table 4

Station	x/c
1	0.0125
2	0.1250
3	0.2500
4	0.5000
5	1.0000
6	1.5000
7	2.0000

Incidence was changed by rotating the blades. Readings were repeated at incidence of -4° and 12°. Beyond these critical values the coefficient of drag increased rapidly (Ref. 14).

This completed one set of readings. The wire grid was then placed immediately before the test section and the above procedure repeated.

The third set was taken with the steel bar grid and spacer duct fitted before the test section.

3.2 Practical problem encountered during experiment:

The flow from cascade exit was striking the side wall of the test section at an angle, when the cascade was set at positive incidence, thus resulting in incorrect measurement of pressure heads.

The side walls of the test section were then Modified as in 2.2.1.

[redacted]

3.3 Date reduction:

The following parameters were deduced from the reading noted:

1. Free-stream velocity (W).
2. Free-stream Reynolds number (Re).
3. Free-stream turbulence intensity (Tu).
4. Mean velocity in the wake region (U).
5. Virtual orgin (x_o/c).
6. Coefficient of Drag (C_d).

3.3.1 Free-stream velocity:

For the measurement of free-stream velocity the total head and the static head was noted with the help of pitot static tube. The free-stream velocity was then determined from the following relation.

$$W = \sqrt{2(H_o - h_{static})g(\rho_w/\rho_a - 1)}$$

ρ_w and ρ_a are the density of water and air respectively at the temperature and pressure of surrounding atmosphere. 'g' is the acceleration due to gravity.

3.3.2 Free-stream Reynolds number:

The free-stream velocity being known the Reynolds number was determined from the formula

$$Re = \rho_a W c/\mu .$$

Where μ is the coefficient of viscosity for air at the surrounding temperature and pressure.

3.3.3 Free-stream turbulence intensity:

With the help of constant temperature hot wire anemometer, root mean square value of A.C. voltage in millivolts, D.C. bridge voltage at zero

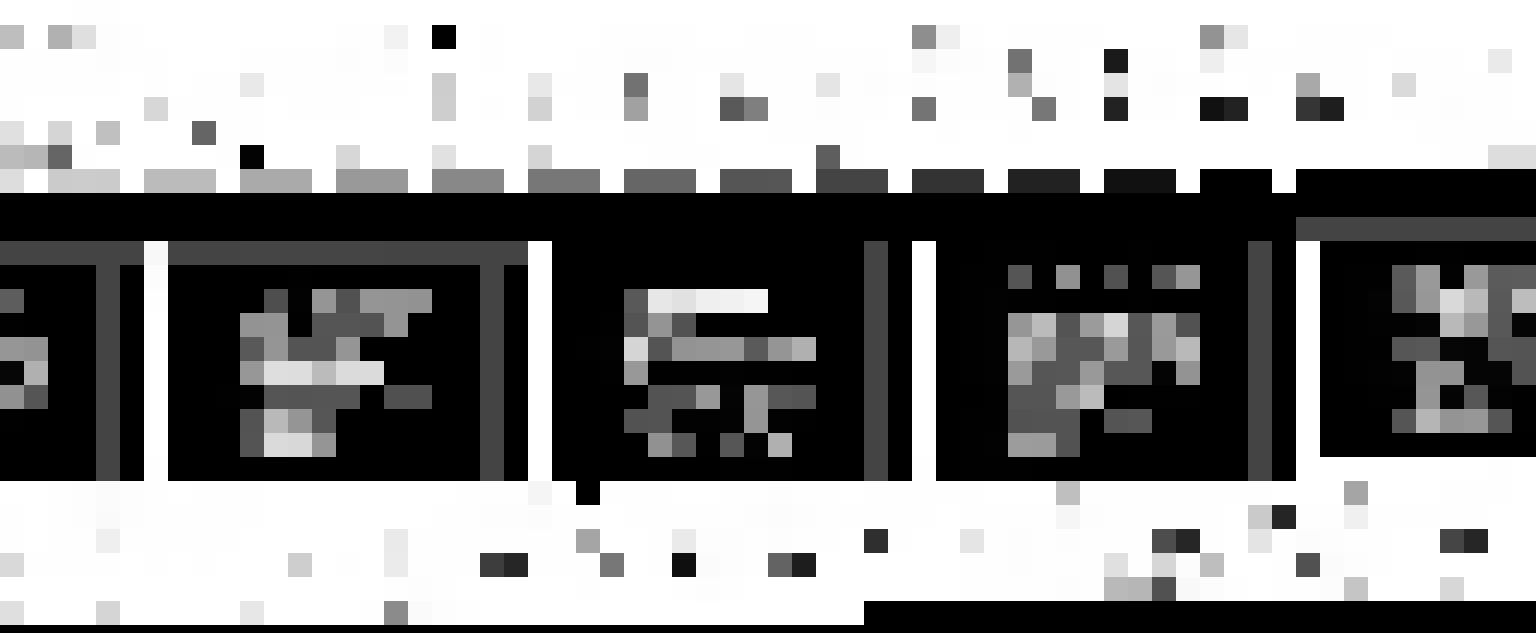

flowvelocity and at the measuced velocity, in volts were noted. Using the following relation the free-stream turbulence intensity was determined.

$$Tu = \frac{100 \times V_{RMS} \times 4V}{1000 (V^2 - V_\infty^2)} \%$$

3.3.4 Mean velocity in the wake region:

Pressure heads were recorded with the help of multimanameter corresponding to the five holes of the prob. Inclination factors K_δ and K_ψ were then calculated as follows.

Inclination factors: $K_\delta = \frac{h_1 - h_2}{h_1 - h_4}$;

$$K_\psi = \frac{h_1 - h_3}{h_1 - h_5} .$$

Corresponding to the values of K_δ and K_ψ the direction of the velocity vector was determined with the aid of the Calibration curves for the inclination factor K (Figure 12). With δ and ψ known the value of V_{12} was determined from calibration curves for the velocity factor V_{12} (Figure 13). The dynamic head was then determined as

$$h_q = \frac{h_1 - h_2}{V_{12}} .$$

With air as flow medium, the velocity was determined from the following formula.

$$U = 4 \, h_q^{\frac{1}{2}} \quad m/s .$$

3.3.5 Virtual origin:

The momentum integral relationship between velocity defect in the wake to the profile

drag is as follows.

$$\frac{U_c}{U_e} = 1 - \frac{K\, C_d^{\frac{1}{2}}}{\left(\frac{x}{c} + \frac{x_o}{c}\right)^{\frac{1}{2}(-m+1)}}$$

Values of x/c and the corresponding values of U_c, U_e etc. obtained from the experiment were substituted to determine the value of x_o/c .

3.3.6 Coeficient of drag:

The coefficient of drag was obtained from observations of pressures in the wake. For determining the drag coefficient, the coefficient of loss of total pressure, and the static pressure coefficient in the wake were obtained as follows.

Total pressure (H_o) in front of the airfoil and free-stream dynamic pressure q_o were obtained from 3.3.1. q_o being equal to $H_o - h_{stat}$. The values of h_1 and h_q were obtained from 3.3.4 and P_{st1} from Figure(14) for the values of δ and ψ of 3.3.4. Static pressure in the wake (p_1) was obtained from the relation $p_1 = h_1 - P_{st1}\, h_q$. Total pressure (H_1) in the wake was then found from the formula $H_1 = p_1 + h_q$.

The value of coefficient of loss of total pressure (H_c) was determined from the relation.

$$H_c = \frac{H_o - H_1}{q_o}$$

and the value of static pressure coefficient in the wake(S) was determined from the relation .

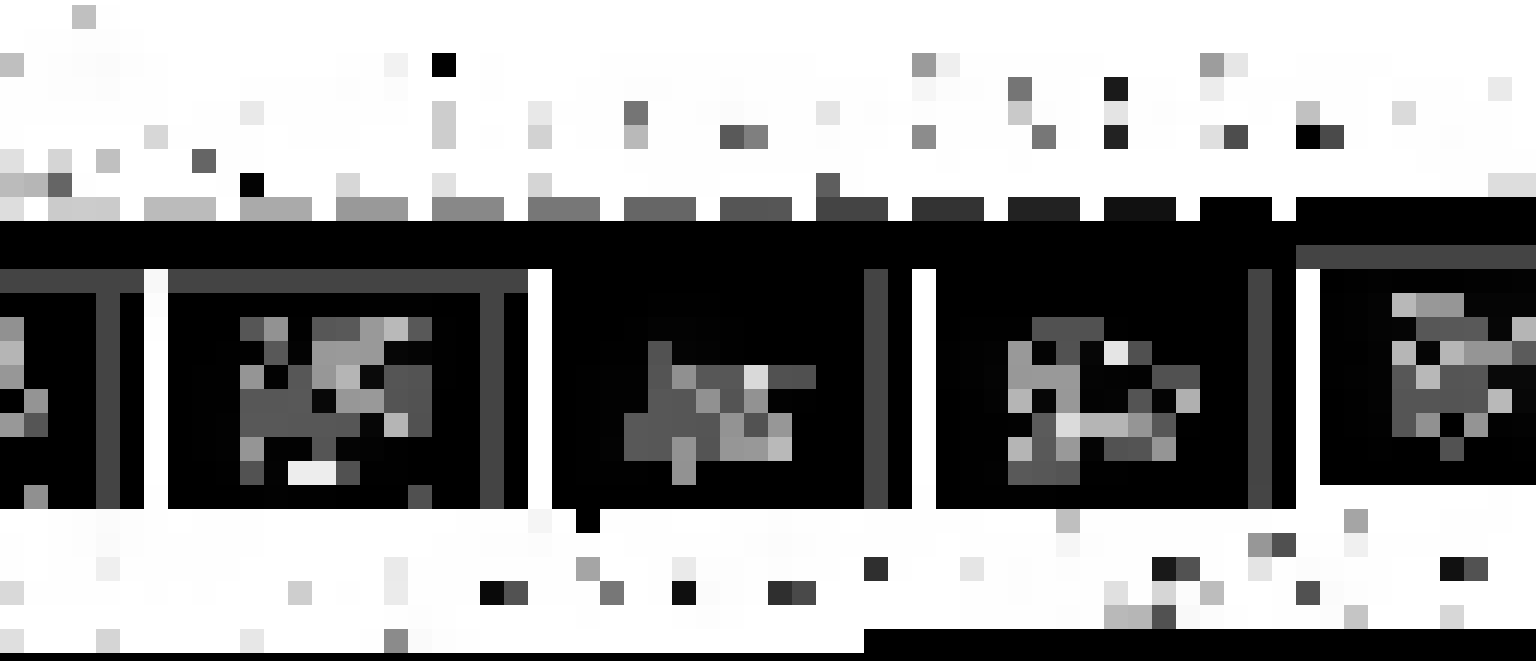

$$S_1 = \frac{H_o - p_1}{q_o} \quad .$$

The drag coefficient was then determined from the formula given below.

$$C_d' = \int_{wake} 2\sqrt{S_1 - H_c}\ \left(1 - \sqrt{1 - H_c}\right) \frac{dy_w}{c} \ .$$

Where y_w is the distance normal to the wake centre-line velocity, from the position of maximum value of H_c to the point at which readings are taken. The value of C_d at an interval of 0.1 cm on either side of wake centre-line velocity were determined. Simpsons rule was then applied to obtain the value of the above mentioned intergral.

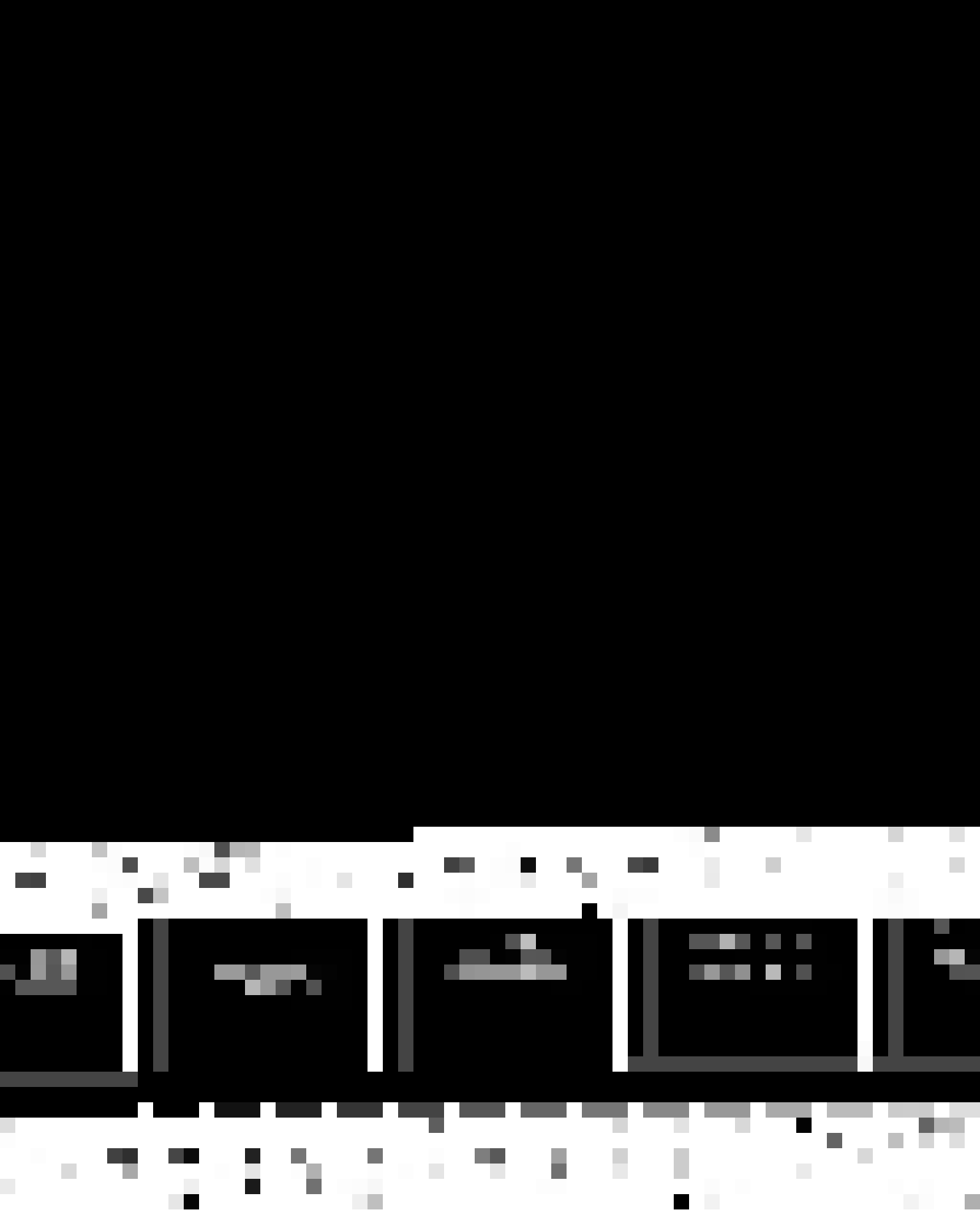

CHAPTER 4

RESULTS AND DISCUSSION

The experimental investigations were carried out at three different free stream turbulence intensities. Without the grids, the turbulence intensity in the cascade tunnel was 1.18%. With the grids, the turbulence intensities were 1.61% and 2.78% respectively. The mean velocity measurements in the wake region were carried out for three incidence angles of $-4^{o}, 0^{o}$, and $+12^{o}$. Beyond this incidence range, the flow was in the stalled region. The measurements were taken on the central blade at the mid span. Flow observed to be two dimensional.

4.1 Mean Velocity Profile:

Figures (15), (16), and (17) show the mean velocity profiles across the wake for an angle of incidence of -4^{o} for the three values of free stream turbulence.

The mean velocity profiles are asymmetric about the wake center line ($y/c = 0$). This asymmetry is maintained at locations downstream of the trailing edge as well. The velocity defect decreases in the downstream direction. Far downstream the wakes of adjacent airfoils interact. With increase in the turbulence intensity, the ratio of centerline velocity to wake edge velocity decreased. At $x/c = 0.9125$, it has a value of 0.60 at turbulence level of 1.18% compared to 0.56 at $Tu = 2.78\%$. At $x/c = 2$, this ratio recovers to 0.91 for $Tu = 1.18\%$ and 0.94 at $Tu = 2.78\%$. Thus

wake decay appears to be faster for the case of higher turbulence in free stream.

Figures (18),(19) and (20) show the plots of mean velocity profiles across the wake for angle of incidence of 0^{o} for the same values of turbulence intensities. The velocity distributions are again asymmetric as in the case of previous incidence angle. The ratio centreline to wake edge velocity is 0.65 compared 0.60 in the previous case at Tu=1.18%. There is decrease in this value with increase in turbulence intensity. The centreline velocity recovers to 94% of wake edge velocity at $x/c = 2.0$ in all the three cases.

Velocity defects are larger for the case of incidence angle of $+12^{o}$ (Figures 21, 22, 23). At $x/c = 0.0125$, the centre-line velocity is only 30% of wake edge velocity. However it recovers to a value of about 88% at $x/c = 2.0$.

Asymmetry in the velocity distributions is more pronounced closer to the trailing edge. However it is apparent even at $x/c = 2.0$.

Using scaling velocity as the difference between the maximum and minimum velocity ($U_o = U_e - U_c$), and two different scaling lengths L_{os} and L_{op} for suction and pressure side respectively), the mean velocity data has been reduced to a single curve in Figures 24, 25 and 26. These figures for 12^{o} incidence are typical of plots at other incidence angles. It is seen that similarity in velocity distribution exists for the three

turbulence intensities. L_{os} and L_{op} have been defined as per Raj and Lakshminarayana (5). L_{os} and L_{op} are distances on the suction and pressure sides of the wake centre-line, from the point of minimum velocity to a point where velocity is $\frac{1}{2}(U_e - U_c)$.

In Figure(29), $U_o L_o / U_{et} c$ has been plotted for $+12^o$ incidence. This factor is nearly constant with downstream distance. It showed a similar trend for -4^o and 0^o incidence angles.

4.2 Variation of wake centre-line velocity with down stream distance:

Figure (30) to Figure (35) show the variation in wake centre-line velocity with down-stream distance in simple as well as logarithmic scales. x_o/c has been obtained following the procedure of Raj and Lakshminarayana (5). The value of x_o/c is in the range of 0.019 to 0.032. Effect of stream turbulence on U_c/U_e does not seem to be appreciable at present levels of turbulence intensities. x_o/c values in the present experiments are in good agreement with the values of Lieblein and Roudebush (4). x_o/c decreases with the increase in free stream turbulence.

4.3 Variation of wake edge velocity with down stream distance:

The wake edge velocity can be expressed as $U_e \sim 1/x^m$, where the value of m is found to be 0.0875, 0.052 and 0.0349 at incidences -4^o, 0^o, and 12^o respectively. Figure 36 to Figure 41 shows the variation of wake edge velocity in simple as well

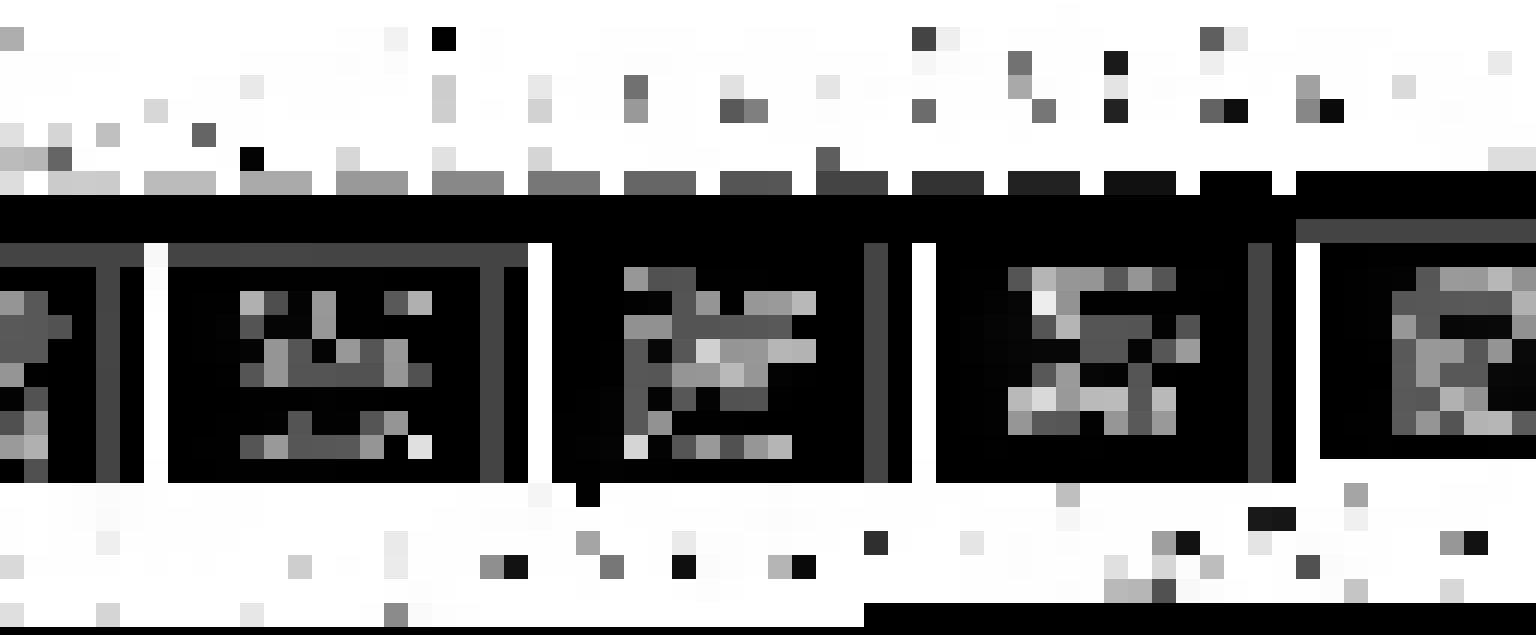

as logarithmic scales. These values are in the range of values obtained by Raj and Lakshminarayana (5). The freestream turbulence does not seem to have an effect on the value of 'm'.

4.4 Coefficient of drag:

The coefficient of drag for the different incidence angles and freestream turbulence are shown in table (5). The value of C_d showed good comparison with the values of C_d obtained by Richard & James (14) in NACA TN 3937 for similar blade profile and inlet angle. There is some decrease in the value of C_d with increase in turbulence intensity.

Table 5.

i	C_d			
	Tu = 1.18%	1.61%	2.78%	Ref. (14)
-4°	0.025	0.023	0.022	0.020
0°	0.017	0.014	0.013	0.015
12°	0.013	0.011	0.011	0.0125

Due to lack of time, turbulence measurements could not be carried out in the wake of cascade.

[redacted]

CHAPTER 5

CONCLUSIONS

(1) A three dimensional spherical probe has been extensively calibrated using a specially designed calibration rig. In addition turbulence grids were designed to give a stream turbulence level upto 2.78% at the cascade inlet.

(2) Detailed measurements of mean velocity distribution in a compressor cascade wake has been carried out at a Reynolds number of 1.31×10^5, a subcritical value. The measurements were made at three incidence angles, $-4^o, 0^o$, and $+12^o$. Asymmetry in velocity distribution is observed even upto $x/c = 2.0$.

(3) Similarity in the mean velocity distribution is observed at the three incidence angles for different values of free stream turbulence. Similarity parameters has been calculated for different cases.

(4) Stream turbulence intensity does not significantly affect the wake decay upto a stream turbulence of 2.78%.

(5) There is a decrease in the value of drag coefficient with increase in turbulence intensity.

(6) In future studies, turbulence measurements in the wake should be included. Wake characteristics can be studied at higher turbulence levels of freestream to see if there is significant effect on wake decay at these values.

THE BIBLIOGRAPHY

(1) Spence, D. A. : Growth of the Turbulent Wake close behind an aerofoil at incidence. C. P. No. 125, British A. R. C. 1953.

(2) Chevrey, R., & Leslie S. G. Dovaszney. : Turbulence measurements in the wake of a thin flat plate. 1969 A. I. A. A. J. 7, 1641.

(3) Bradshaw, P, Ferriss, D. H, & Atwell, N. P. : Calculation of boundary layer development using the turbulent energy equation, 1967 J. Fluid Mechanics. 28, 593.

(4) Lieblein, S. and Roudebush, W. H. : Low-speed wake characteristics of two-dimensional cascade and isolated airfoil section. 1956 NACA Tech. Note No. 3771.

(5) Raj, R. and Lakshminarayana, B. : Characteristics of the wake behind a cascade of airfoils. 1973 J. Fluid Mechanics. 61, 707.

(6) Preston, J. H., Sweeting, N. E. & Cox, D. K, 1945 Aero. Res. Counc. R&M no. 2013

(7) Gustafson, W. A. and Davis D. W. : Analysis of the turbulent wake of a cascade airfoil. 1977. J. of Aircraft, 14, No. 4. 350.

(8) Schlichting And Das. : Dzung, Lang S.

(9) Evans, R. L. : Free-stream turbulence effects on the turbulent boundary layer. Aero. Res. Counc. C. P. No. 1282.

(10) Evans, R. L. and Harlock, J. H. : Calculation of the development of turbulent boundary layers with a turbulent freestream. 1974 J. of Fluid Engineering. 96, No. 4, 348.

(11) Citavy, J. and Norbury, J. F. : The effect of Reynolds number and turbulence intensity on the performance of a compressor cascade

with prescribed velocity distribution (PVD).1977. J. of Mech. Engg. Science. 19, No. 3, 93.

(12) Eagleson, P.S., Huval, C.J. and Perkins, P.E. 1961 M.I.T. Hydrodynamics Lab TR no. 46.

(13) Gupta, A.K., and Sullerey, R.K. :Flow properties behind flame stabilisers. Technical Report AE-23/78 (I.I.T. Kanpur)

(14) Richard, F. and James C. Emery, : A comperison of typical national gas turbine establishment and NACA axial flow compressor blade sections in cascade at low speed. 1957 NACA. TN. 3937.

(15) Hegge Zijmen, B.C. 1929 Proc. R. Akad., Amsterdam 32, 658-63.

(16) Nowack, C.F.R: improved calibration method for a five-hole spherical pitot prob. 1970. J. of Physics Sec. E. Vol. 3 No. 1-2, 21.

Other references:

(17) Abbott, H. Ira, Albert E. Von Doenhoff, and Louis S. Stivers, Jr. :Summary of Airfoil data. 1945. NACA TR824, 259. (Supersedes NACA WRL-560)

(18) Hersig, L. Joseph, Emery, James C., and Erwin, John R. : Systamatic two-dimensional cascade tests of NACA 65-series compressor blades at low speeds, 1956. NACA TN 3916. (Supersedes NACA RM L51G31)

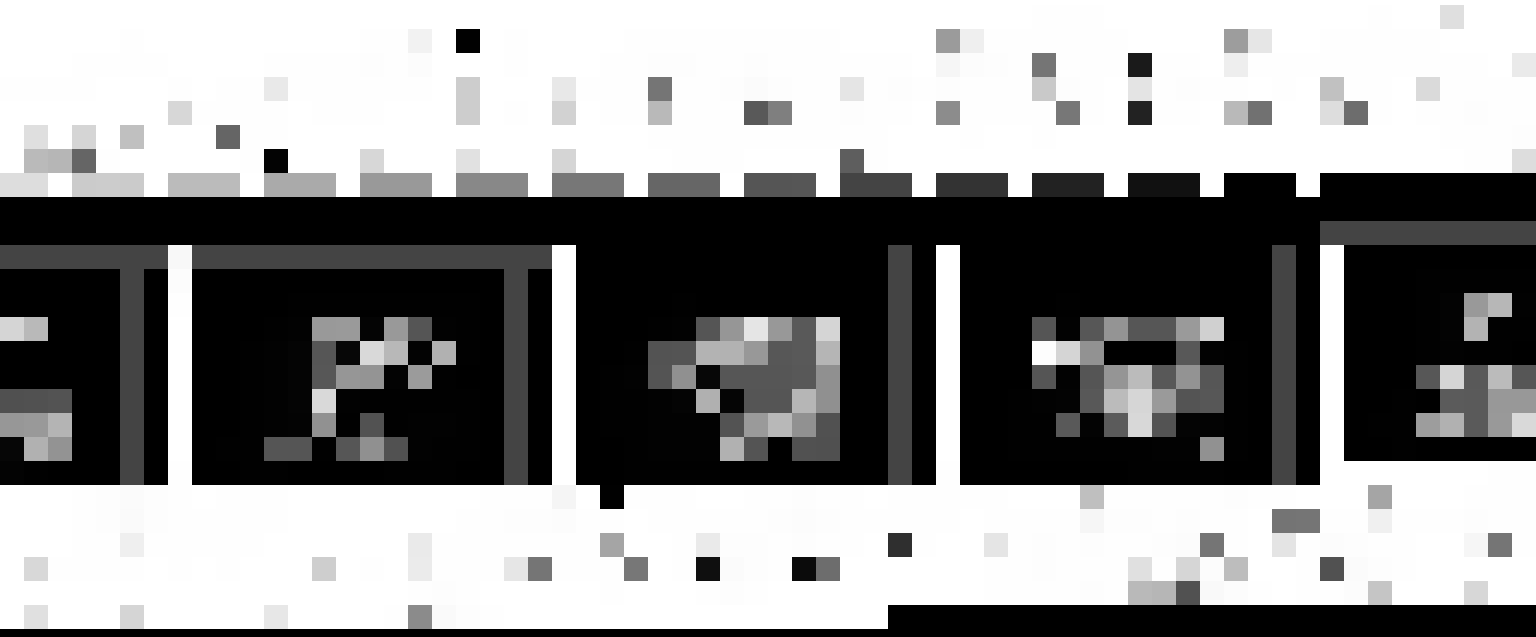

FIG 1. BLADE

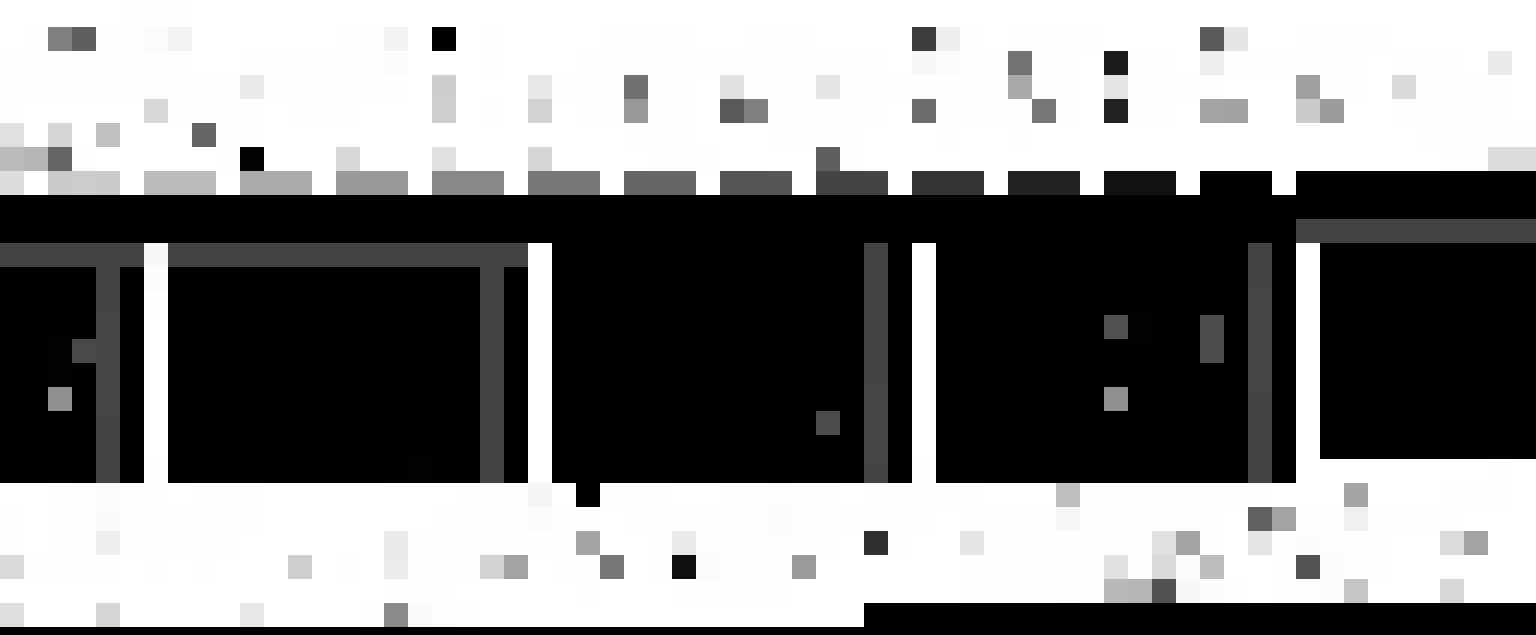

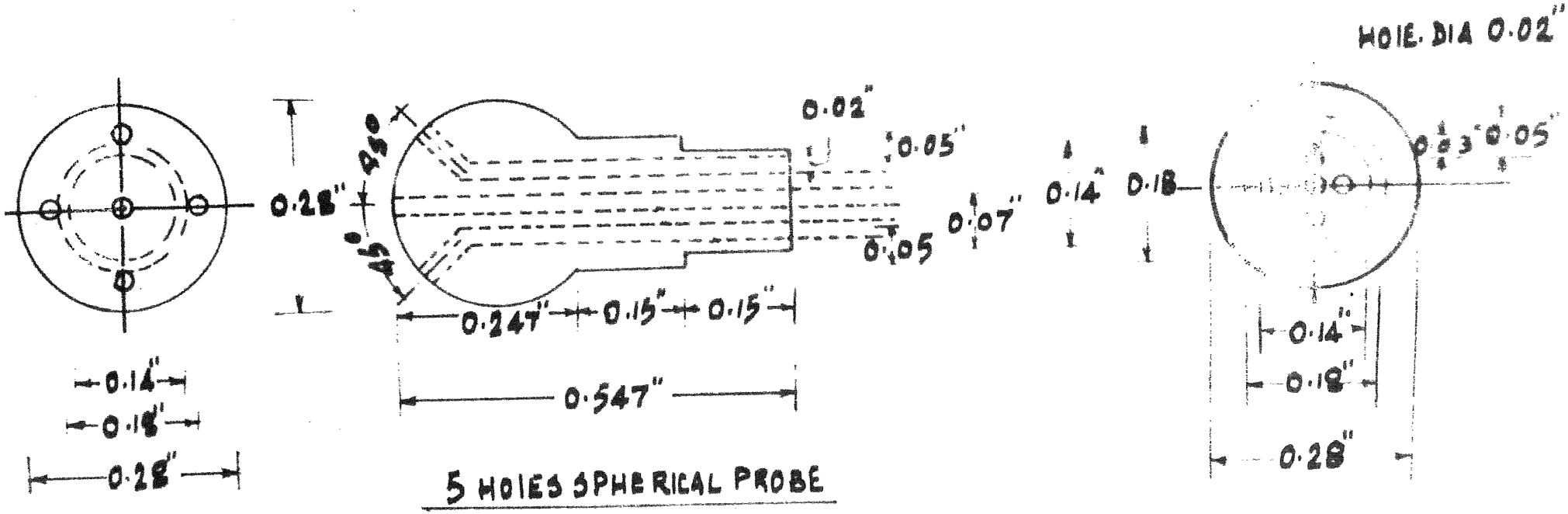

5 HOLES SPHERICAL PROBE

FIG. 2

ALL DIMENSIONS IN INCHES.

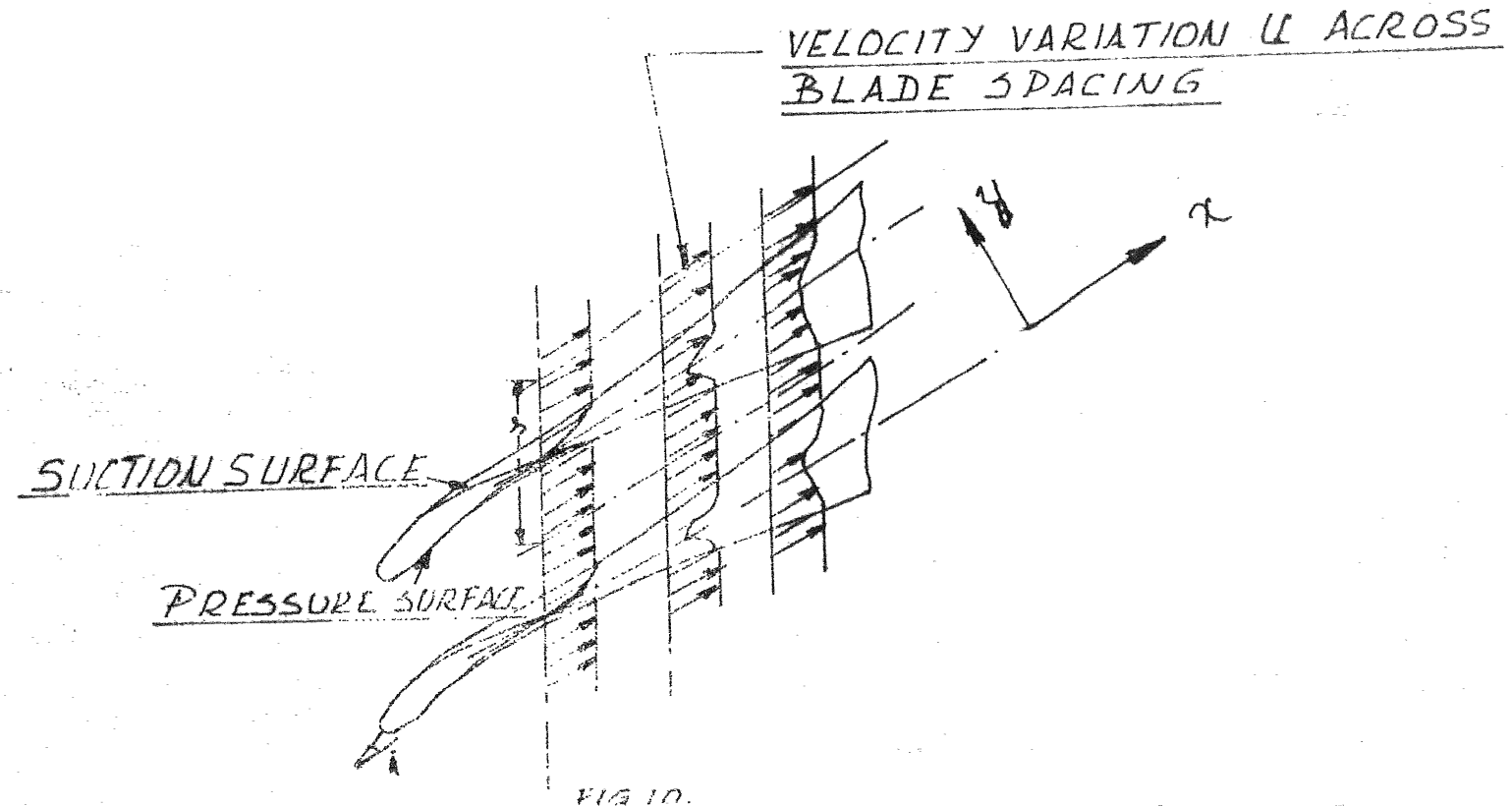

FIG 10.

SCHEMATIC REPRESENTATION OF DEVELOPMENT OF SURFACE BOUNDARY LAYERS AND WAKE IN FLOW ABOUT CASCADE BLADE SECTIONS.

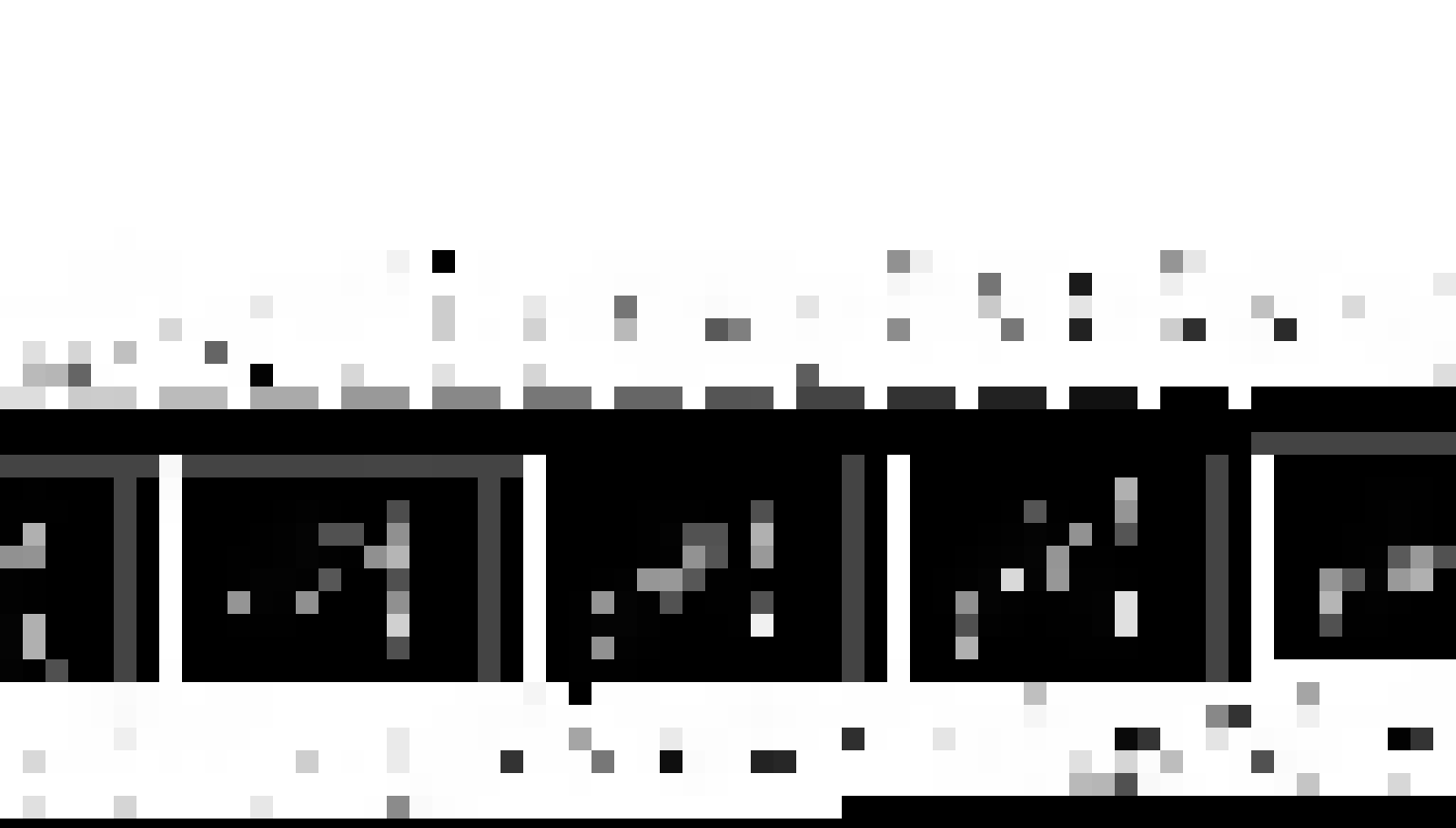

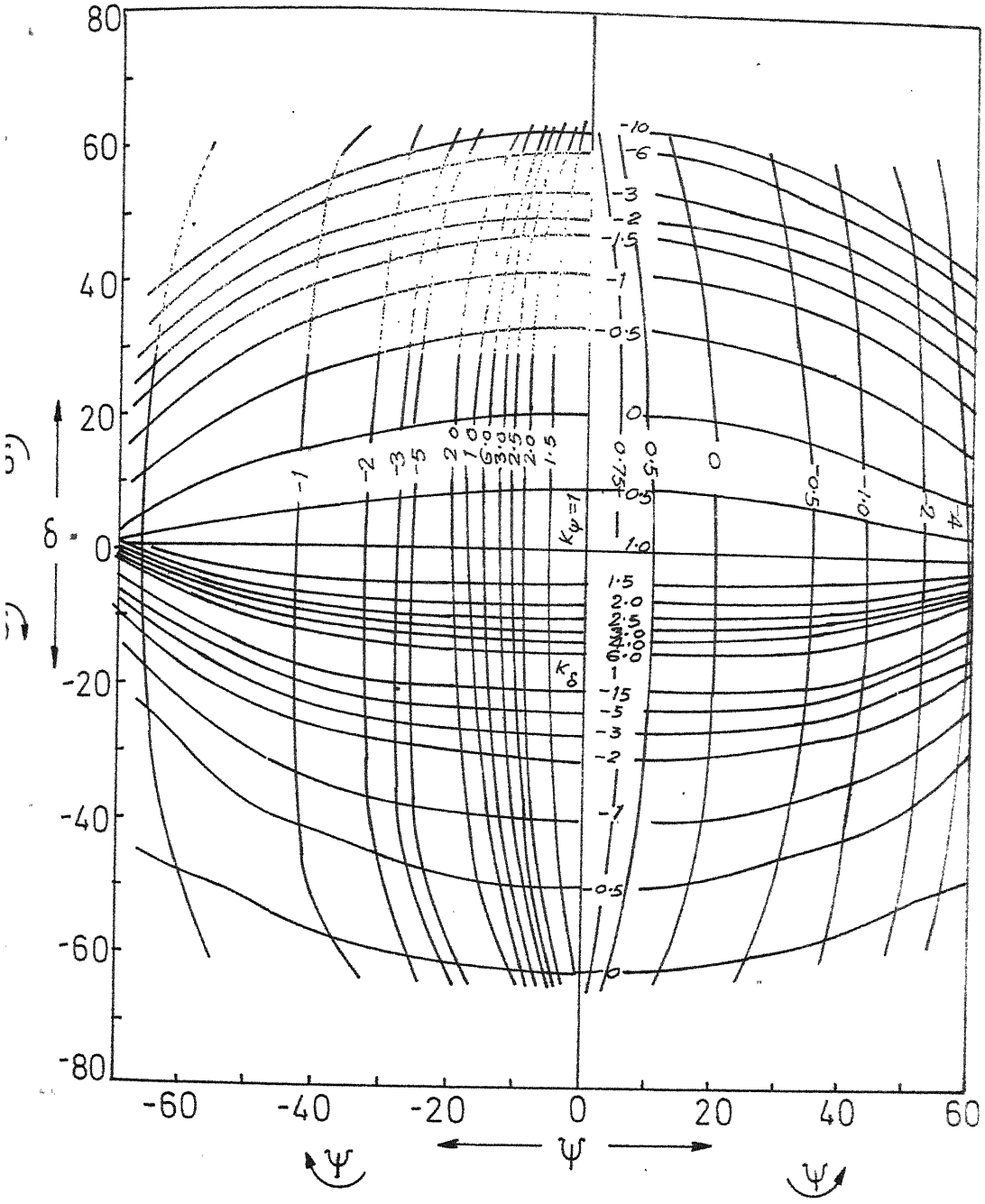

Fig.12 Calibration curves for the inclination factors K_δ & K_ψ

جمعية حقوق الإنسان

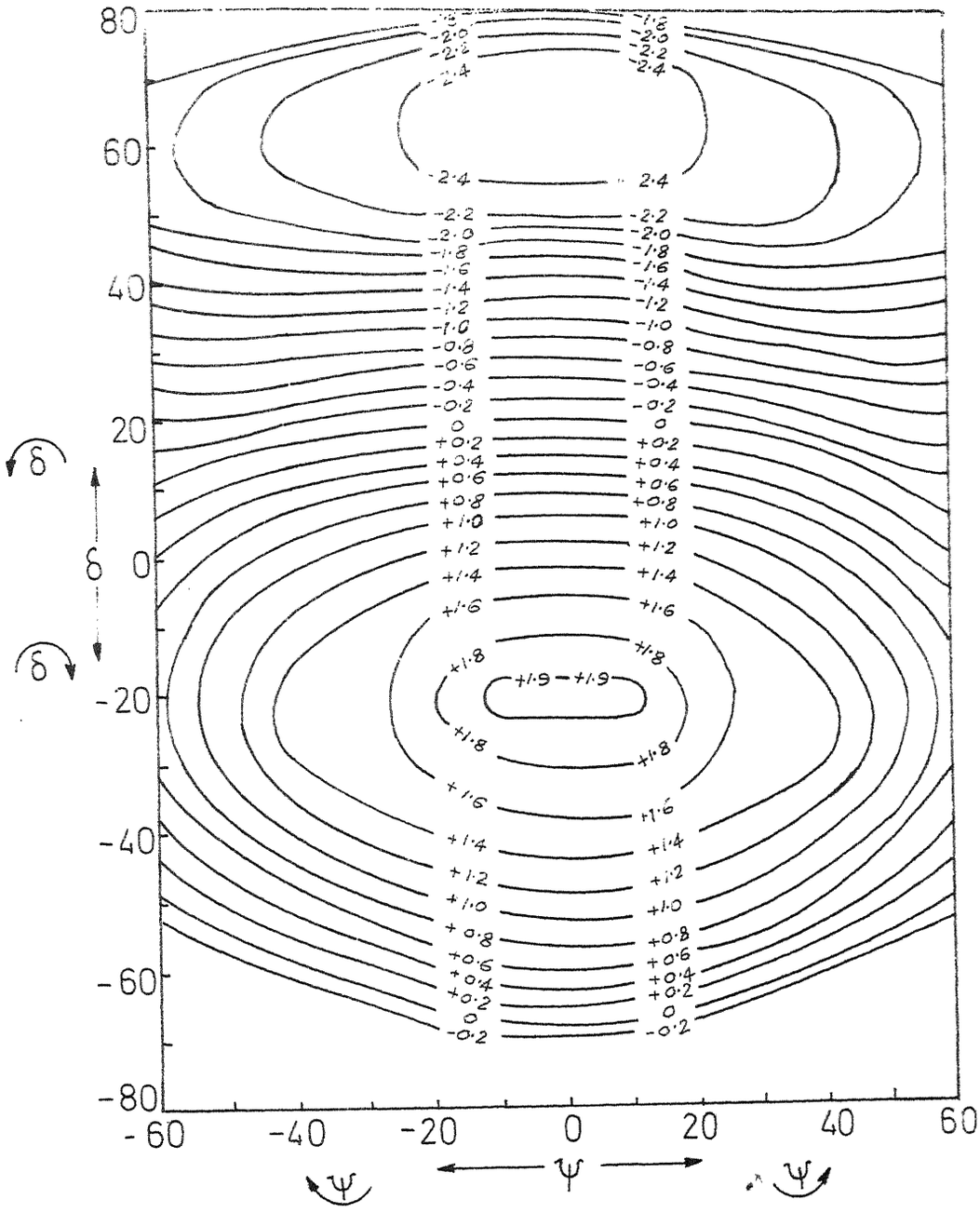

Fig.13 Calibration curves for the velocity factor V_{12}

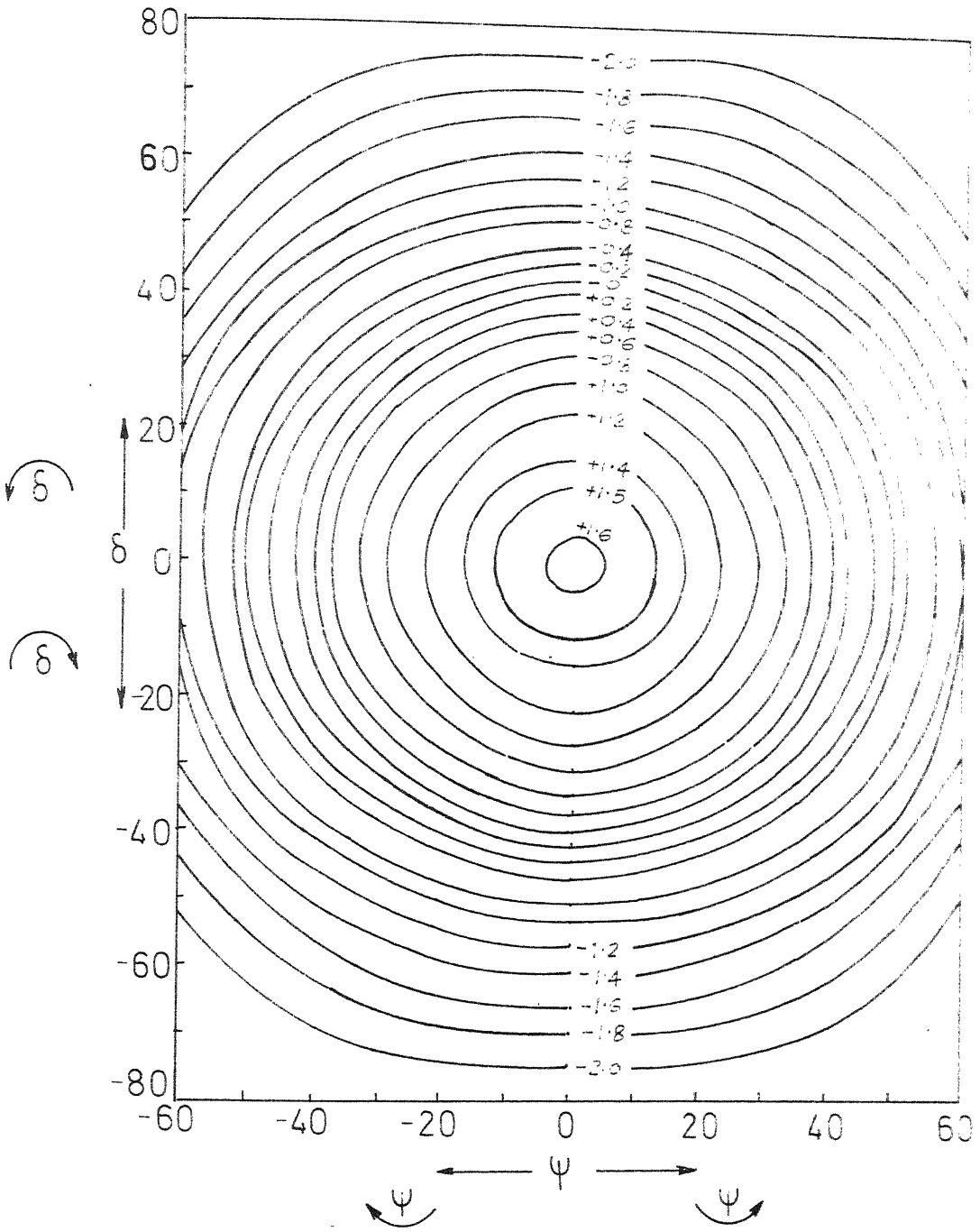

Fig.14 Calibration curves for the static pressure factor $P_{st\,1}$

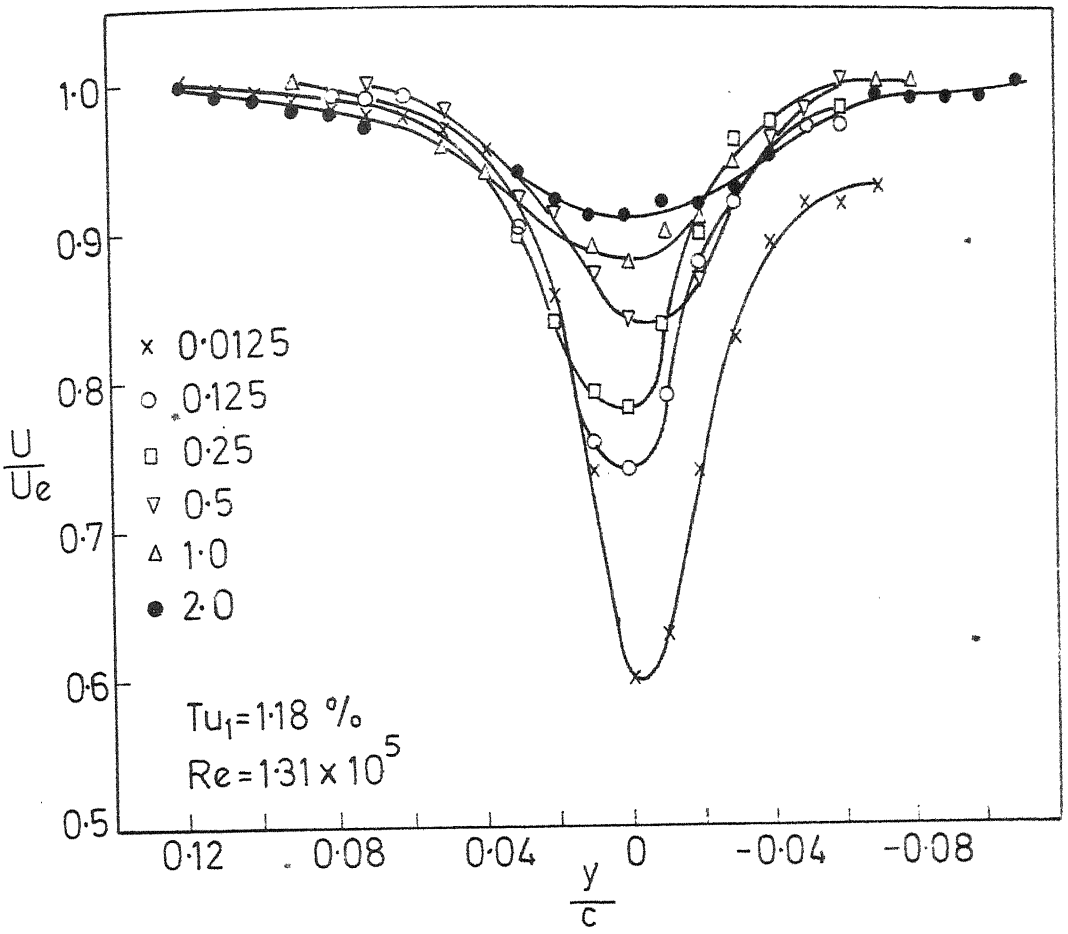

Fig.15 Mean velocity profile at -4° incidence

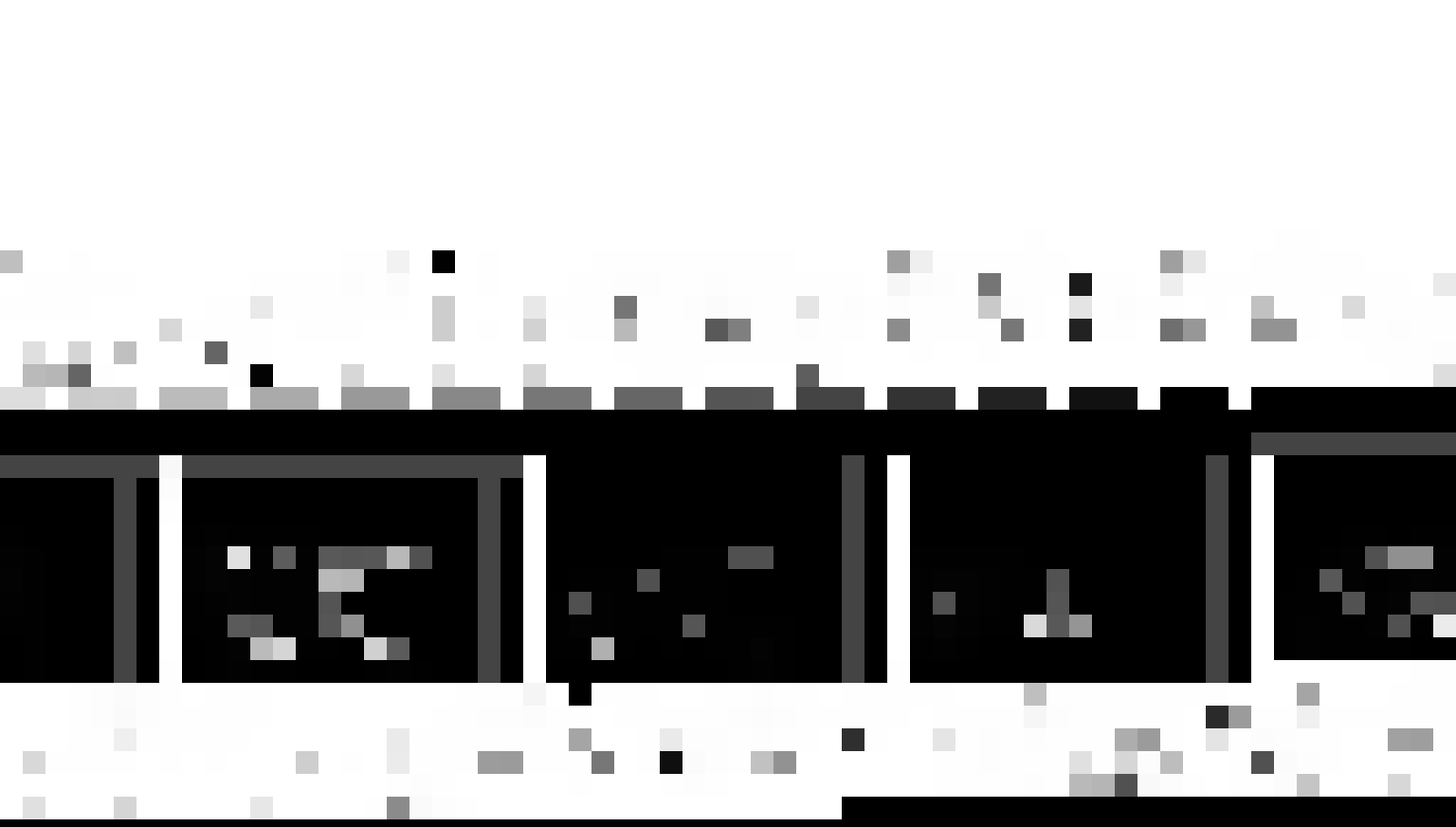

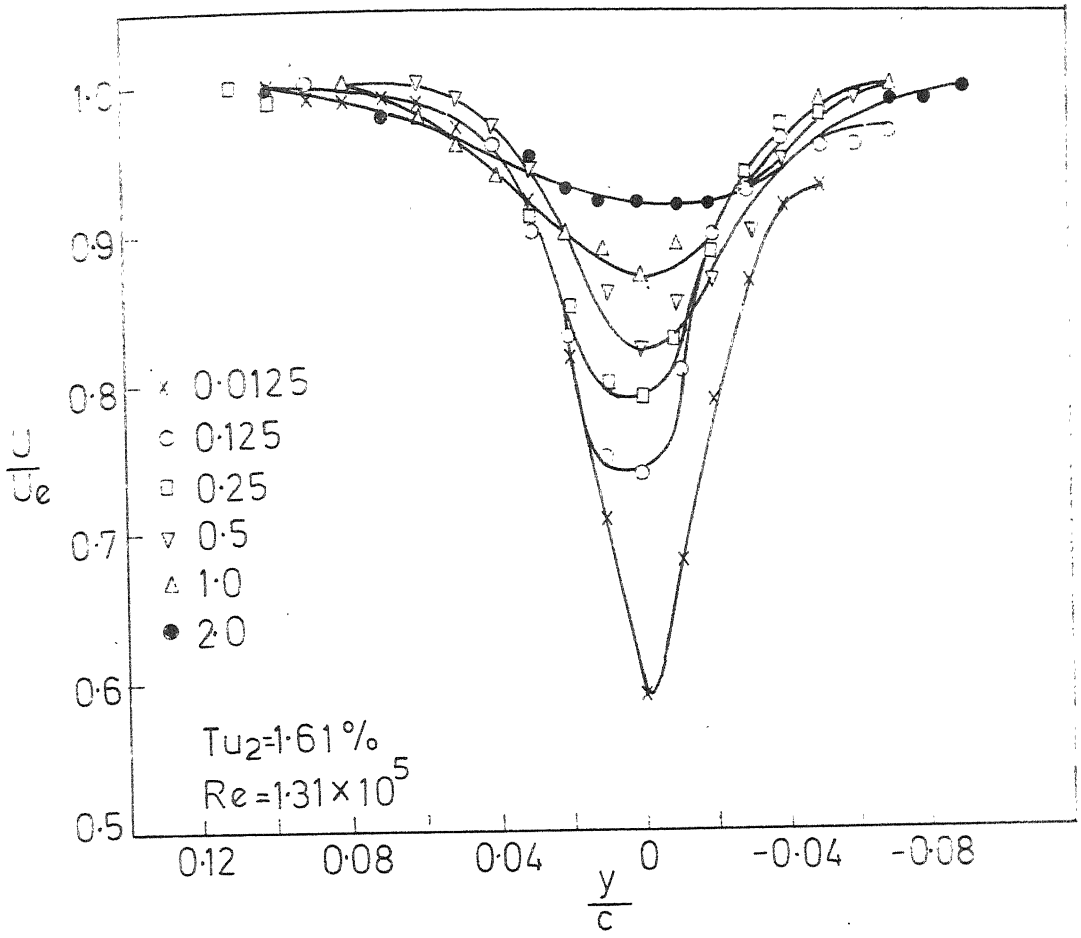

Fig.16 Mean velocity profile at -4° incidence

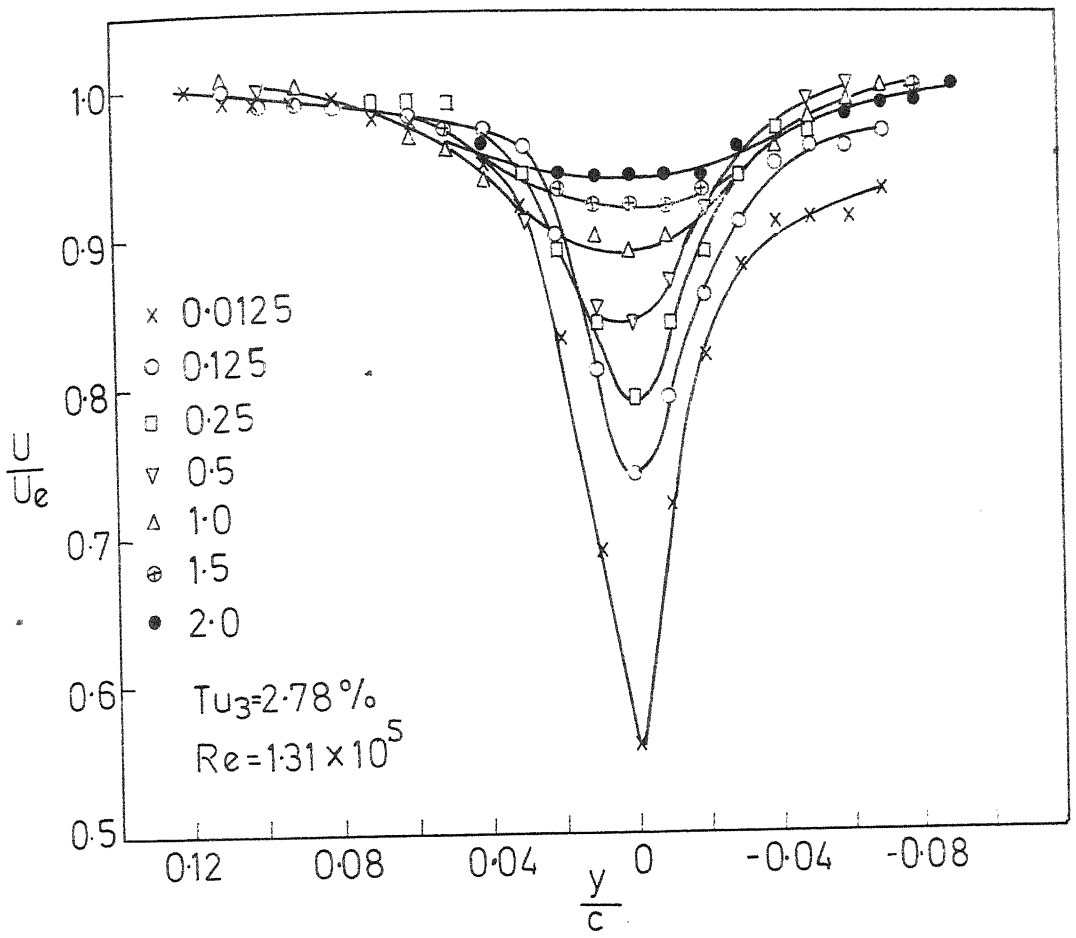

Fig.17 Mean velocity profile at -4° incidence

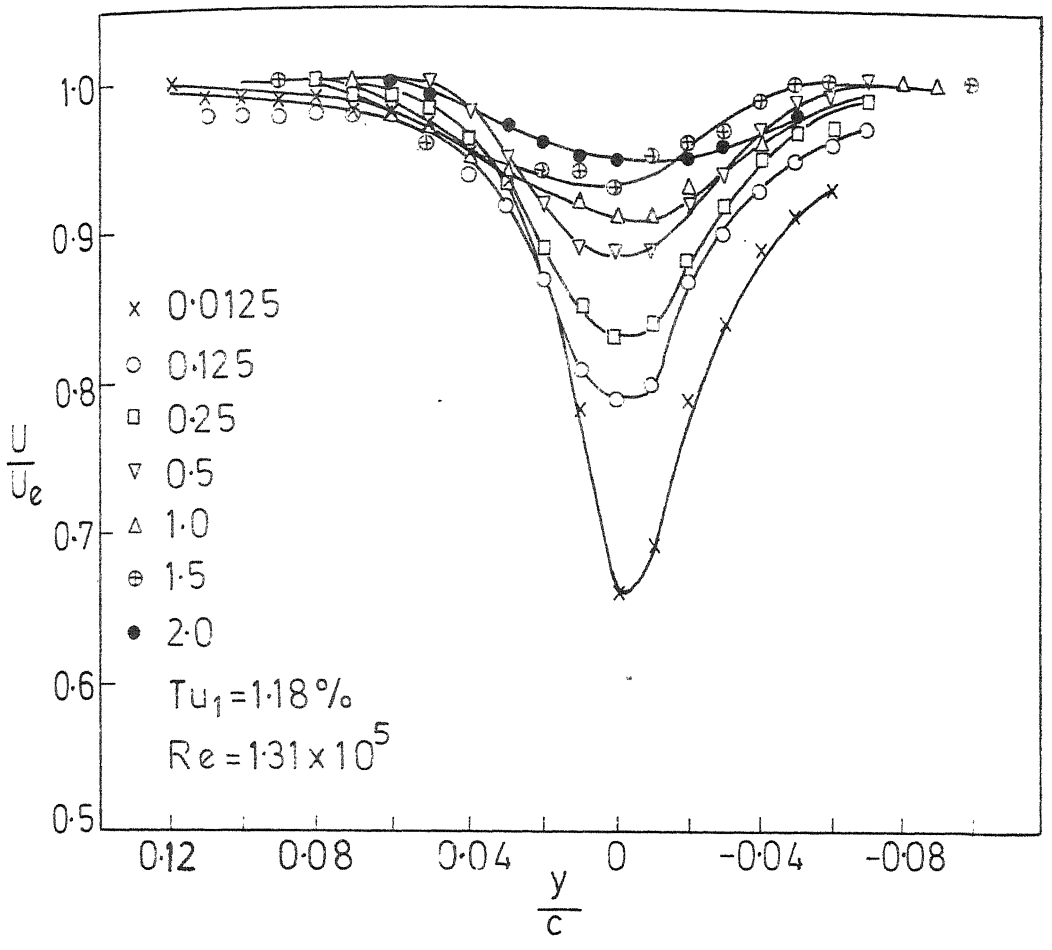

Fig.18 Mean velocity profile at 0° incidence

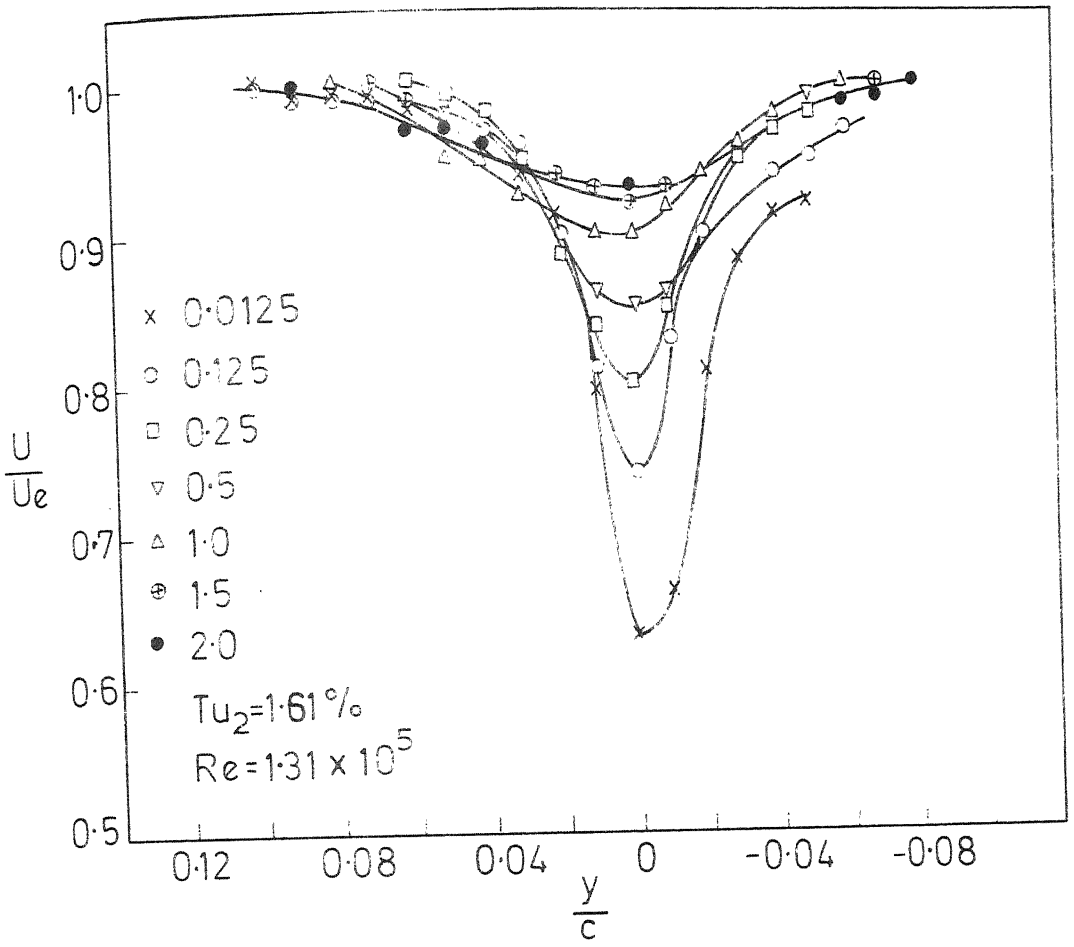

Fig.19 Mean velocity profile at 0° incidence

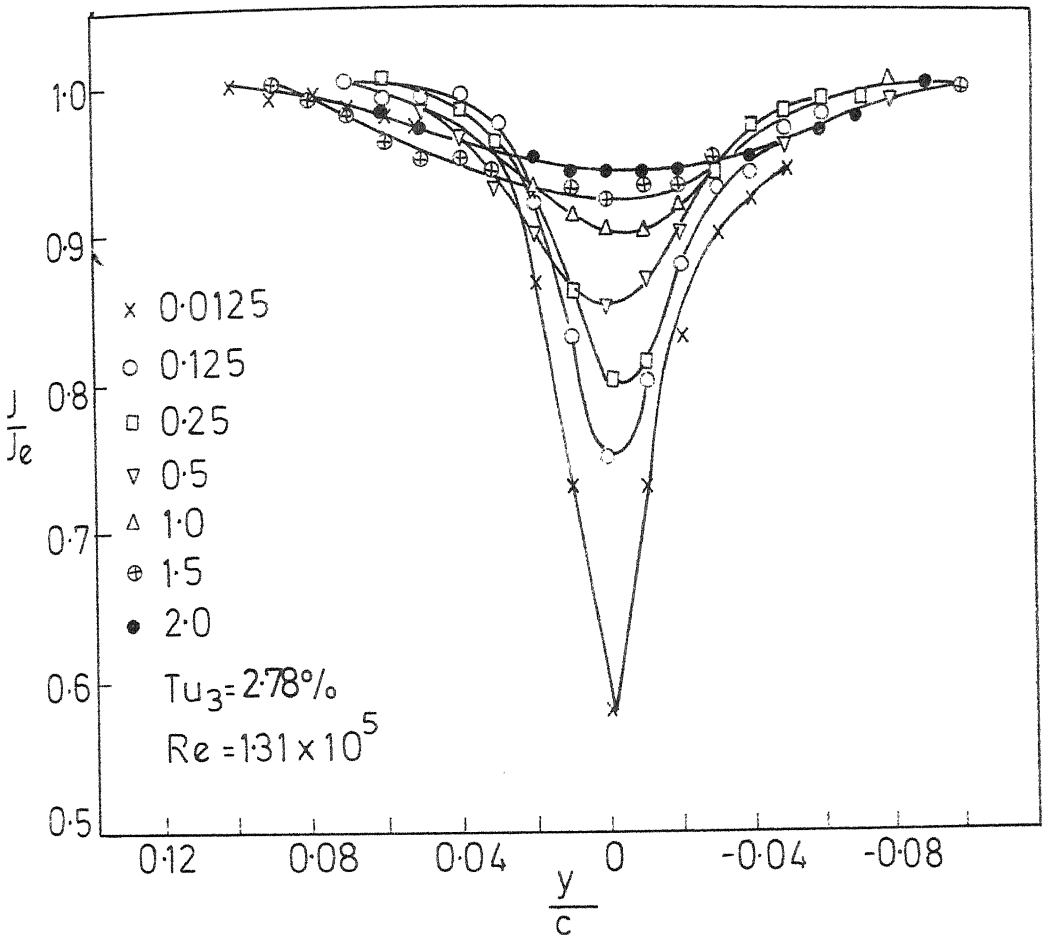

Fig.20 Mean velocity profile at 0° incidence

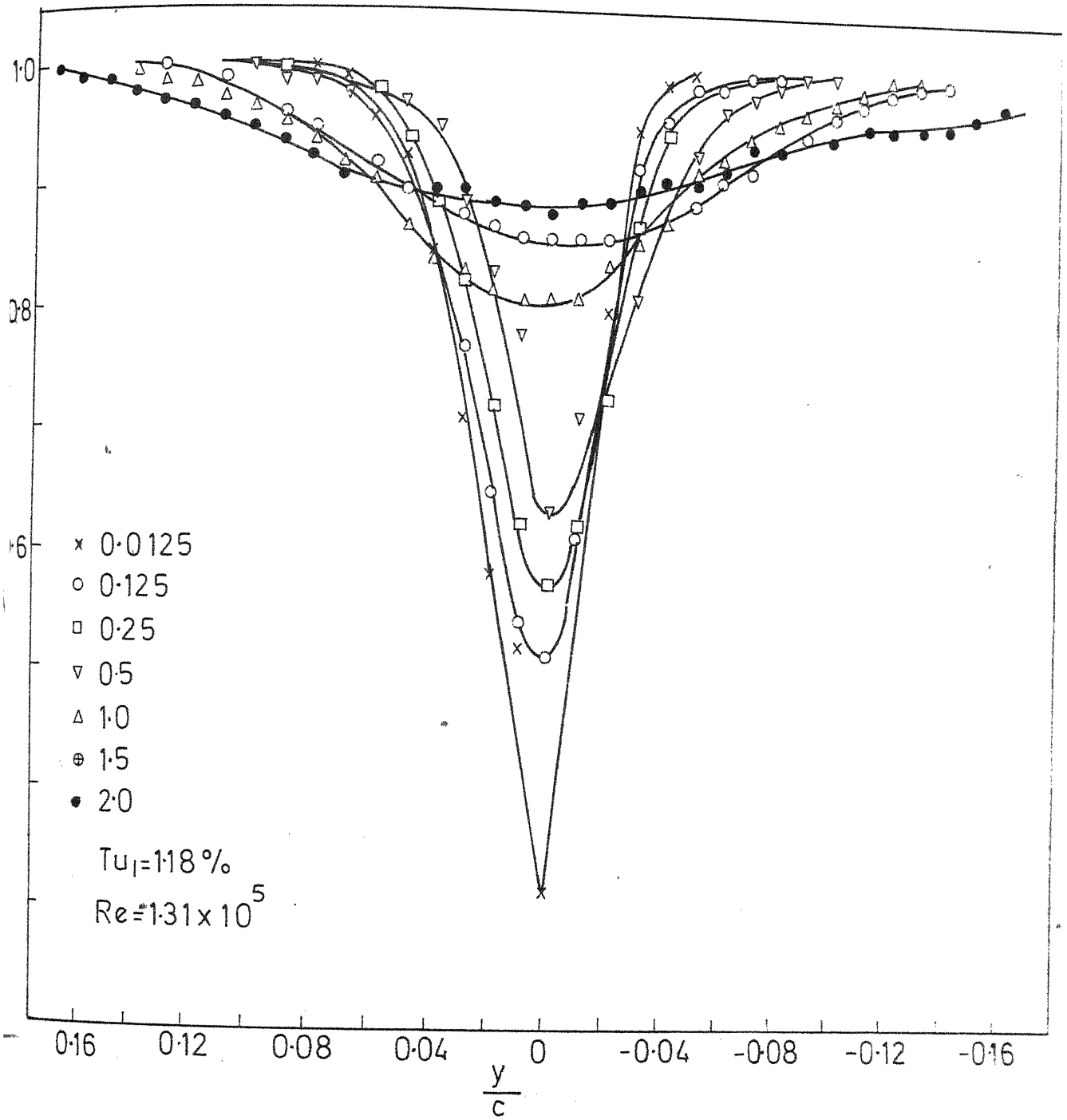

Fig.21 Mean velocity profile at 12° incidence

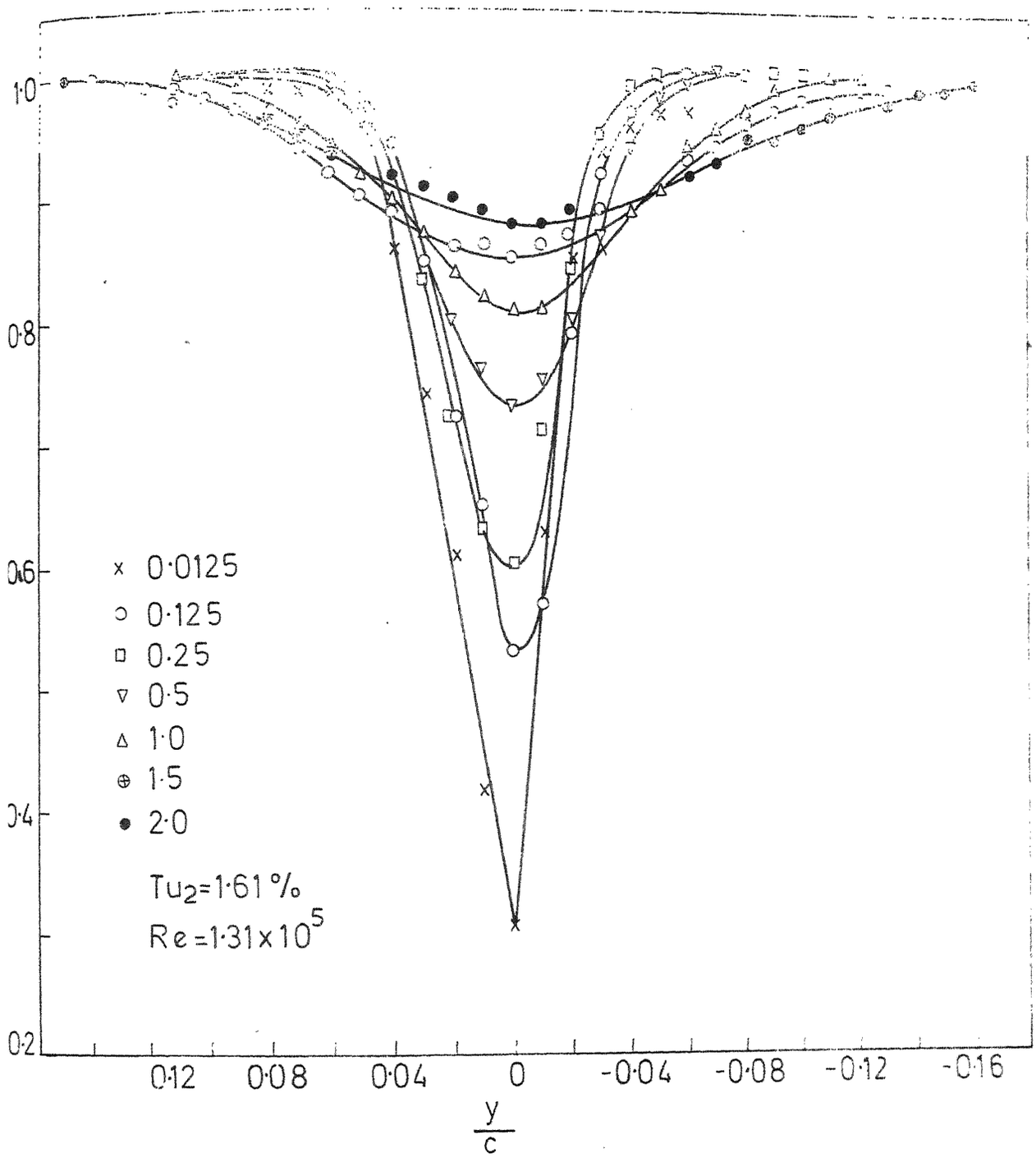

Fig. 22 Mean velocity profile at 12° incidence

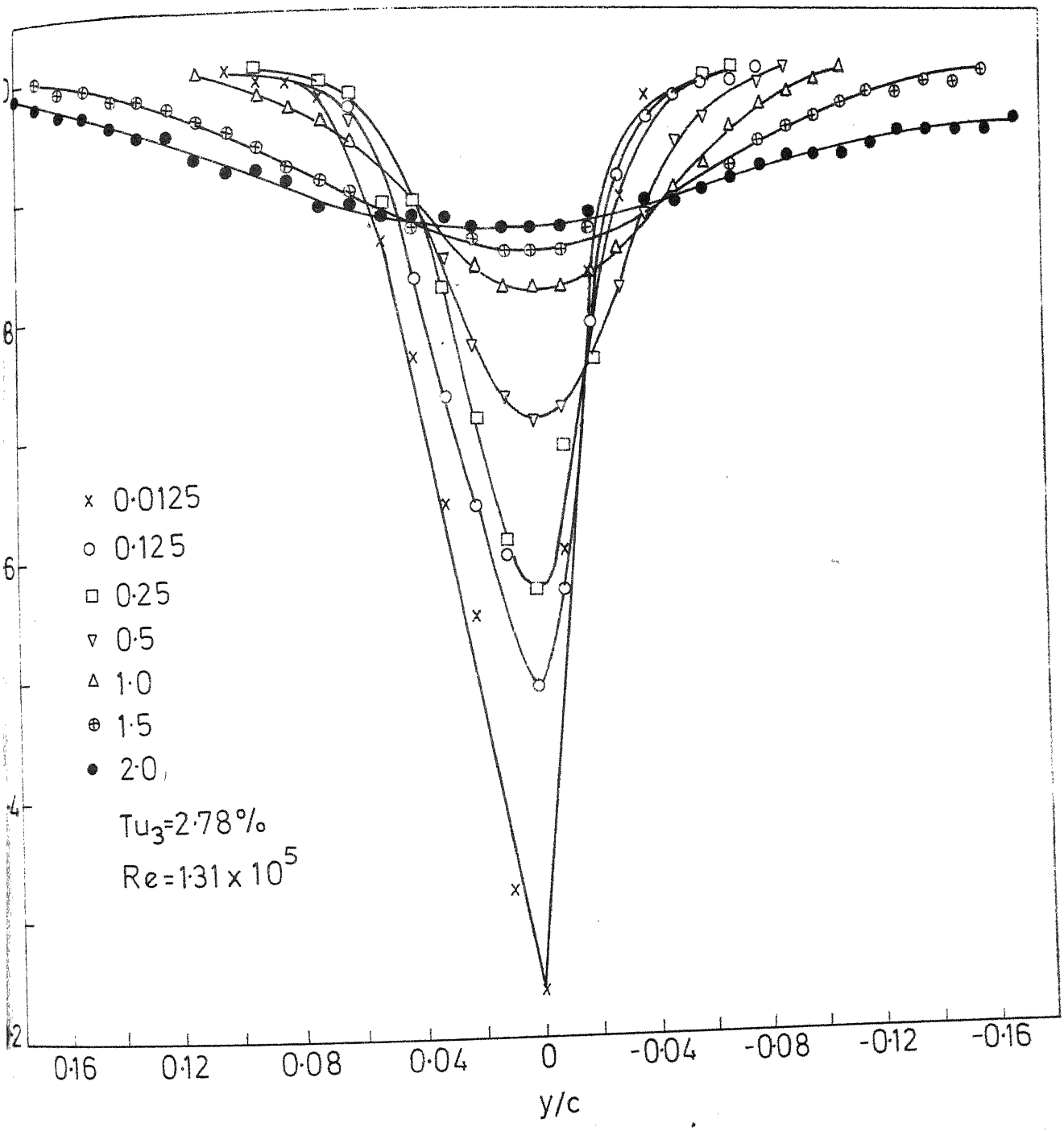

Fig.23 Mean velocity profile at 12° incidence

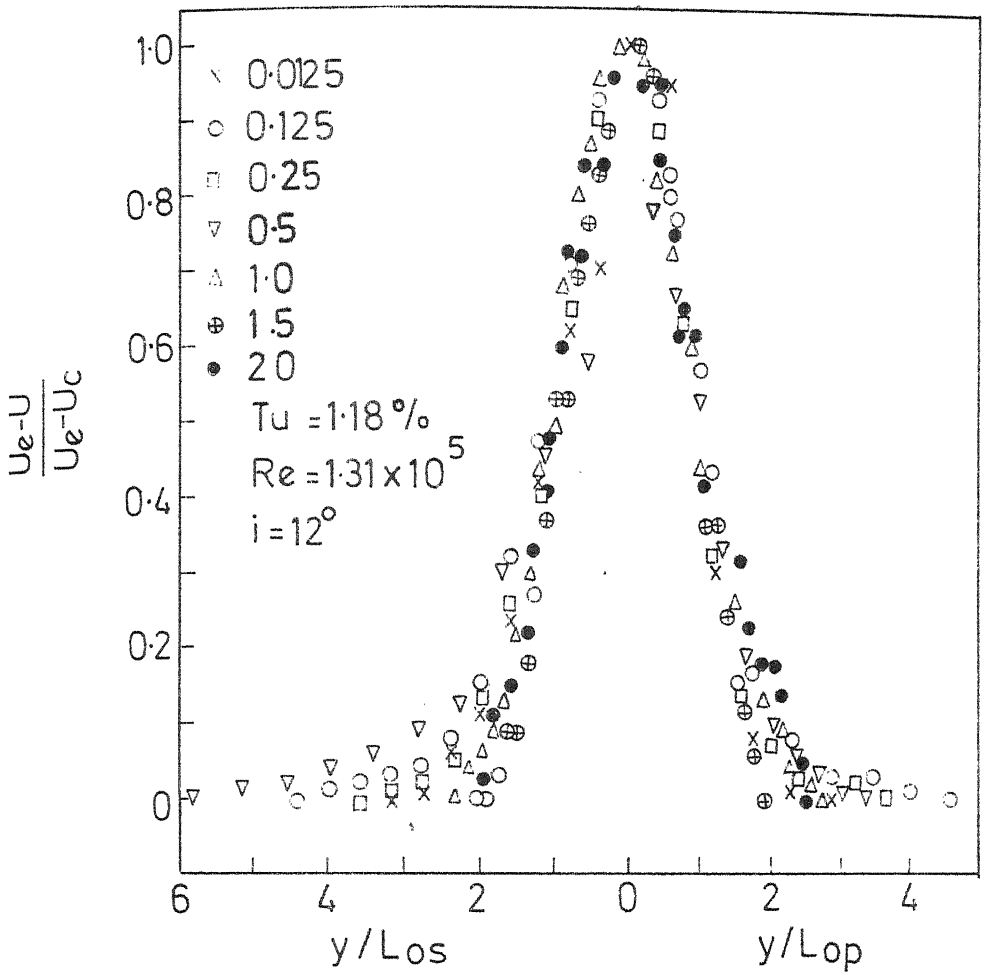

Fig. 24 Similarity in mean velocity profiles

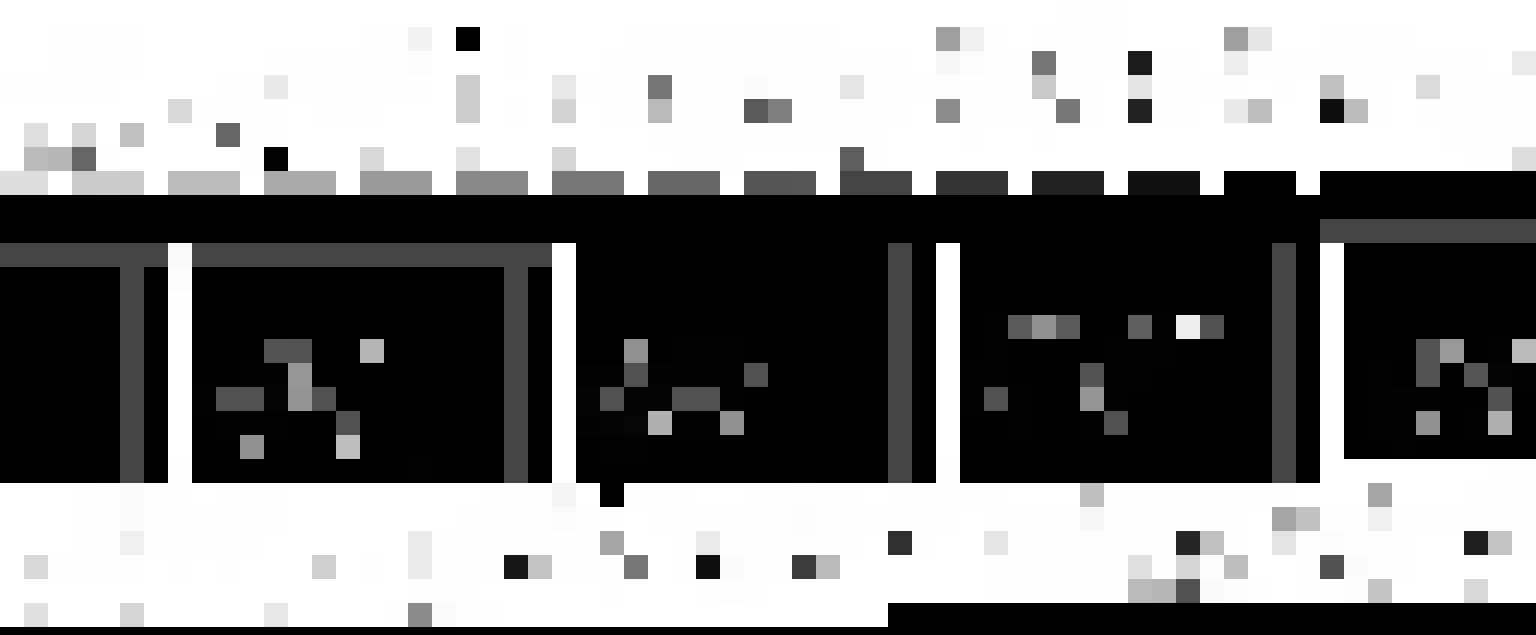

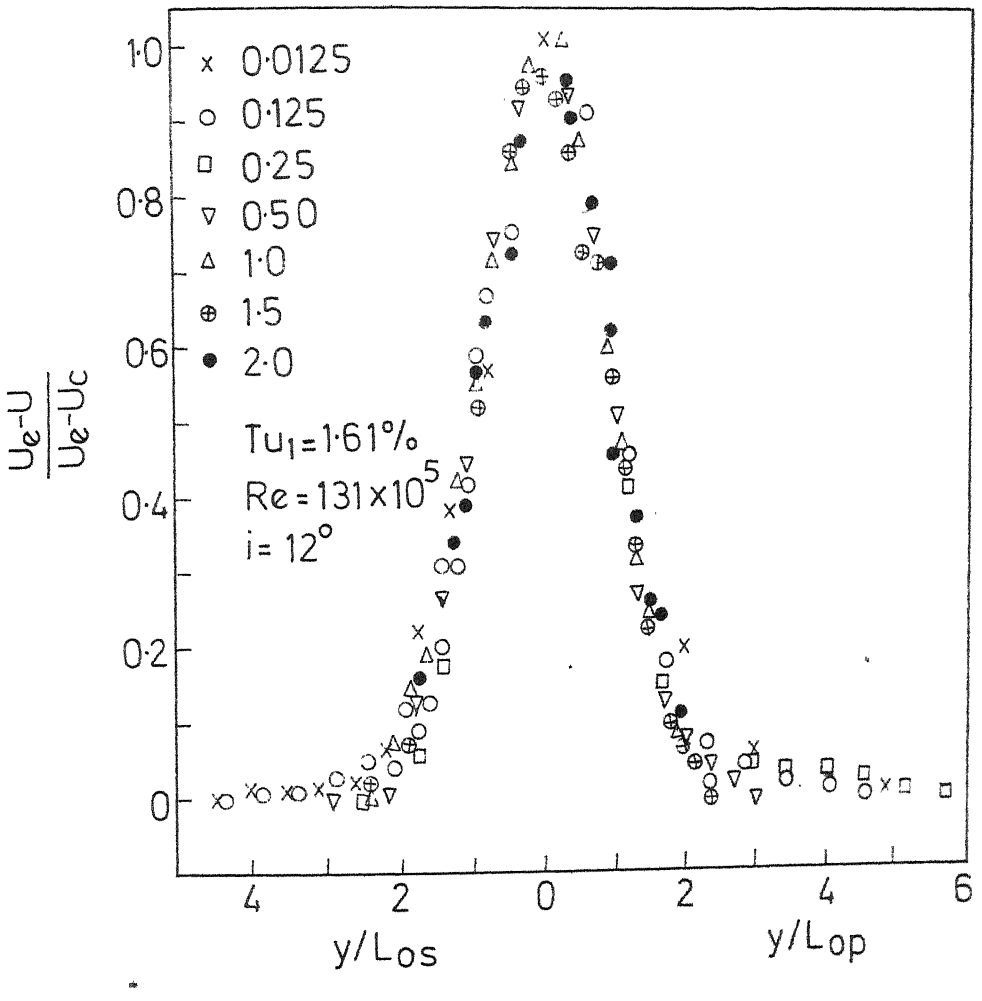

Fig.25 Similarity in mean velocity profiles

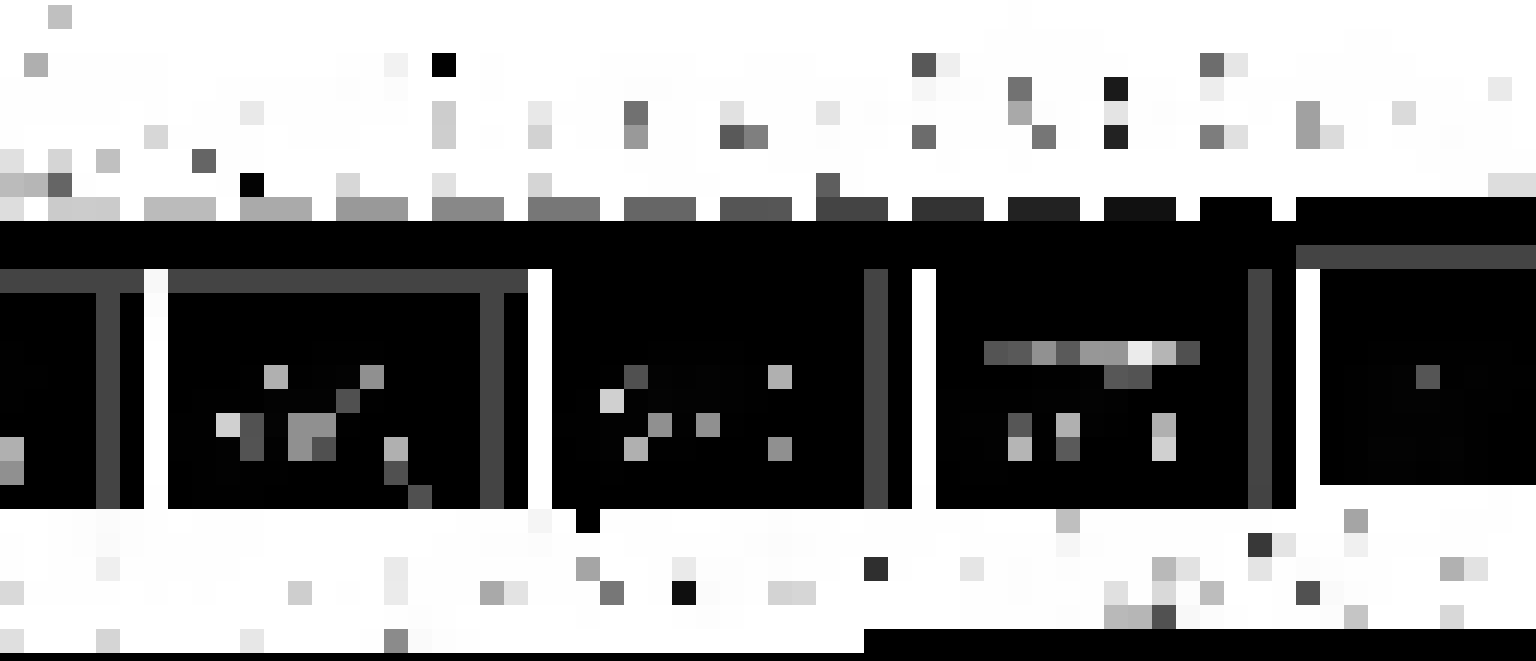

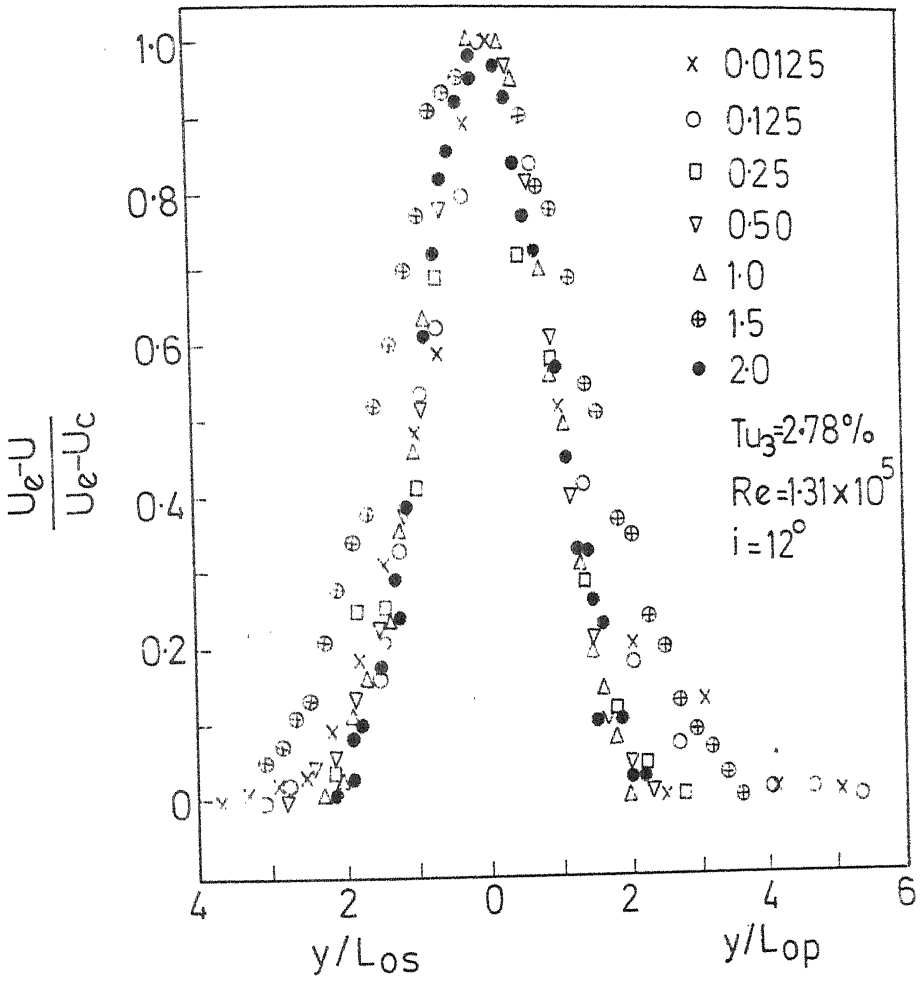

Fig. 26 Similarity in mean velocity profiles

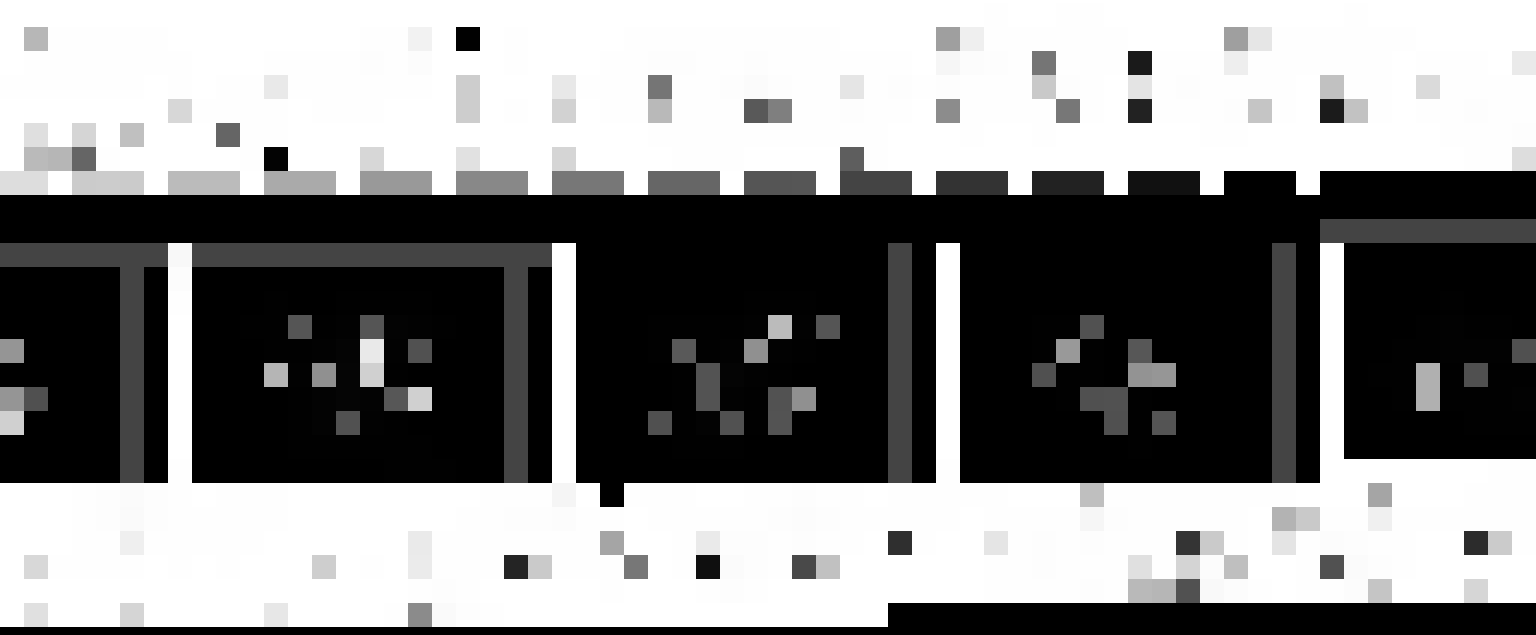

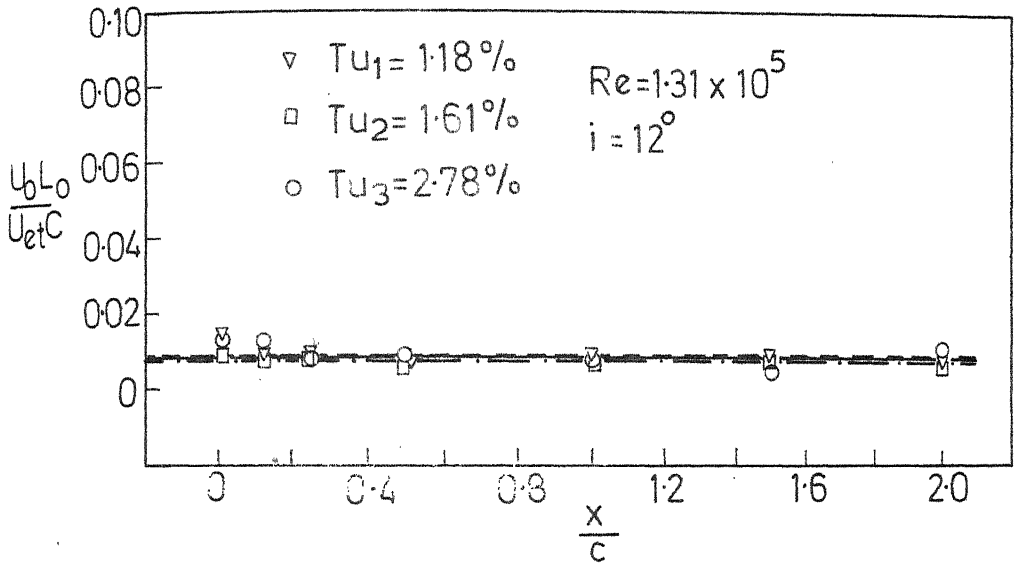

Fig.29 Variation of $U_o L_o / U_{et} C$ with downstream distance

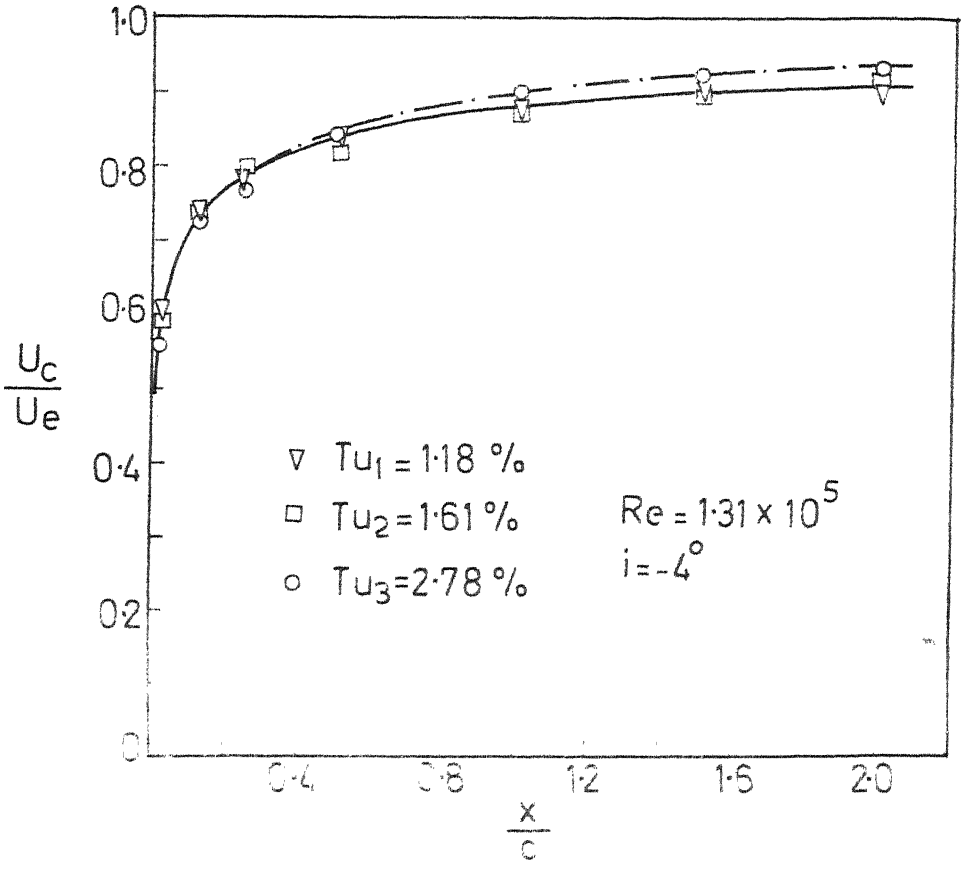

Fig. 30 Variation of wake centre line velocity with downstream distance

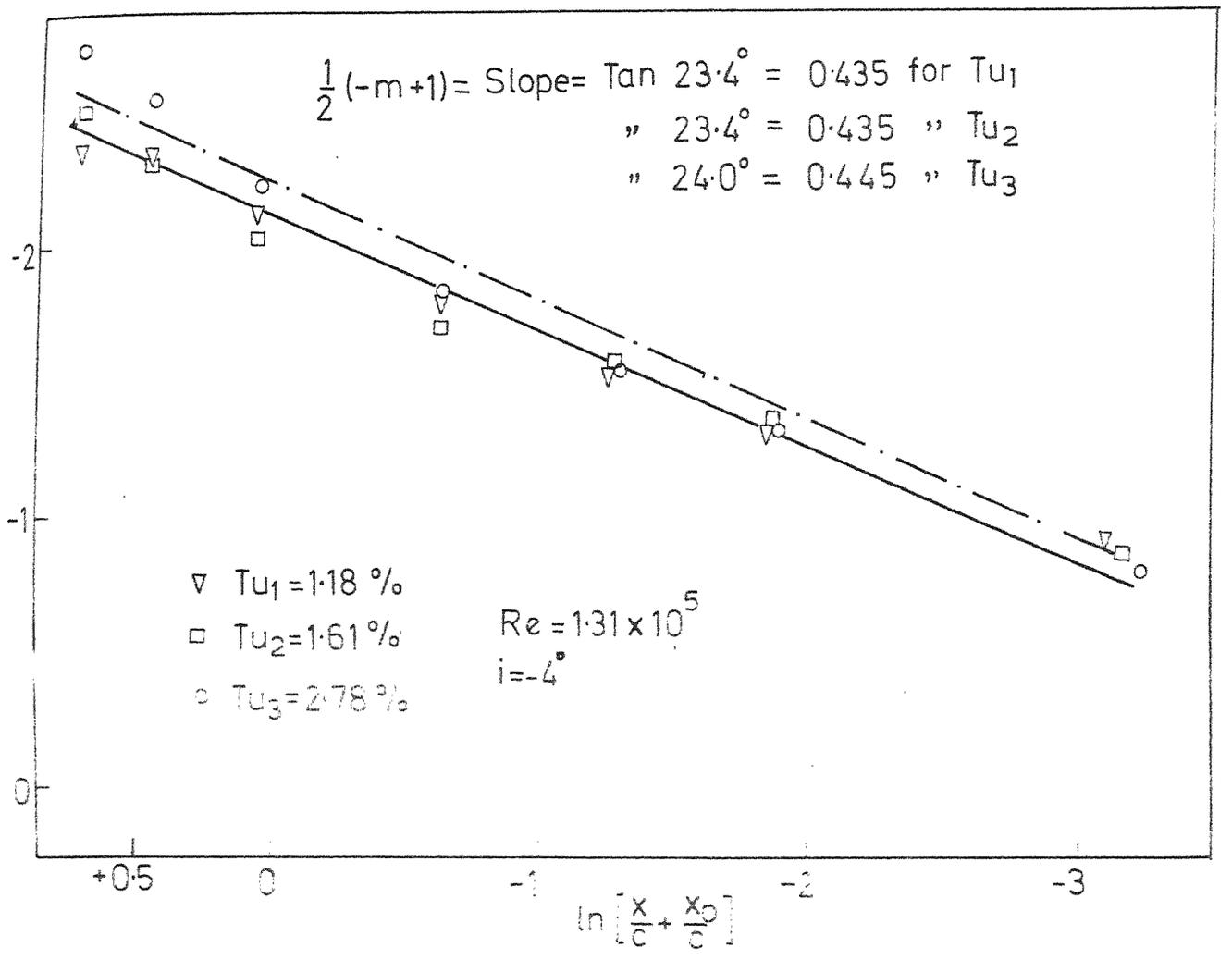

Fig.31 Variation of wake centre line velocity with downstream distance logarithmic

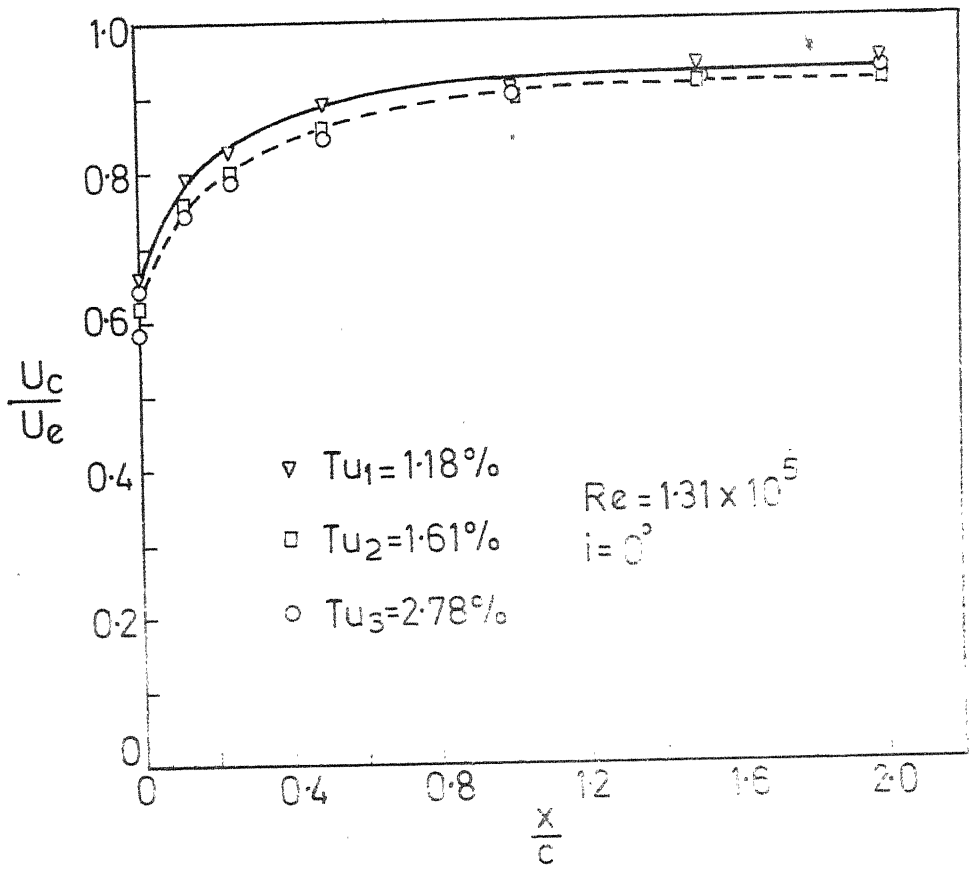

Fig.32 Variation of wake centre line velocity with downstream distance

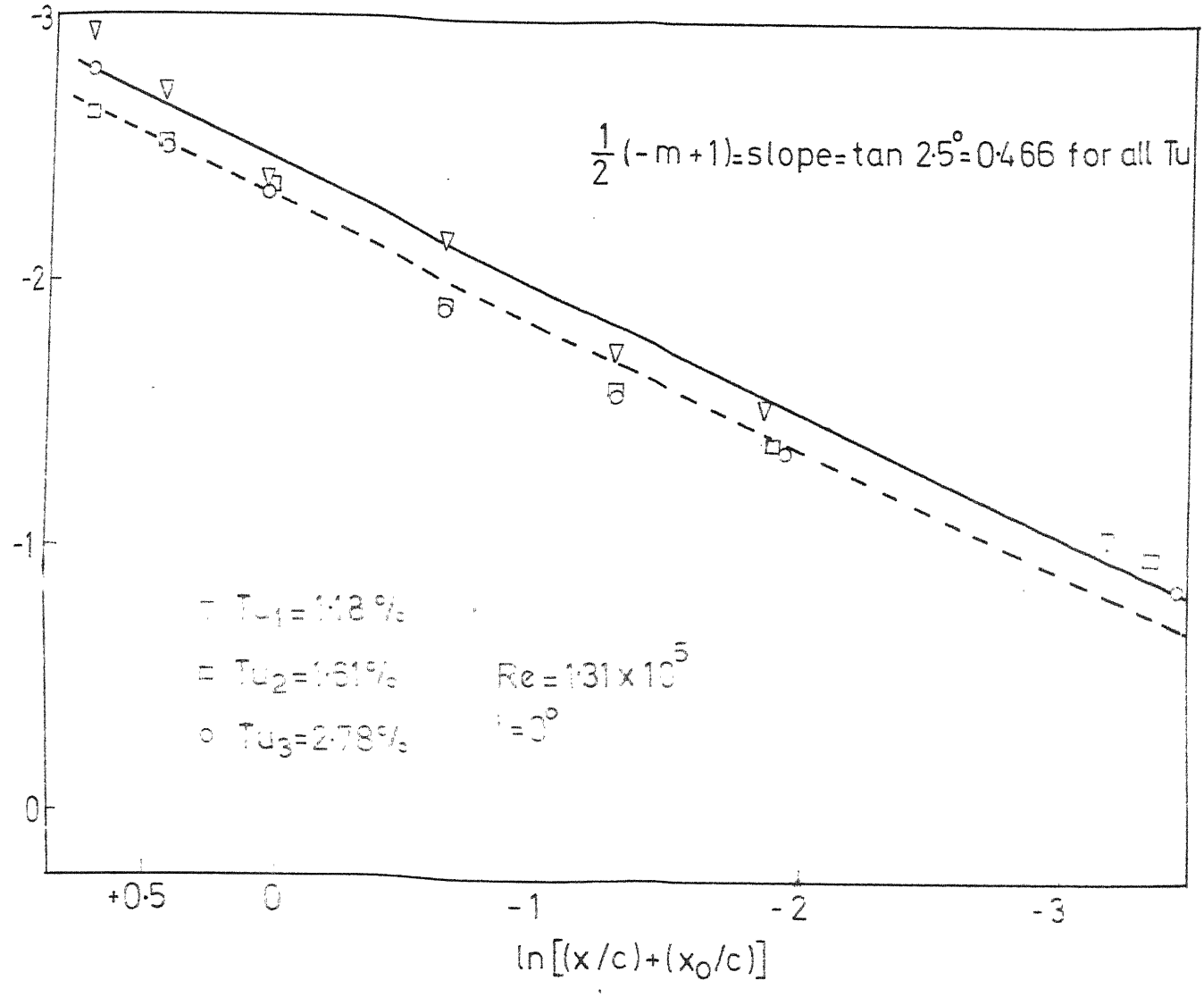

Fig.33 Variation of wake centre line velocity with downstream distance logarithmic

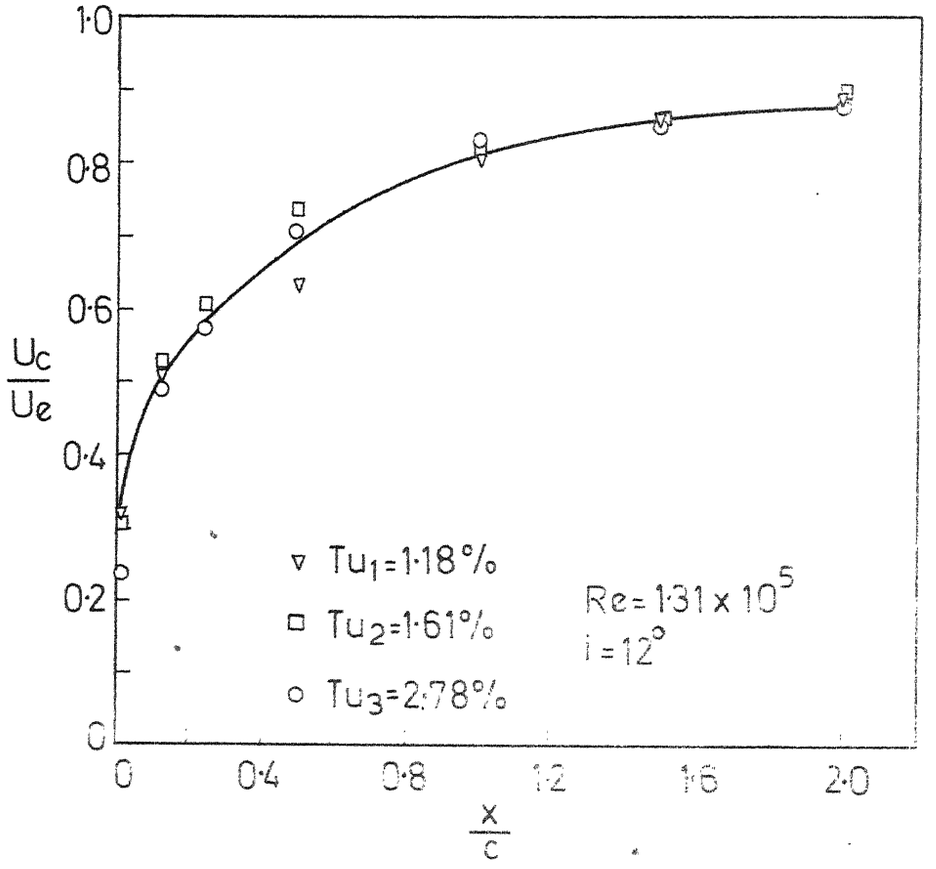

Fig.34 Variation of wake centre line velocity with downstream distance

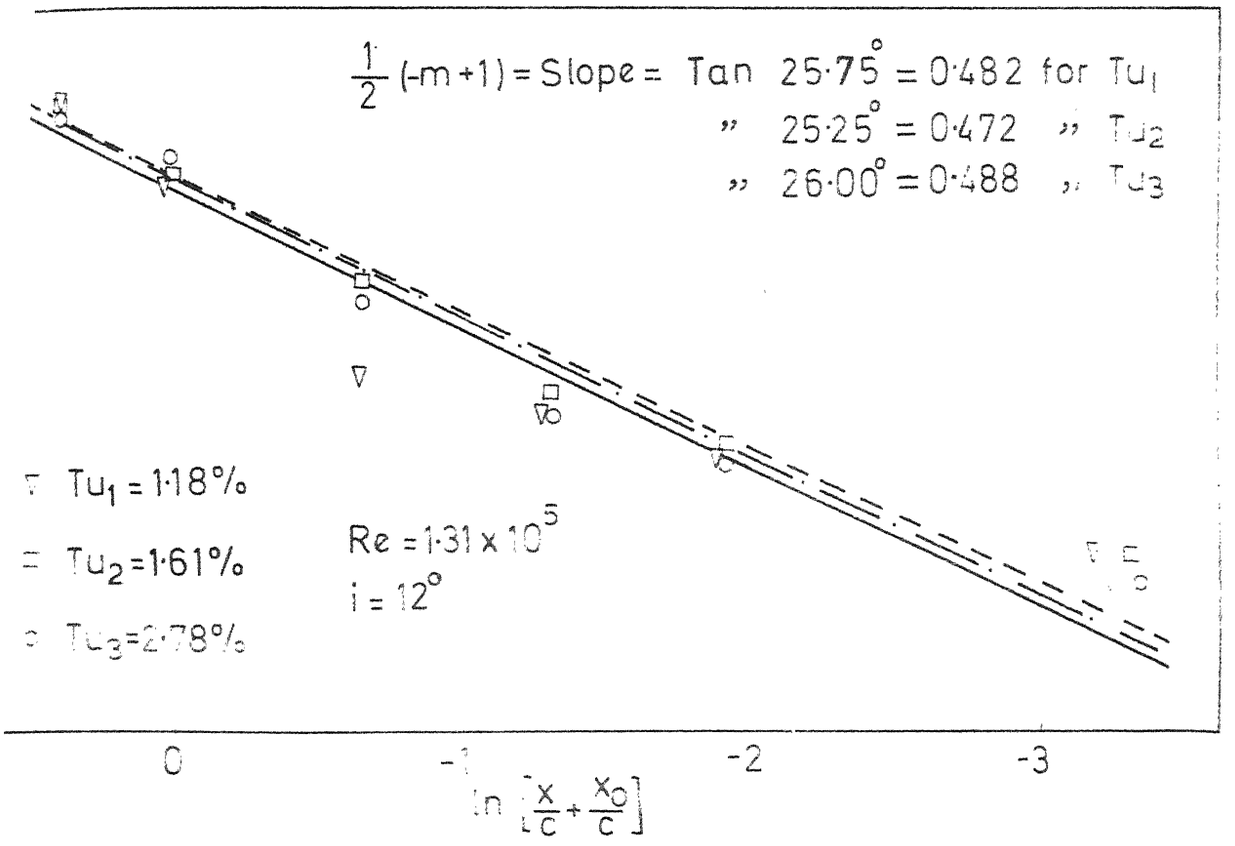

Variation of wake centre line velocity with downstream distance logarithmic

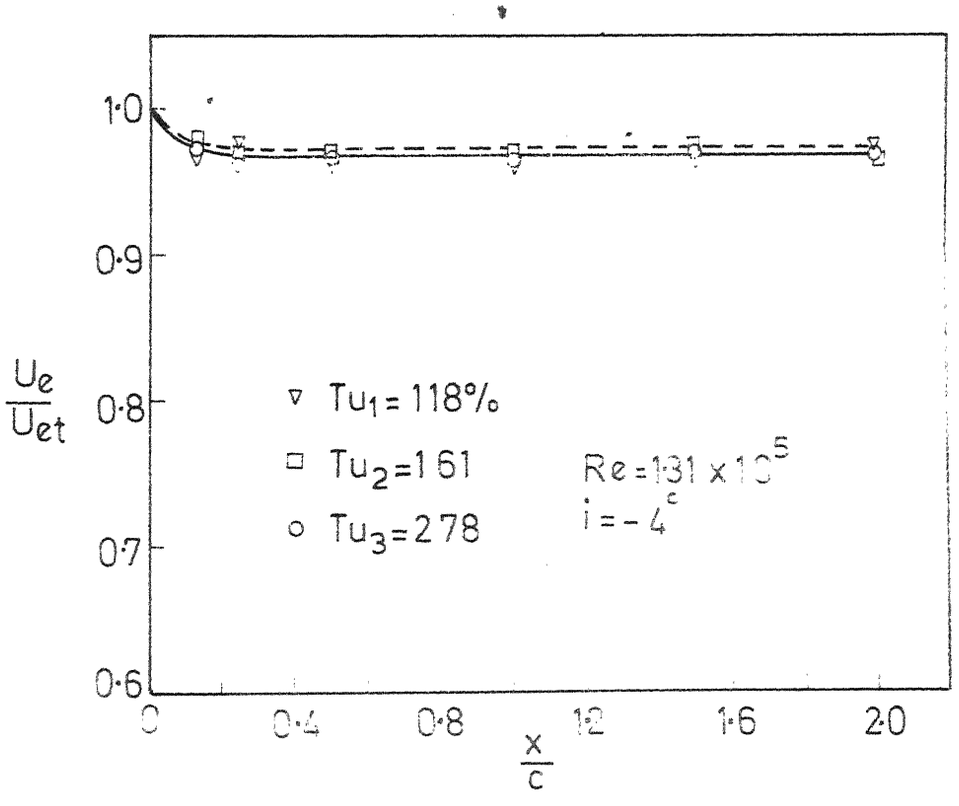

Fig.36 Variation of wake edge velocity with downstream distance

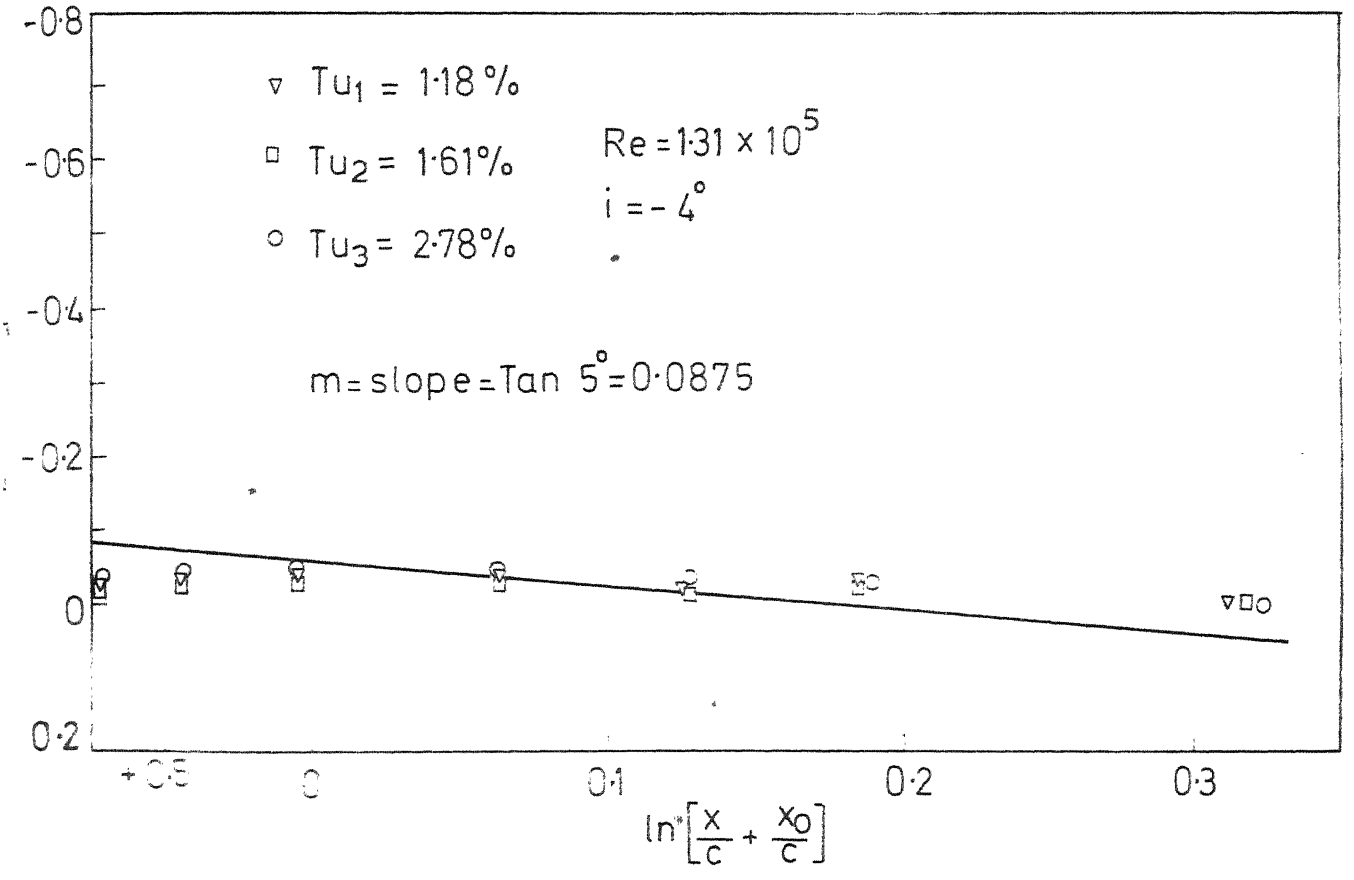

Fig.37 Variation of wake edge velocity with downstream distance logarithmic

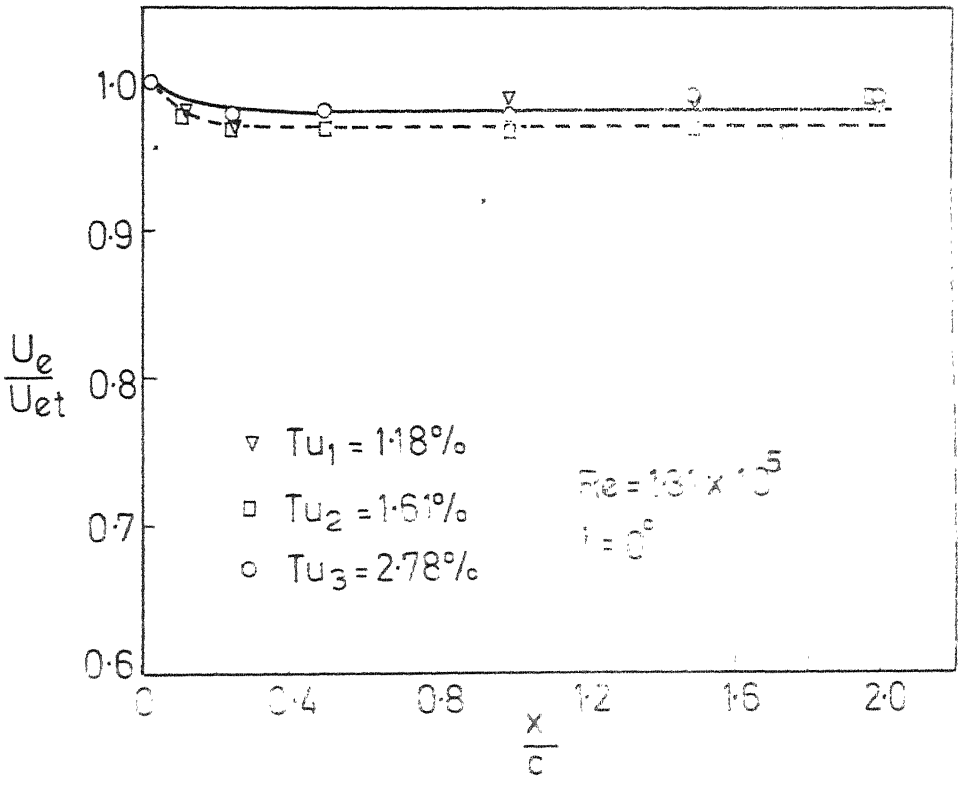

Fig.38 Variation of wake edge velocity with downstream distance

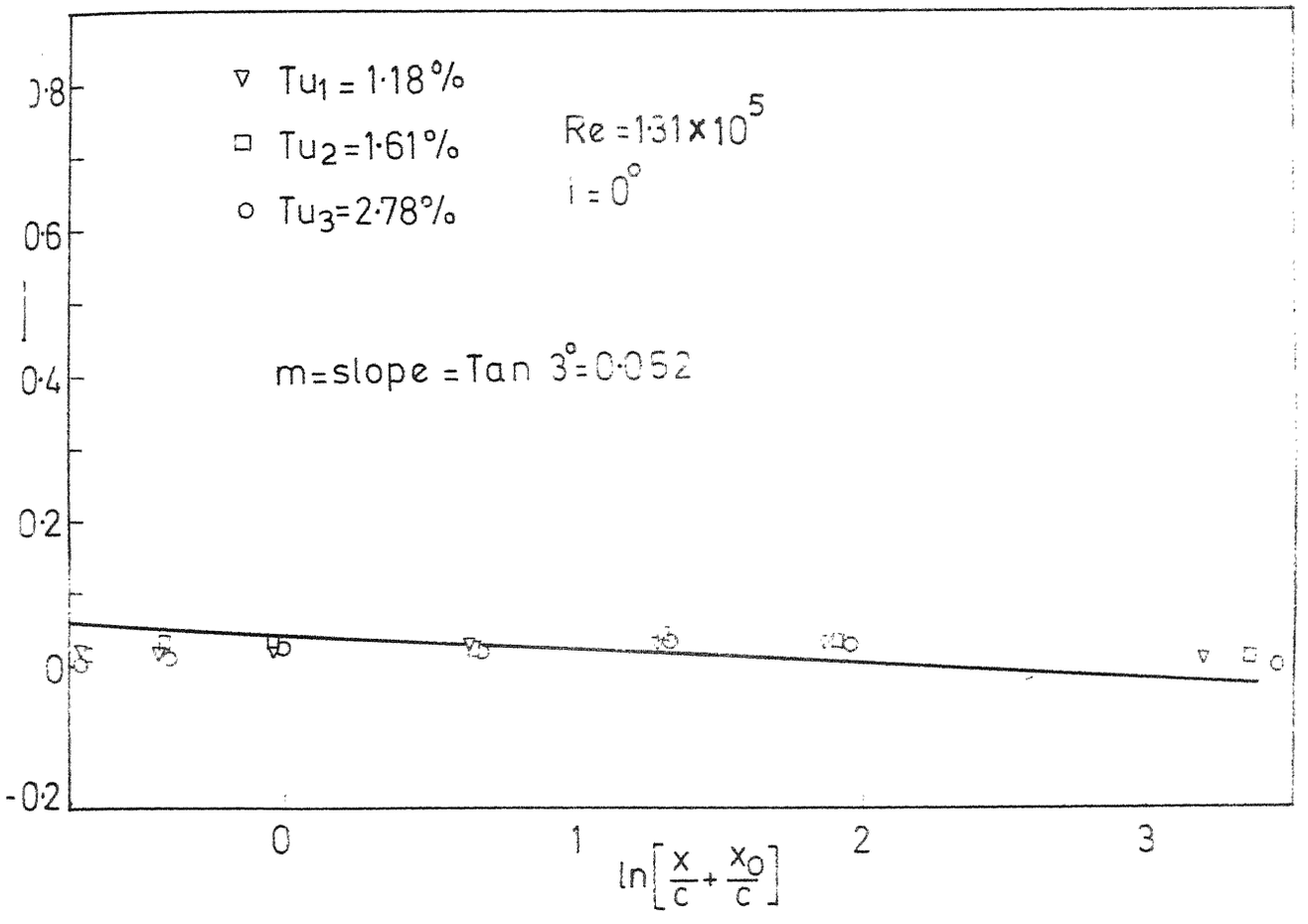

Fig. 39 Variation of wake edge velocity with downstream distance logarithmic

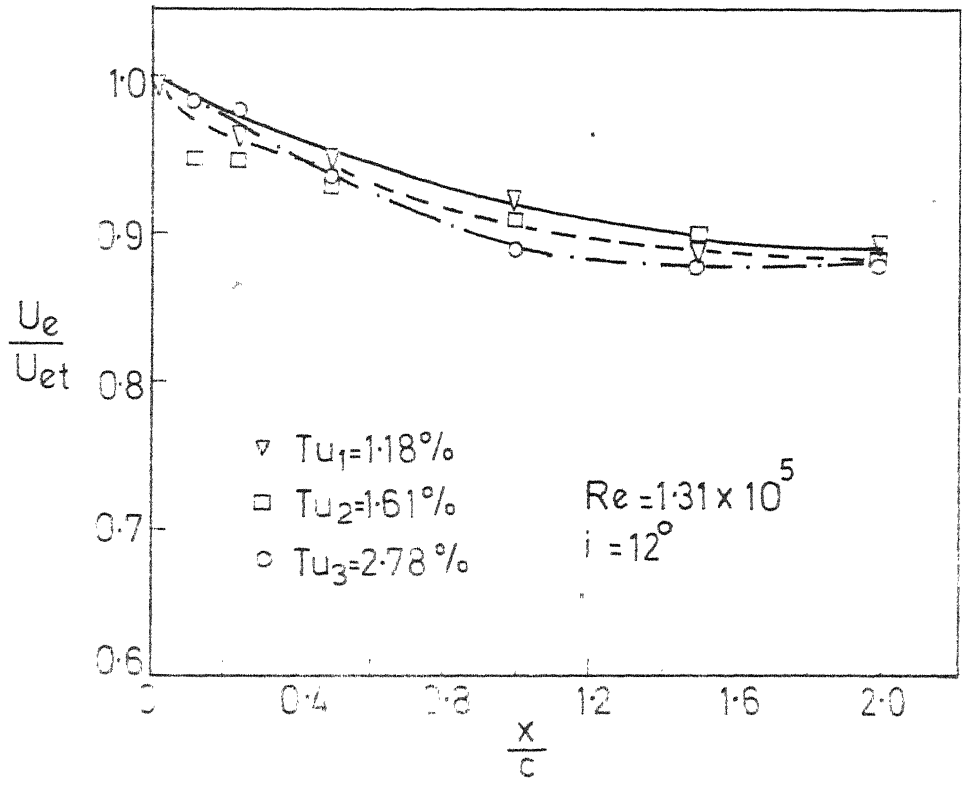

Fig.40 Variation of wake edge velocity with downstream distance

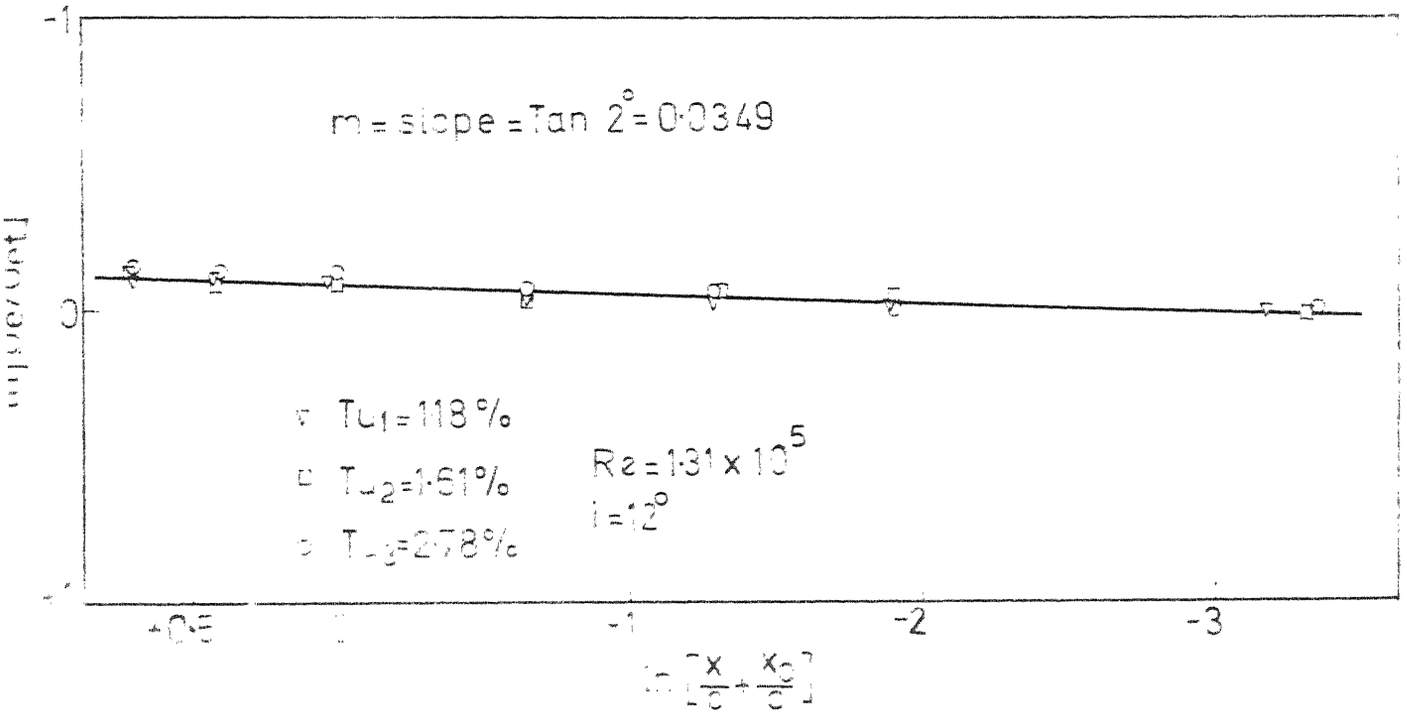

Fig.41 Variation of wake edge velocity with downstream distance logarithmic

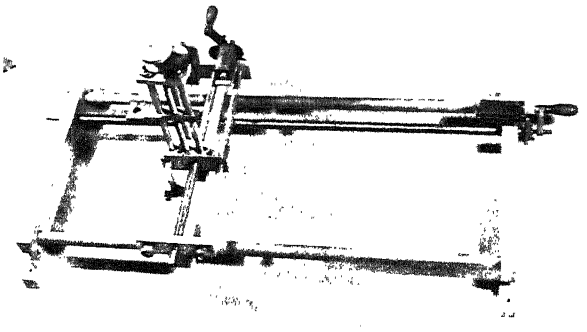

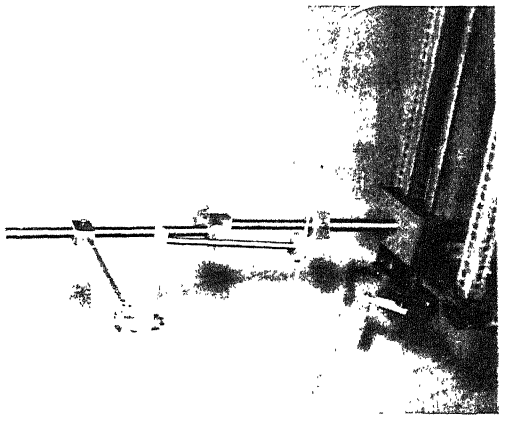

[redacted]

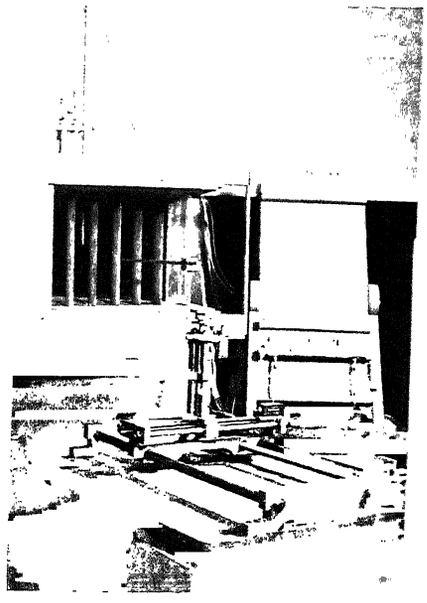

ing

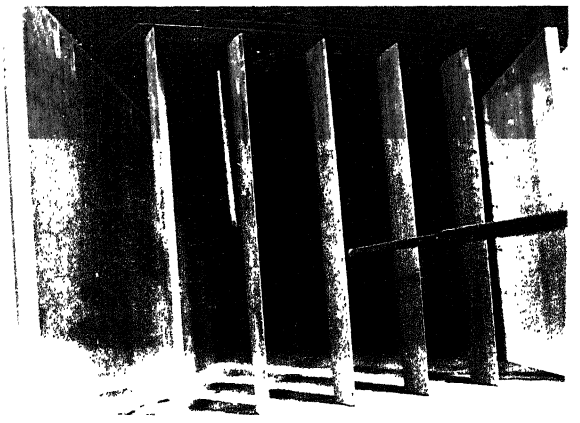

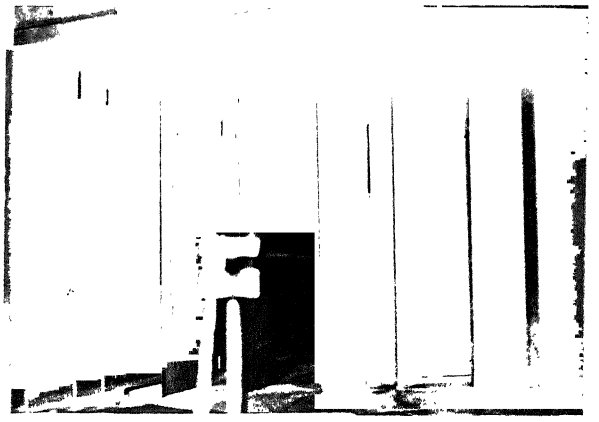

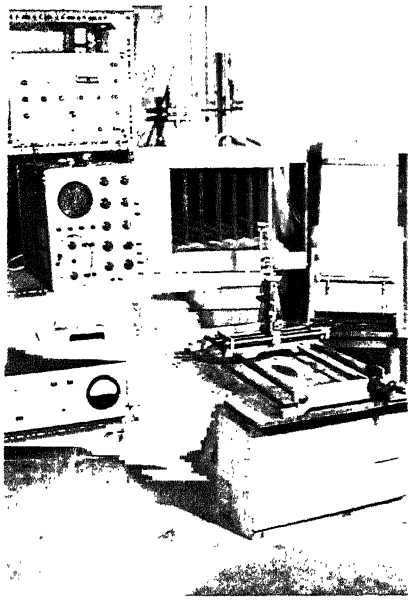

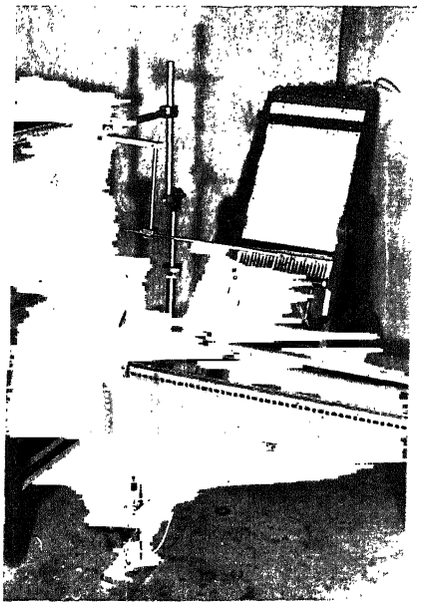

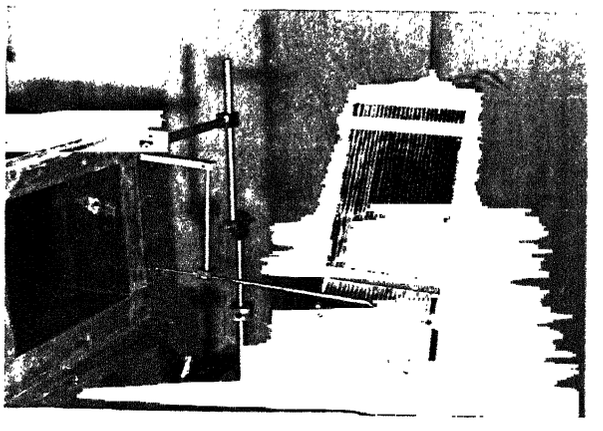

كتاب الصلاة